Universitatea
Transilvania
din Brașov

INTERDISCIPLINARY DOCTORAL SCHOOL

Faculty of Mechanical Engineering

Adrian Ștefan MAZILU

CONTRIBUTIONS TO THE ENERGY OPTIMISATION OF THERMAL ENGINES

SUMMARY

Scientific Supervisor

Prof. dr. eng. Veneția SANDU

BRAȘOV, 2025

CONTENTS

1. INTRODUCTION

The doctoral thesis entitled "Contributions to the Energy Optimization of Thermal Engines" falls within the fundamental field of Engineering Sciences, branch of science Mechanical Engineering, Mechatronics, Industrial Engineering and Management, field of doctoral studies Mechanical Engineering [1].

Actuality and opportunity The doctoral thesis results from the European Union regulations on energy efficiency in transport (in the context of Directive 2012/27/EU [2]) as well as in the policies supporting sustainable mobility [3]. From a scientific point of view, the topicality of the doctoral research is the modernity of the advanced exergetic models and the opportunity of the proposed energy efficiency techniques is the progress in the engineering of motors and energy recovery systems, as well as in the field of related engine instrumentation – sensors, controllers, and advanced testing stands.

Theme The doctoral thesis is in accordance with the Operational Plan for Institutional Development of Transilvania University of Brașov, [4], especially with the operating strategy of the ICDT (Research and Development Institute of Transilvania University) on whose high-performance infrastructure most of the applied research presented in the paper was based. The theme of the thesis is centred on the attributes *energetic* and *exergetic* used in the context of engine analysis or heat balance; according to the argumentation in Chapter 2, the first term will refer to the energy itself, and the second, to the energy recoverable from real, irreversible processes.

The need for this work is motivated by the requirement to increase the effective efficiencies of engines which means a better use of the energy stored in the fuel; this also reduces the rate of depletion of the world's fossil fuel reserves. The relationship between the composition of the fuel and the CO_2 emission of the engine is one of proportionality, based on the mass carbon content of the fuel; CO_2 is the main product of the combustion of fossil fuels that contributes to the greenhouse effect.

Alignment with international policies on energy efficiency and pollutant emissions. The European Green Deal proposes plans for measures aimed at achieving climate neutrality in the European Union by 2050; quantitatively, it aims to reduce greenhouse gas emissions by at least 55% compared to 1990 levels by 2030. The estimates of greenhouse gas emissions from heavy-duty vehicles are 25-40% of those allocated to road transport in the European Union, being estimated to be over 6% of total greenhouse gas emissions. The transport strategy to reduce emissions includes drastically reducing emissions by 90% by 2050; The field of road transport is proving to be more easily adaptable to the requirement to reduce greenhouse gas emissions than air or maritime transport, which is why the pressure on the effective efficiency of heavy-duty vehicle engines requires energy recovery from the other hot sources of the engines.

Energy efficiency is the most cost-effective way to reduce emissions and the environmental impact of internal combustion engines, both in industry and transport. "Europe cannot afford to waste energy" says Directive (EU) 2023/1791 on energy efficiency [5], so the future objectives are to reduce energy consumption by 11.7% by 2030, compared to the situation in 2020.

At the same time, the transition to zero carbon emissions has the goal of 2050. For this, increased attention is needed on the transport sector, with the obligation to reduce final energy consumption, but also on the industrial sector, the energy supply and storage sector, as well as district heating and cooling. About 40% of the total energy destined for road transport is used for urban mobility, both for passenger transport and freight transport. Figure 1.1 shows the impact of European directives on CO_2 emissions from light-duty vehicles over two decades since 2000, for the European Union, Iceland, Norway and the United Kingdom. There is a clear downward trend in emissions as the European directives are adopted, the first being in 2009, and the objectives until 2030 are relatively aggressive with obvious decreasing thresholds (from 130g/km in 2015 to a target of 59.4g/km in 2030) [6].

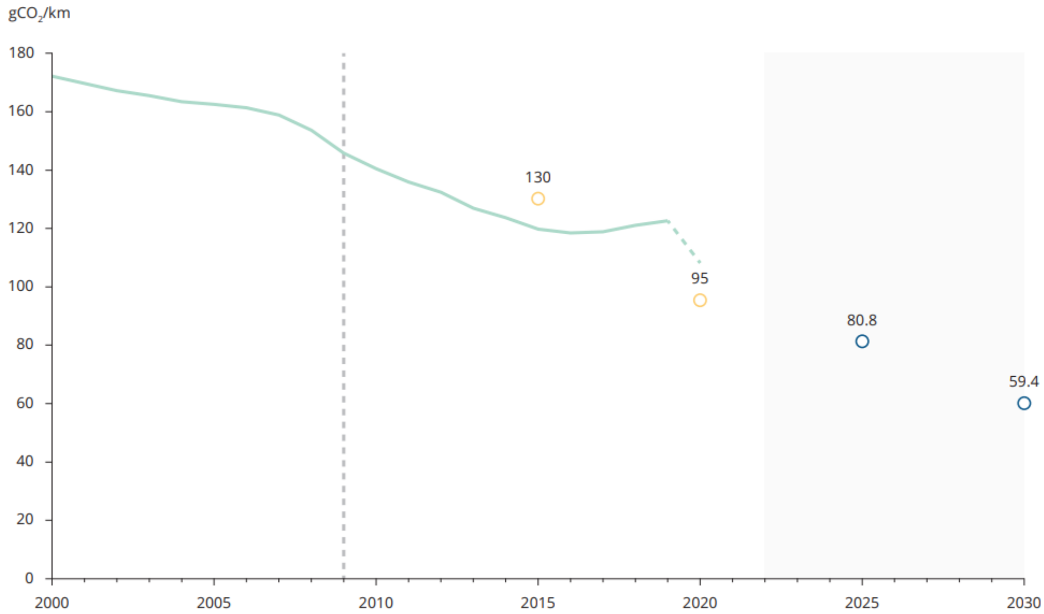

Fig. 1.1 Average CO2 emissions per kilometre for new light-duty vehicles [6]

The current trends in the development of internal combustion engines - especially the directions of energy optimization - have marked the identification of strategies that increase effective efficiency, simultaneously with the reduction of polluting emissions; among them are: the implementation of new combustion modes involving the stratification of the air-fuel mixture, the improvement of the supercharging process, the recirculation of exhaust gases (EGR – Exhaust Gas Recirculation) perfecting the scavenging process, multiple injections, increased injection pressure, simultaneous injection of two types of fuel, variable valve timing through control of intake and exhaust valve opening, reduction of friction losses, as well as the electrification of engine systems including thermal and energy management.

Traditional turbocharged Diesel engines have effective efficiencies of around 44% according to [8]. In a conventional Diesel engine with an effective efficiency of 43%, the fuel energy distribution is 28% through the exhaust system (including 4% pumping losses), 28% through the cooling media (coolant, lubricant) and 1% for other indeterminate heat losses [7]; the current data in the literature are convergent, the average values of the percentages in the engine energy balance being illustrated in Figure 1.2.

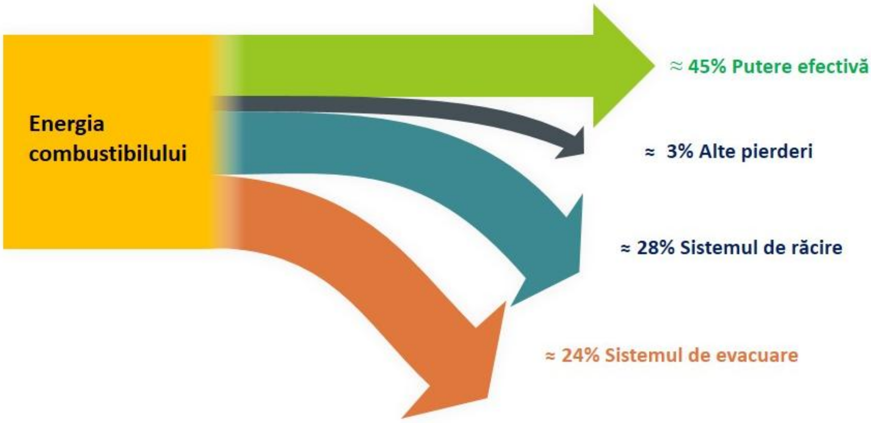

Fig. 1.2 Averaged energy balance of the internal combustion engine (Adaptation after [8])

In this thesis, the laws of thermodynamics, which describe the qualities of energy to be conserved and transformed, will be relevant. The first law of thermodynamics is called the law of energy conservation. The second law of thermodynamics is widely used in the design of thermal systems to establish the maximum possible efficiency of these systems; it refers to the quality of energy, and the introduction of the term "exergy" represents a way to quantify this concept.

Figure 1.3 shows the distribution of energy and exergy according to the research of a conventional Diesel engine [9]. In this case, the heat transfer takes place towards the walls of the combustion chamber, the piston and the lubricating agent, and in terms of the amount of heat released to the environment, it is largely lost through the exhaust gases, and can no longer be used to produce mechanical work. From an exergetic point of view, part of this heat is represented by the irreversibility of the fuel combustion process, while the rest is represented by the irreversibility of the heat discharged to the environment.

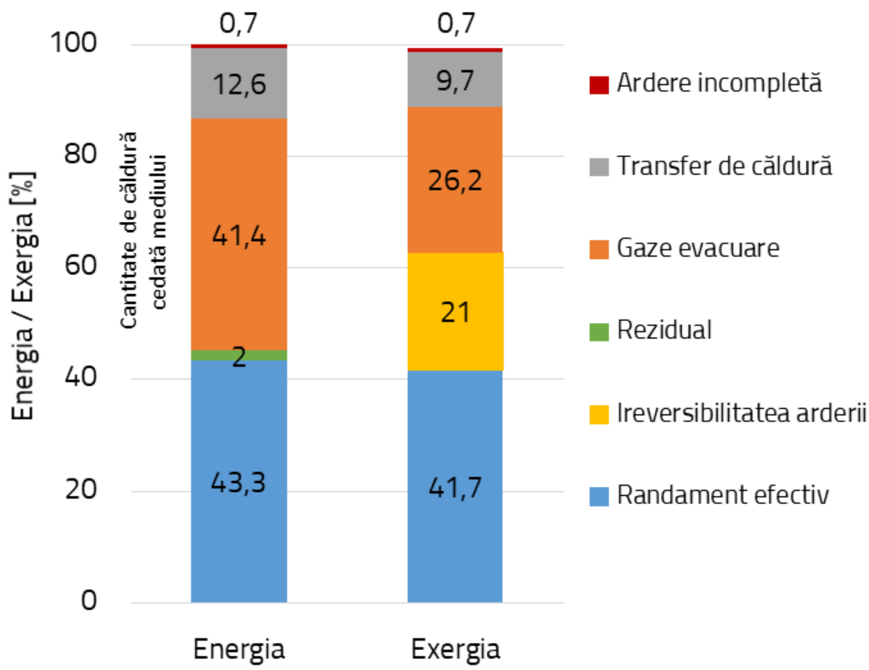

Fig. 1.3 Distribution of energy and exergy in the internal combustion engine (adaptation after [9, 11])

Current literature presents several technologies for the energy optimisation of internal combustion engines. These include: **thermal insulation techniques** for the combustion chamber (LHR – Low Heat Rejection) [10], which involves using thermally insulating materials such as ceramics to achieve a thermodynamic cycle as close as possible to adiabatic; **variable valve timing mechanisms**, which can increase the effective efficiency of the engine at high speeds, with potential fuel consumption reductions of up to 5.4% [12] and an improvement in effective efficiency of 1.5%; the use of **Homogeneous Charge Compression Ignition (HCCI)** engines, which can lead to significant fuel consumption reductions of up to 25% [14]; the use of **Reactivity-Controlled Compression Ignition (RCCI)** technology, managing to produce an indicated efficiency of up to 56% [17], **improving the injection process** [20,21] with an effective efficiency of 49%, and **using heat recovery systems** that add 4-7% to the effective efficiency.

Doctoral research directions are **theoretical** and **applied.**

- the theoretical directions aimed at fundamental research and energy-exergy modelling of internal combustion engines, as well as the development of computational models to support the in-depth evaluation of energy and exergy terms.
- At the experimental level, the research directions aim at the instrumental integration of the engine testing configurations, oriented on the specific measurements indicated in the performance standards and in the specific operating cycles.

The objectives corresponding to these research directions are:

1.1. Fundamental research of the energy balance as a mathematical application of the analysis of internal combustion engines based on the principles of thermodynamics, with a view to fuel economy and energy recovery.

1.2. Analysis of internal combustion engines using the second law of thermodynamics, for various types of air intake: naturally aspirated, turbocharged, with and without intercooling.

1.3. Study of the influence of some constructive and functional parameters of the engines, such as load, speed, compression ratio, excess air coefficient and fuel properties for the purpose of evaluating the terms in the energy and exergy balance.

1.4. Modelling of exergy from an entropic perspective considering the irreversibility of real processes – complementing the energy balance with an exergy balance, as well as highlighting exergetic losses through specific Sankey diagrams.

1.5. Improving energy and exergy models - completing the extended exergy balance by refining and adding new terms.

2.1. Study of the current state of the stands/test benches for all categories of internal combustion engines, in terms of ignition systems, nature of fuels, their destination, as well as specific measuring equipment (engine torque, fuel consumption, air flow, temperature, pressure, speed), with sub-system of sensors and dedicated probes.

2.2. Integration into the ICDT L9 engine laboratory of the experimental engine equipped according to the requirements of the test program.

2.3. Application of the exergy model to Diesel engines - naturally aspirated, turbocharged with and without intercooling, critical evaluation of the initial model manifested in the identification and study of the influence of certain parameters on the terms in the balance.

2.4. Evaluation of the energy recovery potential from the thermal sources of the engine in different operating regimes and cycles; prefiguration of the multi-criteria optimisation and control function of engine parameters with heat recovery systems (Waste Heat Recovery Systems) in the management of modern engines.

In the context of this doctoral thesis, the iterative approach involved the development of energy models and then their experimental testing and validation. Such a cycle allows the identification of possible model deficiencies, allowing progressive improvement, according to **the Agile method.**

In terms of interdisciplinarity, the method uses a close interaction between design-development, implementation, testing and corrective measures, ensuring that problems are solved in the early stages (modelling) and appropriate adjustments can be made to prevent the effects of these problems from propagating. One of the key principles of the method is flexibility. In the context of this doctoral thesis, adaptability to changes in scope, unforeseen requirements or challenges – for example, infrastructure issues or even pandemic restrictions – was important.

Research resources:

- Documentary Database – publications regarding the current state of research in the field, mainly "review" and research articles;
- The Experimental Database – provided mainly by ICDT, but also by collaborations with Brașov's industry, especially with the "Avantec" company, which also took over the research base and archive of INAR Brașov – the Research Institute of Road Vehicles in Romania.

The organization of the thesis corresponds to the research areas presented (Figure 1.4):

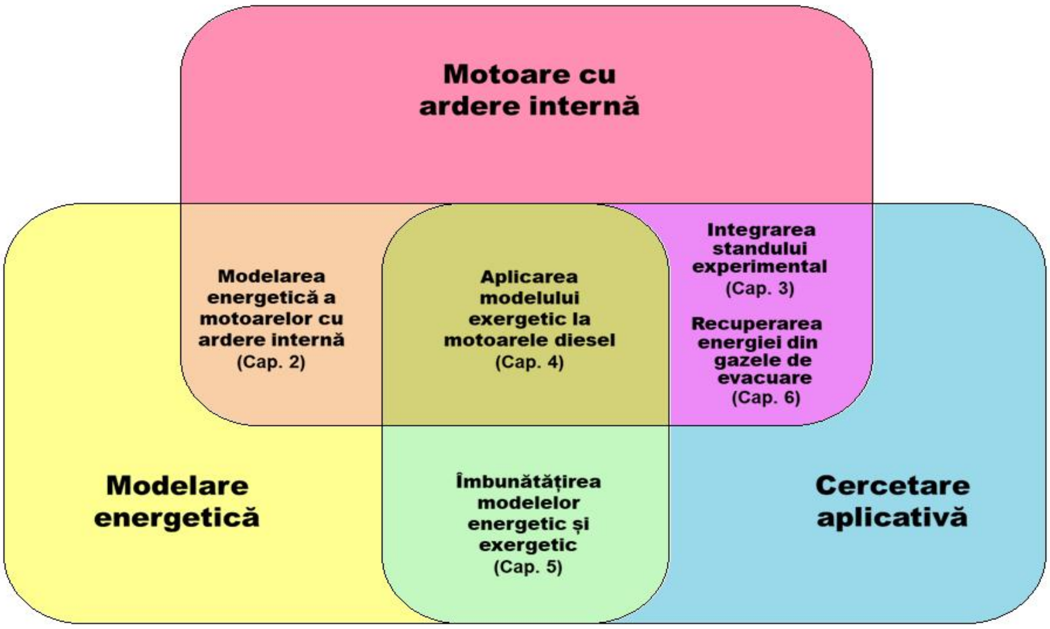

Fig. 1.4 Areas of doctoral research

2. ENERGY MODELING OF INTERNAL COMBUSTION ENGINES

2.1 Energy model

Energy balance theory

The energy model represents the mathematical form of the energy balance, being in fact the analysis applied to the engine of the first principle of thermodynamics. The purpose of knowing the energy balance terms is to increase the effective power, and implicitly the effective efficiency, and to diminish the collateral terms. The engine is considered to be an open thermodynamic system, surrounded by an imaginary contour, for which the input and output energies are analysed, relative to the unit of time. The main terms of the balance are the effective power P_e, the heat flow discharged through the cooling systems (coolant, lubricant) $\dot{Q_{rac}}$, the heat flow from the exhaust system $\dot{Q_{ga}}$; to these three terms is added the residual term $\dot{Q_{rez}}$, which closes the balance sheet and which includes other terms that were not included in the first three, as well as measurement errors. There are other more detailed organizations of the energy balance that include either in the residual term, or as a distinct term, the contribution of heat transfer by convection-radiation from the engine surface to the environment, incomplete combustion, gas exchange from the intake-exhaust, gas leaks in the crankcase or mechanical losses. Classifying these balance terms and fitting them into the estimated percentages is actually more difficult because these terms are not isolated, there are heat losses that are redistributed; e.g. references [31, 32] show that part of the residual term that includes the heat released by the engine surface actually comes from the heat produced by friction and partly taken up by the cooling system.

The assessment of energy balance terms is based on the following equations:

$$\dot{Q_{cb}} = P_e + \dot{Q_{ga}} + \dot{Q_{rac}} + \dot{Q_{rez}}$$

$$\dot{Q_{cb}} = \dot{m_{cb}} H_i$$

$$P_e = 2\pi n M_e$$

$$\dot{Q_{ga}} = \dot{m_{ga}} c_{pga} T_{ga} - \dot{m}_a c_{pa} T_a - \dot{m}_f c_{pcb} T_{cb}$$

in which the mass balance results: $\dot{m_{ga}} = \dot{m}_a + \dot{m_{cb}} - \dot{m_{bb}}$

$$\dot{Q_{rac}} = \dot{m_{rac}} c_{prac} \left(T_{rac,e} - T_{rac,i}\right)$$

$$\dot{Q_{rez}} = \dot{Q_{cb}} - (P_e + \dot{Q_{ga}} + \dot{Q_{rac}})$$

where $\dot{m_{cb}}$- fuel flow, H_i - lower heating value of the fuel, n - engine speed, M_e- engine effective torque, $\dot{m_{ga}}$- exhaust gas flow, $\dot{m}_a$ - air flow rate, $\dot{m_{bb}}$ - the mass flow of crankcase gases (blow-by). It can be seen that the contribution of the sensible heat of the fuel in the energy balance equation has been introduced in the formula, as recommended by several references, for better accuracy [33, 34]. The customization of these formulas will be carried out for the case of experimental determinations in Chapters 5 and 6.

Evaluation of energy terms

Classical literature [31, 35] specify the percentages of these balance sheet terms for engines running on conventional fuels (Table 2.1):

Tab. 2.1 Energy share of the main energy balance terms (adaptation after [31, 35])

Engine type	Term [%]			
	effective	cooling	exhaust	residual
Compression-ignition engines	33-38	16-35	23-37	2-6
Spark-ignition engines	25-28	17-26	36-45	3-10

The percentages of the energy terms reflected the technological progress, but also the specifics of each use. For example, the reference [33] indicates the effect of increasing efficiency by supercharging, but also the distribution of energies released through different cooling media, according to the data presented in Table 2.2.

Tab. 2.2 Comparative expression of the energy balance terms (adaptation ref. [33])

<table>
<tr><td rowspan="2">Engine type</td><td colspan="6">Term [%]</td></tr>
<tr><td>effective</td><td colspan="3">cooling</td><td>exhaust</td><td>residual</td></tr>
<tr><td>Naturally aspirated diesel engine (2.5 l car)</td><td>33</td><td colspan="3">25</td><td>34</td><td>8</td></tr>
<tr><td rowspan="3">Turbocharged diesel engine (250 kW)</td><td rowspan="2">effective</td><td colspan="3">cooling</td><td rowspan="2">exhaust</td><td rowspan="2">Radiation convection</td></tr>
<tr><td>liquid</td><td>oil</td><td>air-supercharging</td></tr>
<tr><td>38</td><td>25</td><td>3</td><td>10</td><td>20</td><td>4</td></tr>
</table>

The current literature records significant increases in the percentages of effective efficiency compared to those in the tables above; for diesel engines currently used in heavy-duty vehicles, this percentage is in the range of 38-47%.

2.2 Exergetic model

Theoretical premises

Classical thermodynamics examines thermodynamic processes as sequences of intermediate equilibrium states that thermodynamic systems traverse at infinitely slow speeds, in a reversible way. Unlike these ideal reversible processes, real processes are irreversible and do not take place under conditions of thermodynamic equilibrium. That is why technical thermodynamics, of the processes in thermal machines, had to adapt the classical theory to the obvious reality; For example, it has been found that the transformation of heat into mechanical work is not total, which has led to the idea that energies are qualitatively different in terms of their ability to transform from one form to another.

Thus, the energies were classified into:

- ordered energies, which can be totally transformed into any other form of energy (mechanical-kinetic and potential energy, electrical energy, mechanical work) without depending on the conditions of the environment;

- unordered energies, which can be partially transformed into ordered energies (heat, internal energy, enthalpy) and which depend on the state conditions of the thermal processes and the conditions of the environment.

The attribute of ordered/unordered refers to the degree of arrangement and mobility of some particles in the thermodynamic system; For example, a crystalline solid body has its atoms positioned in a well-defined, very ordered network, while the molecules of a gas move freely in all directions, their positions and speeds being unknown, so their arrangement is chaotic and unpredictable. This property is closely related to the concept of entropy, which is a measure of the degree of disorder in a system. Quantitatively, both types of energies, ordered or unordered, respect the principle of energy conservation. The closer a thermal process comes to the condition of total reversibility, the more the partial transformation of unordered energy into ordered energy tends towards a maximum value. According to the second law of thermodynamics, the entropy of an adiabatic isolated thermodynamic system is constant when the internal processes are reversible; In case of internal irreversibility, the entropy of the system increases. In the case of a thermal machine that exchanges mass and heat with the environment, another component of entropy appears, as a result of the exchange of heat and mass with the outside, which generates external irreversibility.

The increase in entropy as a result of irreversibility leads to a decrease in the ability to transform the energy of a thermodynamic system into mechanical work. The assessment of this capacity was proposed by the physicist Z. Rant in 1956 who gave it the name of exergy. The definition of this quantity is as follows: The exergy of a thermodynamic system in a given state is the maximum amount of ordered energy that can be released by the reversible transition of the system from the given state to equilibrium with the surroundings [36]. As a result of this definition, the part of energy that cannot be transformed into mechanical work was called anergy.

By 1970, about 50 articles on exergy had been published in scientific journals or presented at conferences. In 2004, this number was well over 500. All major journals dedicated to the study of energy publish, on average, 1 or 2 articles on concepts related to exergy in each issue. Since 2000 there has been the "International Journal of Exergy", which has published over 1000 articles to date. According to Clarivate Analytics, in 2023, approximately 3095 articles about exergy were published on the Web of Science platform, of which 57 were in the field of internal combustion engine exergy. About 2683 have been published by the end of 2024, and 40 of them cover the keywords "internal combustion engine".

Unlike energy, which is conserved, exergy can be destroyed in irreversible processes, turning into unusable energy, into anergy. Irreversibility can be internal or external, as a result of processes that take place either inside the thermodynamic system or in its interaction with the environment. The impact of irreversible thermodynamic processes on the energy conversion capacity of a thermodynamic system into mechanical work is summarized in the Guouy-Stodola theorem, which states that when 1 kg of thermal agent passes through the system, the loss caused by the internal and external irreversibility of the processes π_{ir} is equal to the loss of technical mechanical work produced by internal and external irreversibility, Δl_t.

$$\pi_{ir} = \Delta l_t = T_0 \cdot \Delta S_{ir} \; [\frac{J}{kg\ agent}]$$

In a thermodynamic process, exergy can only be conserved in a reversible process. The loss caused by the internal and external irreversibility of the processes, π_{ir} , is dependent on the ambient temperature, TO , and on the variation of the entropy of the thermal agent-ambient environment thermodynamic system, ΔS_{ir}, as a result of the irreversibility, both internal and external, of the energy processes in which the thermal agent interacts with the ambient environment. Given the fact that the irreversible evolution of real processes is correlated with the increase of entropy, it is imperative to introduce the concept of entropy production into the theory of these processes. Through this approach, it was possible to elaborate an entropic balance equation similar to the balance equations of conserved quantities, such as energy and mass.

This balance, the foundation of the dynamics of irreversible processes, shows that the variation in the entropy of a thermodynamic system is the result of the production of entropy caused by the internal irreversibility of the processes that take place under conditions of imbalance in that system, as well as of the variation in entropy caused by the exchange of heat and mass with the external environment [40, 41]. The main irreversible processes in the field of technical thermodynamics are fuel combustion, heat transfer at finite temperature differences, real compression and expansion processes, throttling (reducing the pressure of the working fluid when passing through very small sections), mixing fluids, and friction.

Analysis of internal combustion engines using the second law of thermodynamics

The application of the second law of thermodynamics to internal combustion engines is based on a mathematical model of the various processes inside the cylinder and engine subsystems, formulated in the reference [41]. For the most general case of supercharged and intermediately cooled heat engines, the main irreversibility comes from:

- irreversible process of fuel combustion;
- irreversible processes of air compression in the compressor and expansion in the turbine;
- irreversible process of exhaust under pressure and temperature differences;
- irreversible throttling processes of the working fluid as it passes through the engine's ducts, during intake into the compressor, passage through the intercooler and through the turbine;
- irreversible intake-scavenging process;
- irreversible heat transfer processes between the exhaust gases and the ambient environment at the turbine outlet, between the compressed air and the surroundings at the cooler outlet, between the gases exhausted from the engine and the scavenging air;
- irreversible mechanical friction processes inside the engine.

The application of the second law of thermodynamics to internal combustion engines is based on mathematical models of the internal processes. A simplified model, called "single-zone," considers the working fluid homogeneous with the properties of air. This hypothesis simplifies the calculation and provides reasonable accuracy. Non-homogeneous models consider distinct zones for the air-fuel mixture and exhaust gases. The engine is an open system with energy and mass exchanges with the environment. The energy released by combustion is obtained by applying the first law of thermodynamics.

In order to simplify the calculation model, the following assumptions are also necessary:

- the working fluid is considered an ideal gas;
- pressure and temperature are homogeneous within the thermodynamic system;
- the properties of the gas are considered invariable with temperature and pressure;
- heat of the combustion gases is uniformly distributed in the combustion chamber and cylinder;
- blow-by gases are neglected, applying the principle of mass conservation;
- enthalpy of the fuel in the injection process is neglected;
- there is no heat transfer between the engine and the environment in the intake, compression, expansion and exhaust processes, but there is heat transfer between the exhaust gases and the environment;

Figure 2.1, using the p-V diagram, shows the simplified model of the thermodynamic cycle used for the analysis of a naturally aspirated, 4-stroke mixed-combustion engine. The parameters associated with the specific processes and quantities are presented in Tables 2.3 and 2.4.

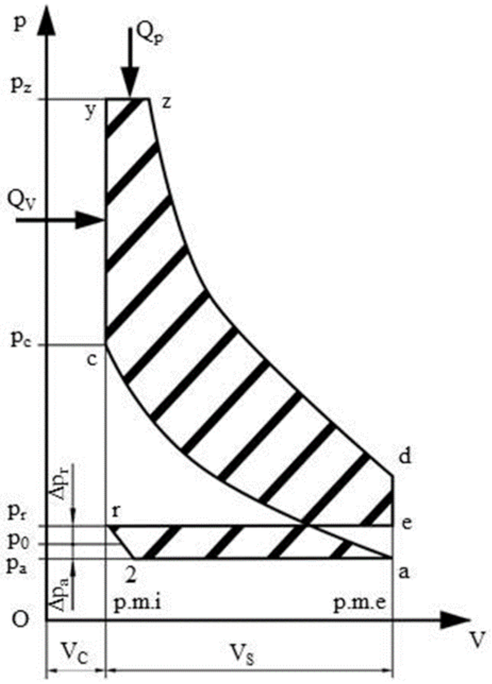

Fig. 2.1 The cycle of the isochoric-isobaric combustion engine represented in p-V (Adapt. after [41])

Tab. 2.3 Thermodynamic processes of the thermodynamic cycle

Process	Name	Specific parameters
2-a	Isobaric Intake Process	$\Psi a=\Delta p_a/p_0$
a-c	Reversible adiabatic compression process	ε
c-y	Isochoric combustion process	λ
y-z	Isobaric combustion process	ρ
z-d	Reversible adiabatic expansion process	(λ / ρ)
d-e	Isochoric Evacuation Process	p_d, p_r
e-r	Isobaric evacuation process	$\Psi_e= \Delta p_r / p_r= (p_r-p_0)/p_r$
r-2	Reversible adiabatic expansion process	T_r, T_a

Tab. 2.4 Specific quantities of the thermodynamic cycle

R	Ideal gas constant [J/kgK]
c_p, c_v	Specific heat of gas at constant pressure/volume
H_i	Lower heating value of fuel [MJ/kg]
ε	Compression ratio
L_0	Stoichiometric value of the amount of air required to burn 1kg of fuel [kg air/kg fuel]
$\Psi_a=\Delta p_a/p_0$	Relative pressure loss in the intake process
$\Psi e=\Delta p_r/p_r$	Relative pressure loss in the exhaust process

For each stage of this process, the thermodynamic parameters were determined and evaluated according to the following steps [41]:

Inlet pressure:

$$p_a = p_2 = (1-\psi_a)\cdot p_0$$

Inlet temperature:

$$T_a = T_2 = T_0 \cdot \frac{1}{1-(1-\frac{T_0}{T_r})\cdot\frac{1}{\varepsilon}}$$

Volumetric efficiency:

$$\eta_V = (1-\psi_a)\cdot\frac{\varepsilon}{\varepsilon-1}\cdot(1-\frac{1}{\varepsilon}\cdot\frac{1}{\psi^{\frac{1}{k}}})$$

The compression increases the pressure at the p_c value and the temperature T_c:

$$p_c = p_a \cdot \varepsilon^k$$
$$T_c = T_a \cdot \varepsilon^{k-1}$$

The increase in pressure during the isochoric combustion process is:

$$p_y = \lambda p_c$$

with the parameter λ that can be calculated by knowing the maximum pressure in the engine cylinder.

The temperature increase in the isochoric process is:

$$T_y = \lambda T_c$$

To determine the parameter ρ that defines the y-z process, the energy balance for the combustion process is applied. The total heat of the fuel Q_{ar} is made up of the heat released during the isochoric process Q_v and the heat released during the isobaric process Q_p, where m_c and m_y represent the mass corresponding to the c and y points in Fig.2.1.

$$Q_{ar} = Q_v + Q_p = m_c c_v(T_y - T_c) + m_y c_p(T_z - T_y)$$
$$Q_{ar} = m_c R T_c \cdot \frac{\lambda - 1 + k\lambda(\rho-1)}{k-1} = m_{cb} H_i$$

The mass of thermal agent m_{ag} differs depending on the type of engine, as follows:

- for compression-ignition (MAC) engines, it is the sum of the mass of fuel injected into the cylinder m_{cb}, *the* mass of air introduced into the engine m_a and the mass of waste gases m_r.

$$m_{ag} = m_{cb} + m_a + m_r = [1 + (1 + \gamma_r)\alpha L_0]m_{cb}$$

- for spark-ignition engines (MAS) represents the sum of the mass of the air-fuel mixture admitted in the m_{ac} *engine* and the mass of the residual gases remaining in the cylinder m_r .

$$m_{ag} = m_{ac} + m_r = (1 + \gamma_r)(1 + \alpha L_0)m_{cb}$$

Calculating the ratio of Q_{ar} to the dislocated volume V_s , we get the quantity q_{ar} that is called the combustion heat relative to the unit of displacement and with which ρ can be determined:

$$q_{ar} = \frac{Q_{ar}}{V_s} = \frac{m_{cb}H_i}{V_s} = p_c \cdot \frac{\lambda - 1 + k\lambda(\rho - 1)}{(k - 1)(\varepsilon - 1)}$$

$$\rho = 1 + \frac{k - 1}{k}\left(\frac{\varepsilon - 1}{p_z}q_{ar} - \frac{1}{k - 1} \cdot \frac{\lambda - 1}{\lambda}\right)$$

The maximum temperature of the cycle is at the z-point:

$$T_z = \rho T_y$$

Average T_{mar} combustion temperature :

$$T_{mar} = T_c \cdot \frac{(\lambda - 1) + k\lambda(\rho - 1)}{\ln(\lambda \cdot \rho^k)}$$

Temperature and pressure at the end of the expansion stroke:

$$T_d = \frac{T_z}{\left(\frac{\varepsilon}{\rho}\right)^{k-1}};\ p_d = \frac{p_z}{\left(\frac{\varepsilon}{\rho}\right)^{k}}$$

Residual exhaust gas coefficient:

$$\gamma_r = \frac{1}{\rho\varepsilon\lambda^{\frac{1}{k}} - 1}$$

The exhaust gas temperature T_r is determined using the hypothesis of an adiabatic process with constant k, during the free exhaust of combustion gases. During scavenging, an isobaric process takes place in which fresh gases are mixed with the burnt gases remaining in the engine cylinder, preserving the enthalpy of the gases.

$$T_r = T_d \cdot \left(\frac{p_r}{p_d}\right)^{\frac{k-1}{k}}$$

In order to identify the balance equation of losses generated by irreversibility, it is necessary to use the energy and entropic balance equations integrated between the inlet and outlet sections of the engine:

$$\sum Q = I_2 - I_r + \sum L_t$$

$$S_2 - S_r = \sum \Delta S_Q + \sum \Delta S_{irin}$$

In the above equations $I_2 - I_r$ represents the increase in the enthalpy of the agent during the heat exchange ΣQ and the mechanical work performed ΣL_t , S_2 - S_r represents the increase in the entropy of the agent during the heat exchange with the ambient environment $\Sigma\Delta S_Q$ and the internal irreversibility of the working processes $\Sigma\Delta S_{irin}$.

It is obtained:

$$\sum E_Q = \Delta E + L + \sum \Pi_{\mathrm{irin}},$$

which represents the balance equation for losses caused by irreversibility. ΣE_Q is the total exergy of the heat absorbed by the working fluid during intake and the combustion process.

ΔE represents the loss of exergy through the heat released by the exhaust gases to the environment in the isobaric cooling process from temperature T_r to T_0 :

$$\Delta E = \Pi_{Qe} = |Q_e| - T_0 \cdot |\Delta S_{Qe}|,$$

Q_e is the heat available in the exhaust gases, and ΔS_{Qe} is the change in entropy of the exhaust gases.

The term $\Sigma\Pi_{irin}$ describes the sum of losses caused by the irreversibility of inlet and outlet processes, such as throttling or finite pressure and temperature differences.

The balance equation for losses caused by the irreversibility of the working processes of the internal combustion engine can be written as follows:

$$\begin{cases} Q_{ar} = L + \Pi_{Qea} + \Pi_{irar} + \Pi_{ire} + \Pi_{la} + \Pi_{le} \\ Q_{ar} = L + \Pi_{Qer} + \Pi_{ir\Delta Ta} + \Pi_{irar} + \Pi_{ire} + \Pi_{la} + \Pi_{le} \end{cases},$$

and in a restrained form:

$$Q_{ar} = L + \sum_{j=1}^{n} \Pi_{irj}$$

Part of the heat produced by fuel combustion is transformed into mechanical work, while the rest are the losses caused by the internal and external irreversibility of the cycle. Exergy losses can be expressed in three ways: in energy units, Π_x [MJ], as energy reported per unit mass of fuel π_x [MJ/kg], or as energy reported to the energy released by fuel combustion, expressed as a percentage $\bar{\pi}_x$ (%):

$$\pi_x = \frac{\Pi_x}{m_{cb}};$$

$$\bar{\pi}_x = \frac{\pi_x}{H_i}.100\ (\%)$$

The exergy losses generated by irreversibility for the naturally aspirated engine are as follows:

The loss caused by combustion irreversibility:

$$\Pi_{irar} = T_0 \cdot \Delta S_{Qar} = T_0\left(\Delta S_{Qv} + \Delta S_{Qp}\right) = T_0 m_{cb}(c_v \ln\frac{T_y}{T_c} + c_p \ln\frac{T_z}{T_y}) = m_{cb} R T_0 \cdot \frac{1}{k-1} \cdot ln\lambda\rho^k$$

The loss caused by the irreversibility of combustion in relation to the fuel unit results:

$$\Pi_{irar} = \frac{(1+\gamma_r)(1+\alpha L_0)}{k-1} m_{cb} R T_0 \ln\lambda, \text{ for MAS;}$$

$$\Pi_{irar} = \frac{1+(1+\gamma_r)\alpha L_0}{k-1} m_{cb} R T_0 \ln\lambda\rho^k, \text{ for MAC;}$$

Loss caused by the irreversibility of the exhaust process:

$$\Pi_{ire} = T_0 \Delta S_{ire} = \frac{k}{k-1} \cdot (1+\alpha L_0) m_{cb} R T_0 \ln\frac{T_e}{T_r};$$

Loss caused by the irreversibility of throttling during intake:

$$\Pi_{la} = T_0 \Delta S_{la} = (1+\alpha L_0) m_{cb} R T_0 \ln\frac{1}{1-\psi_a};$$

Loss caused by the irreversibility of the throttling during exhaust:

$$\Pi_{le} = T_0 \Delta S_{le} = (1+\alpha L_0) m_{cb} R T_0 \ln \frac{1}{1-\psi_e};$$

Exergy loss of heat to the environment:

$$\Pi_{Qea} = |Q_{ea}| - T_0 |\Delta S_{Qea}| = \frac{k}{k-1} \cdot (1+\alpha L_0) m_{cb} R T_0 (\frac{T_e}{T_0} - \frac{T_a}{T_0} - \ln \frac{T_e}{T_a})$$

In the case of turbocharged and intercooled engines, additional factors are present compared to the naturally aspirated engine, which determine the irreversibility of the processes [41]:

- irreversibility of air compression in the compressor and expansion in the turbine;
- irreversibility of heat transfer at finite temperature variation in the intercooler;
- irreversibility of throttling processes when passing through the compressor, heat transfer in the intercooler and exhaust gas exit from the turbine;

The parameters specific to thermodynamic processes are presented in Table 2.5.

Tab. 2.5 Thermodynamic processes [42]

	Process	Name	Specific parameters
Compressor	0-1	Air intake into the compressor at $p_1 < p_0$	$\Psi_1=(p_0-p_1)/p_0$
	1-s	Air compression, irreversible adiabatic	k, p_s, T_s
Intercooler	s-s'	Isobaric air cooling	$\tau = \Delta T_R / \Delta T_{Rmax}$
	s'-2	Isothermal air throttling in cooler at , Δp_2	$\Psi_2=(p_s-p_2)/p_s$
Engine	2-a'	Isobaric intake process	$\Psi_a=(p_2-p_a)/p_2$
	a'-a	Irreversible scavenging process	β
	a-c	Adiabatic compression process	ε
	c-y	Isochoric combustion process	λ
	y-z	Isobaric combustion process	ρ
	z-d	Adiabatic expansion process	(λ/ρ)
	d-e	Adiabatic free exhaust process	p_d, p_r
	e-t	Isobaric forced exhaust process	$\Psi_e=(p_r-p_t)/p_r$
Turbine	t-3	Irreversible adiabatic expansion process of exhaust gases	k
	3-e_T	Exhaust of gas with pressure drop to p_0	$\Psi_3=(p_3-p_0)/p_3$

Similar to the naturally aspirated engine, the thermodynamic parameters are determined: pressure at the compressor inlet (p_1), pressure at the cooler outlet (p_2), intake pressure (p_a), temperature at the compressor outlet (T_s), temperature at the cooler outlet (T_2), air density at the cooler outlet (ρ_2), air temperature at the engine inlet (T_a), temperature increase coefficient (φ_a). The following are calculated: pressure and temperature at the end of compression (p_c , T_c), pressure increase ratio in isochoric combustion (λ), volume increase ratio in isobaric combustion (ρ), total heat released in combustion (Q_{ar}), heat of combustion reported per unit cylinder volume (q_{ar}), maximum cycle temperature (T_z), temperature and pressure at the end of expansion (T_d , p_d), pressure of the exhaust gases (p_r). The following are evaluated: gas temperature in the exhaust manifold (T_e), exhaust gas concentration (γ_r), exhaust gas temperature (T_r), scavenging process temperature (T_b), scavenging factor (β), gas temperature before the turbine (T_t), exhaust gas temperature at the turbine outlet (T_3), and pressure at the turbine outlet (p_3).

Finally, the exergetic losses specific to the supercharged engine are calculated: combustion losses (π_{irar}), heat transfer in the cooler (π_{QR}), heat transfer between the exhaust gases and the environment (π_{QeT}), irreversibility of compression in the compressor (π_{irS}), irreversibility of expansion in the turbine (π_{irT}), irreversibility of scavenging during intake (π_{irba}), irreversibility of the exhaust process (π_{ire}), irreversibility of heat transfer between exhaust gases and scavenging air ($\pi_{\mathrm{ir\Delta T_{eb}}}$), compressor throttling (π_{laS}), intercooler thorttling (π_{lR}), engine intake throttling (π_{laM}), engine exhaust throttling (π_{leM}), and turbine outlet throttling (π_{leT}).

The numerical model evaluates the cycle indicated mean pressure (p_{mc}) and the engine cycle thermal efficiency (η_t). The cycle indicated mean pressure is equivalent to the engine indicated mean pressure (p_{mi}). The formulas for p_{mc} are valid for both engine types.

The thermal efficiency of the engine cycle (η_t) is the ratio of indicated work to the heat released by combustion, similar to the indicated efficiency (η_i). The difference between them appears in the heat term (released vs. available). The ratio of the two heat terms is the incomplete combustion efficiency, which in this model is considered equal to unity (total combustion). So. $\eta_t = \frac{p_{mc}}{q_{ar}} = \eta_i$.

Based on the quantities and equations presented above, a calculation program was built that allowed the determination of the pressures and temperatures in the cycle, the indicated efficiency, the indicated mean pressure, as well as the exergetic losses related to the fuel energy, previously formulated π_i .

3. EXPERIMENTAL TEST BENCH INTEGRATION

This chapter describes the classic stands for testing internal combustion engines of the Research Institutes (INAR, INMT BRAȘOV), with a more detailed presentation of the modern stand used within the Research and Development Institute (ICDT) of the Transilvania University of Brașov. The research infrastructure provided by the ICDT includes the internal combustion engine test cell of the Research Center for High-Tech Automotive Products.

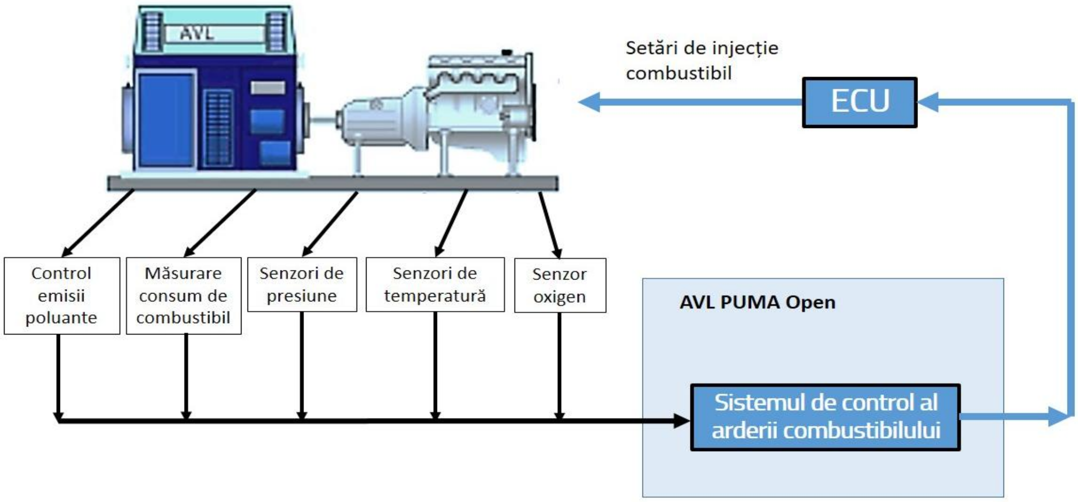

Fig. 3.1 AVL Test Stand Diagram [50]

The main components of the test stand are the electric dynamometer, the research engine, the unit for controlling the coolant (at the engine inlet and outlet) as well as the oil (in the sump or on the circuit), the unit for controlling the air intake into the engine and monitoring the exhaust gases. The general configuration of the setup (Figure 3.1) shows continuous closed-loop operation of the engine-dynamometer system. The test stand at the ICDT uses a test cell controlled by AVL Puma Open software as the main control panel and a modular AVL 5402 single-cylinder engine, reconfigurable for different ignition types and fuels. The stand includes a reversible electric dynamometer, coolant and oil temperature control systems, an air supply system (turbocharging simulator), and a data acquisition system (AVL Indicom). The experimental research is based on a stand with a modular AVL single-cylinder, four-stroke engine, reconfigurable as both a spark-ignition engine and a compression-ignition engine (AVL 5402), adapted for different fuel types (diesel, petrol, vegetable oil esters, oxygenated compounds), having the combustion chamber configuration in the piston crown in the omega shape illustrated in Fig. 3.14, and the technical data in Tab. 3.2. The injection pressure is provided by a Bosch Common Rail CP4.1 injection system.

The main specific quantities were the fuel mass flow rate measured with the AVL 735S, the air mass flow rate measured with the AVL Flowsonix flow meter, the parameters of the intake air supercharging control system type AVL Supercharger 515 Unit, the working fluid temperatures (Pt100, NiCr-Ni), the Optimus AT 420 infrared thermometer, the air velocity near the cylinder block with the portable hot-wire anemometer, AirFlow TA460, the cylinder pressure with the piezoelectric sensor GU21D and other pressures with the piezoresistive sensor APT100, the excess air coefficient with the Bosch LSU 4.9 lambda probe, the conditioning of the coolant and oil temperatures with the AVL 577 unit, and the crankcase gas flow rate with the AVL Blow-by 442S system.

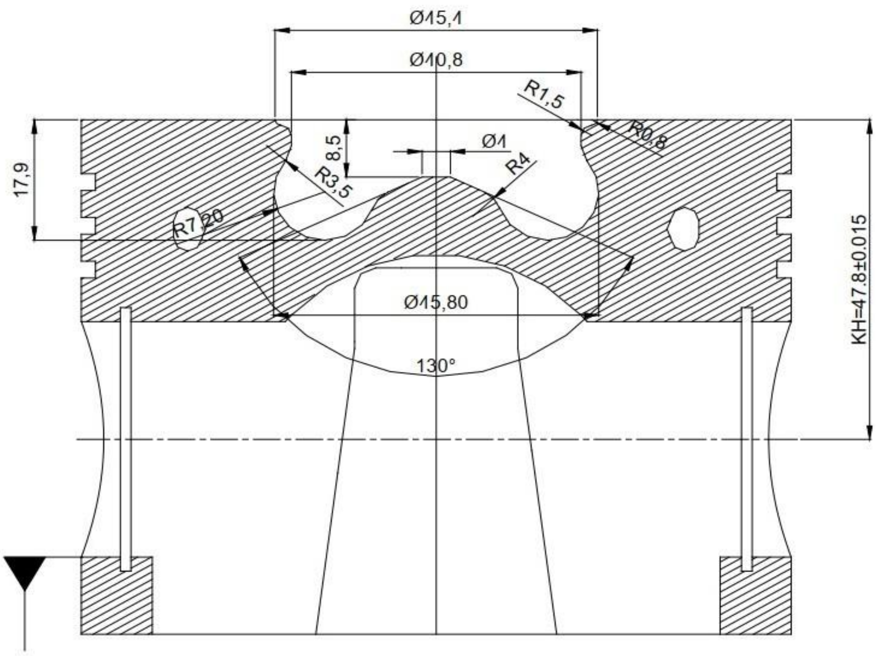

Fig. 3.1 Geometry of the combustion chamber of the AVL 5402 engine [51]

Tab. 3.1 Technical characteristics of the AVL 5402 engine [20, 52]

Parameter	Value	U.M.
Engine type	4-stroke, single-cylinder	-
Stroke/bore ratio	90 / 85	mm
Displacement	510,7	cm^3
Connecting rod length	138	Mm
Combustion type	Direct injection with one injector	-
Rated/maximum speed	4200/4500	rpm
Rated power range (naturally aspirated-supercharged)	6-16	kW
Maximum injection pressure	180	Mpa
Compression ratio	17,5:1	-
High-pressure system	Common rail CP 4.1 Bosch	-
Management system	AVL-RPEMS + ETK7 Bosch	-
Maximum cylinder pressure	17	Mpa
Diameter of valve seat	Intake 24,9 / Exhaust 24,5	mm

The test stand used AVL PUMA Open software for controlling speed, load, and intake air parameters, regulated by the AVL Supercharger unit. Data acquisition was performed with the AVL Indicom and AVL IndiModul 621 systems, monitoring cylinder pressure, injection performance, manifold pressures, and other operational parameters. Additionally, the temperatures of the engine's external surfaces and the air velocity in the cell were measured for the analysis of heat transfer by convection and radiation.

The main objective of the AVL engine test programme was to analyse the energy and exergy balance of the AVL 5402 single-cylinder compression-ignition engine under various operating regimes, varying speed, load, and intake air parameters. The engine was operated within a speed range limited to 1600-3600 rpm for comparability. The tests included naturally aspirated operation and simulated turbocharging at different pressures (100mbar, 250mbar, 400mbar), using diesel fuel according to standard EN 590 and SAE 15W40 oil. The engine load was varied between 25%, 50%, 75%, and 100%. Injection included a main injection and a pilot injection per cycle, controlled via the AVL Fire software module, without modifying specific injection parameters during the tests.

Figure 3.2 shows specific AVL Fire data such as speed, load, injection pressure, as well as injection timing and injected fuel quantity per stroke for the pilot and main injection.

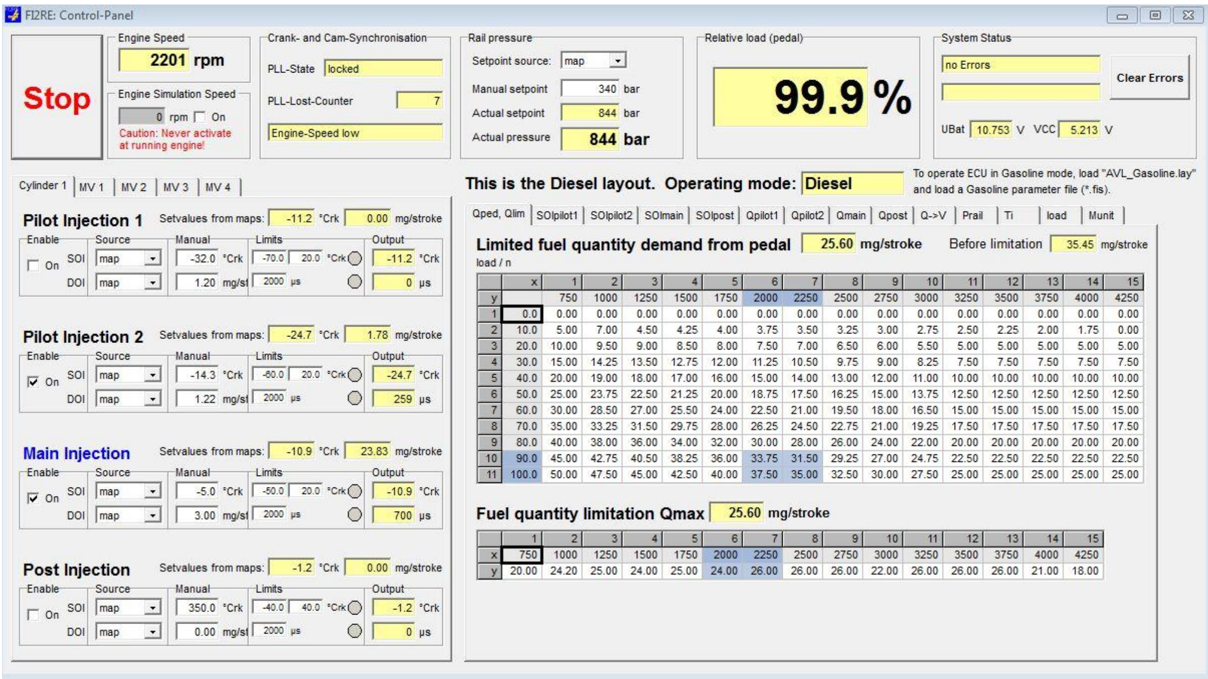

Fig. 3.2 Screenshot from AVL Fire software at rated speed and full load

Using the software integrated into the test stand, AVL PUMA Open (Figure 3.3), it was possible to set the speed and load as input data, controllable via the three-phase asynchronous electric motor. Furthermore, the PUMA programme is used to display in real time the hourly fuel consumption, exhaust gas pressure, oil pressure, atmospheric pressure, exhaust gas temperature, and excess air coefficient, offering the possibility to calculate derived specific quantities, such as effective power and engine torque.

Summarising what has been described in this chapter, a retrospective look at technical progress in recent decades indicates a considerable decrease in measurement errors, with two notable achievements: the PT100 reduces the error by 50 times, and the error for fuel consumption decreases by 8 times, according to Table 3.1.

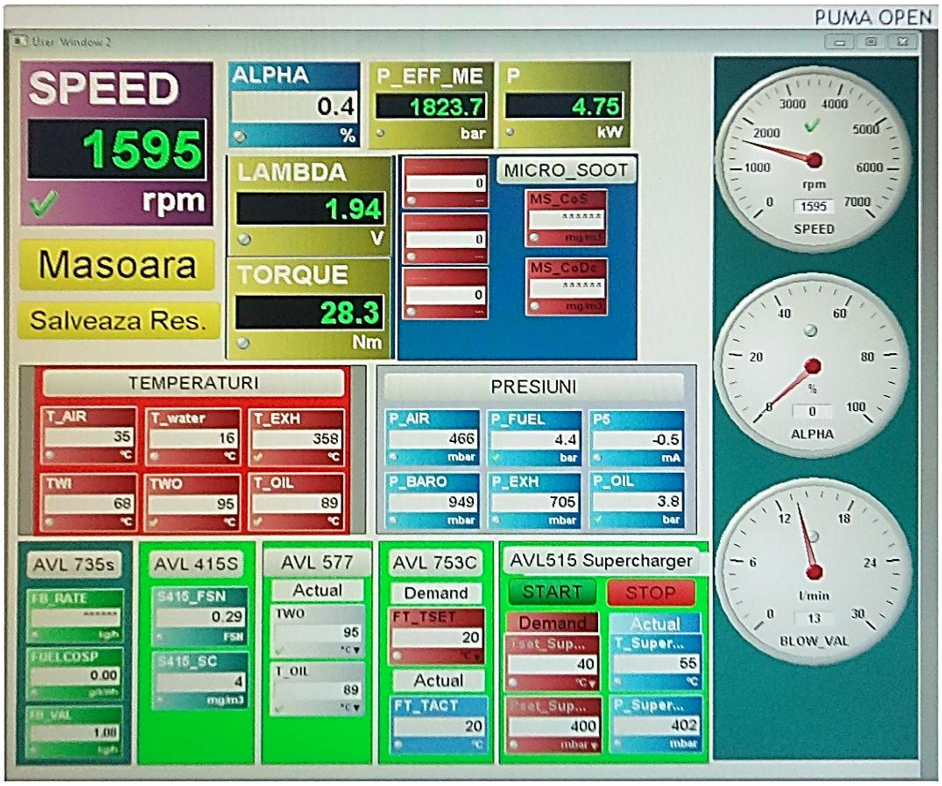

Fig. 3.3 PUMA Open AVL Interface

Tab. 3.1 Evolution of measurement errors

Parameter	Measurement errors [45]	Measurement errors [50]
Exhaust gas temperature, Pt100	±5K	±0,1K
Exhaust gas temperature, NiCr-Ni	±2K	±1,5K
Fuel consumption	1%	0,12%
Air consumption	±2%	<±1%

An advanced performance complex system (high capacity, resolution/accuracy, controllability) was integrated, offering capabilities to close automatic control loops in real time. The experimental research resulted in the integration of a significant test configuration (measurement - control via data acquisition - sensors) and actuators. The significance of this solution lies in opening up possibilities for monitoring and automatic control strategies that can be transposed into ECU (Electronic Control Unit) implementations. This modern approach combines Instrumental Informatics with Mixed Reality, placing these contributions in the category of advanced engineering development techniques (mechanical, robotics, instrumentation, communications) which are part of the objectives of ICDT Brașov [50].

4. APPLICATION OF THE EXERGETIC MODEL TO DIESEL ENGINES

Chapter 4 presents the validation of the initial exergy model described in Chapter 2. The study uses the calculation programme with its exergy model to evaluate performance and exergy losses under various operating conditions and engine configurations. For this, a series of experimental engine data, recorded on test stands, was used. To this end, a database was compiled consisting of internal combustion engines for road vehicles and tractors developed and produced in Romania. The development activities for these engines took place over several decades at research institutes in Brașov, at the INAR Institute - Research Institute for Road Vehicles, which later became the commercial company SC INAR SA, and INMT - National Institute of Thermal Engines, Brașov branch. To obtain the necessary data, permission was requested and obtained to consult the INAR archive (Annex 4.1.1), the common repository for engine test bulletins. Eight types of four-stroke, direct-injection compression-ignition engines, all manufactured in Romania, were analysed, ordered by total displacement (3,12-13,8 litres), detailed in Table 4.1. For some of these, the naturally aspirated (N), turbocharged (T), and turbocharged with intake air cooling (RI) variants were considered.

Tab. 4.1 Main characteristics of the investigated engines

No.	Engine Code	Type of air intake	Cylinder configuration	Rated speed (rpm)	Maximum torque speed (rpm)
1.	D127	N	4-cylinder in-line	3200	1600
		T		2800	1600
2.	392-L4	N	4-cylinder in-line	2800	1600
		T		2800	1800
		RI		2600	1600
3.	550-L6	N	6-cylinder in-line	2800	1800
		T		2700	1800
		RI		2600	1700
4.	1035-L6-DTO	T	6-cylinder in-line	2100	1400
5.	1070-L6-DTI	RI	6-cylinder in-line	2150	1400
6.	1230-L6-DTI	RI	6-cylinder in-line	1900	1200
7.	1240-V8-DT	T	8 cylinders in V	2600	1600
8.	1380-V8-DT	T	8 cylinders in V	2200	1400
	1380-V8-DTI	RI		2200	1400

By running the program, a database of the exergetic analysis corresponding to the initial model was obtained, which are presented graphically in the form of Sankey diagrams.

These diagrams are representations of the material and energy balances of thermodynamic systems in their evolution.

The data processing and presentation of the results was carried out as follows:

- **for each engine** , the results obtained from the exergetic analyses of the two representative operating regimes were compared: the full load at nominal speed regime and the full load at maximum torque speed regime, being commented upon comparatively with data from the scientific literature, categorised by intake type (N, T, and RI);

- **for each class of engines, defined by the type of intake** (N, T, RI), the homologous terms from the exergetic balances were compared at the corresponding regimes; by numerical simulation, the influence of some parameters on the exergetic terms (N, T and RI) was determined;

Four naturally aspirated engines were analysed: D127, 392-L4, 550-L6 and D30. The calculation program considered five main exergetic terms, representing the losses with the irreversibility of work processes:

- loss caused by the combustion irreversibility - π_{irar}

- loss caused by the exhaust process irreversibility - π_{ire}

- loss caused by the irreversibility of throttling in the intake process - π_{la}

- loss caused by the irreversibility of throttling in the exhaust process - π_{le}

- loss of exergy of heat released to the environment - π_{Qea}

The terms for the irreversibility of working fluid throttling in the intake and exhaust processes are very small, almost negligible.

The exergetic losses of the four engines are illustrated in Annex 4.2.1 (which also includes a detail of the calculation program). They are characterized by high values of combustion irreversibility π_{irar} and heat exergy loss to the environment π_{Qea}, both in the range (20-24%).

The loss caused by the irreversibility of the exhaust process, π_{ire} , falls within the range (1,3-1,95%), and the sum of the losses due to throttling of the intake and exhaust is about 2%.

The influence of engine speed on exergetic terms shows that π_{irar} increases slightly with engine speed, while π_{Qea} decreases slightly. π_{ire} decreases with speed, and the sum of throttling losses increases. These trends are similar to those in the specialised literature [40].

The exergetic balances in the form of Sankey diagrams plotted for the two representative full load speeds of the 392-L4-D engine are illustrated in Figure 4.1:

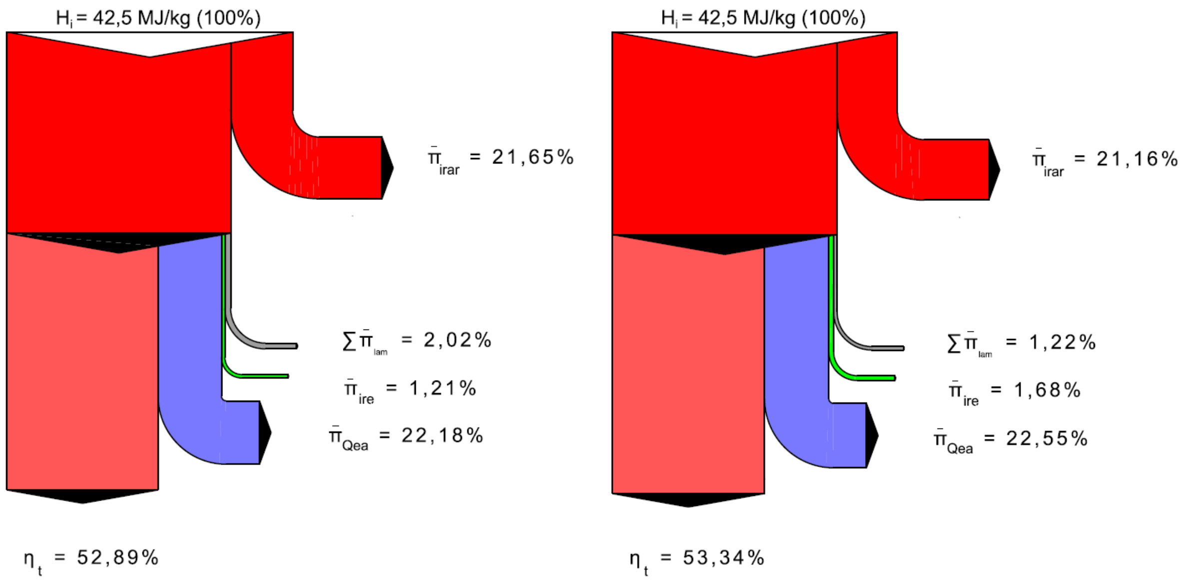

2800 rpm 1600 rpm

Fig. 2.21 Sankey diagrams – 392-L4-D engine

Six T engines were analysed. The exergetic balance included eleven terms, specific to the processes in the engine and turbocharger. Additional terms to N engines include:

- exergy loss of heat rejected by the exhaust gases from the turbine to the environment - π_{QeT}
- loss caused by irreversibility of air compression in the compressor – π_{irs}
- loss caused by the irreversibility of gas expansion in the turbine - π_{irT}
- loss caused by irreversibility of intake-scavenging processes - π_{irba}
- loss caused by the irreversibility of heat transfer between the exhaust gas from the engine and the scavenging air - $\pi_{\Delta Teb}$
- loss caused by the irreversibility of throttling in the intake of the engine - π_{laM}
- loss caused by the irreversibility of throttling in the exhaust of the engine - π_{leM}
- loss caused by the irreversibility of throttling in the compressor intake - π_{laS}
- loss caused by the irreversibility of throttling in the turbine exhaust - π_{leT}

The terms of irreversibility of throttling are very small, their sum not exceeding 1%. T engines are characterized by relatively high values of π_{irar}, (16,33-18,70%), but lower than in N engines. The exergy loss of heat rejected to the environment, π_{QeT} (14,53-19,50%) are also lower than π_{Qea} in the N engines. The loss caused by the irreversibility of the exhaust (1,38-2,20%) increases with the decrease in speed. The irreversibility of the π_{irs} compressor (0,48-3,60%) is higher than that of the π_{irT} turbine (0,23-1,34%), both of which increase on average with increasing speed. The terms π_{irba} and $\pi_{\Delta Teb}$ have slight variations. Throttling losses increase with speed.

Intermediate cooling (RI) of the intake air has the effect of increasing the mass of fresh charge in the cylinder. In the list of engines in question there are five turbocharged engines that have been cooled by means of air-to-air coolers.

The calculation program for RI engines includes thirteen exergetic terms, adding two more terms associated with the intercooler:

- exergy loss in the air-to-air heat exchanger - π_{QR}

- exergy loss due to the irreversibility of throttling in the air-to-air heat exchanger - π_{lR}

The sum of the throttling irreversibility terms does not exceed 1.8%. The exergetic losses of the five engines are characterised by high values of combustion irreversibility (18,56-21%), higher than those of turbocharged engines. Exergy losses of heat to the environment (11,78-17,57%) are lower than their only turbocharged counterparts. The exergy loss due to heat transfer in the air cooler varies between 0,22-1,22% with higher values at higher speeds. Losses caused by exhaust process irreversibility fall within the range (1,65-2,48%). And in this case, compressor irreversibilities (0,93-2,71%) are higher than those of the turbine (0,56-1,18%). The terms π_{irba} and $\pi_{\Delta Teb}$ both have a small variation, the first 0,54-0,83%, and the second 0,23-1,06%, the first increasing with speed, and the second decreasing as speed increases. Throttling losses are higher than in T engines, explainable by the additional throttling in the intercooler with an average contribution of 0,2%. Total throttling loss values oscillate within the range 0,67-1,75%, increasing with increasing speed.

Compared to the T case, applying RI confirms the notable increase in combustion irreversibilities, characterised by the range (16,33–18,70)% for T, to the range (18,56–21)% for RI. On the other hand, the loss with the heat exchange of the exhaust gases at the turbine outlet, π_{QeT}, decreased in RI, (11,78–16,34%) compared to T (14,53–19,50%).

The qualitative influence of **increasing engine speed** on the balance terms for the three engine types, averaged over the presented engines, is summarised in Table 4.2.

Tab. 4.2 Response of exergy terms to increasing engine speed

	π_{irar}	$\pi_{Qea,T}$	π_{ire}	$\Sigma\pi_l$	π_{irs}	π_{irT}	π_{irba}	$\pi_{\Delta Teb}$	π_{QR}
N	↗	↘	↘	↗	-	-	-	-	-
T	→	↘	↘	↗	↗	↗	↗	↘	-
RI	↗	↘	↘	↗	↗	↗	↗	↘	↗

With the exception of the term π_{irar} , the trend of evolution of exergetic terms can be observed.

The last part of Chapter 4 presents the study of the influence of certain parameters on the terms in the exergy balance. The study used a variational calculation method, applying small variations to the parameters to observe the effect on the terms in the exergy balance. The influences were analysed separately for the N, T, and RI engines..

The following figures illustrate the evolution of some parameters of naturally aspirated, supercharged and supercharged engines with intermediate cooling, at the two specific engine speeds.

In **the case of the naturally aspirated engine**, the parameters considered were atmospheric factors (temperature and pressure), compression ratio and excess air coefficient. The ambient temperature T_0, in the case of testing the two engines was 290K or about 17°C.

In order to study the influence of this parameter on the engine cycle and the exergetic balance, the operation of the engine in the temperature range (273-310K) or 0-37°C was simulated.

The quantities affected by the variation of T_0 are the density of the intake air, ρ_0, the cycle temperatures as well as T_{mar} - the mean thermodynamic temperature of combustion, the indicated mean pressure, p_{mi}, the cycle indicated efficiency, η_i, the volumetric heat load of the cylinder q_{ar}, and the heat transferred to the environment from the exhaust gases Q_{ea}. In the exergy balance, the most sensitive relative terms are the loss caused by combustion irreversibility, π_{irar},, the loss with the exergy of the heat transferred to the environment π_{Qea}, and the loss caused by exhaust irreversibility, π_{ire} .

With increasing ambient temperature, there is a decrease in air density ρ_0, explainable by the equation of state for air, considered an ideal gas: $\rho_0 = \frac{p}{RT_0}$. The cycle process temperatures T_a, T_c, T_y, T_z, T_d also naturally increase with T_0. The results of the numerical models applied for the 392-L4-D and 550-L6-D engines are presented in parallel.

The trend of increasing T_{mar} with T_0 is evident for both engines, having higher values for maximum torque speed, as shown in Figure 4.2.

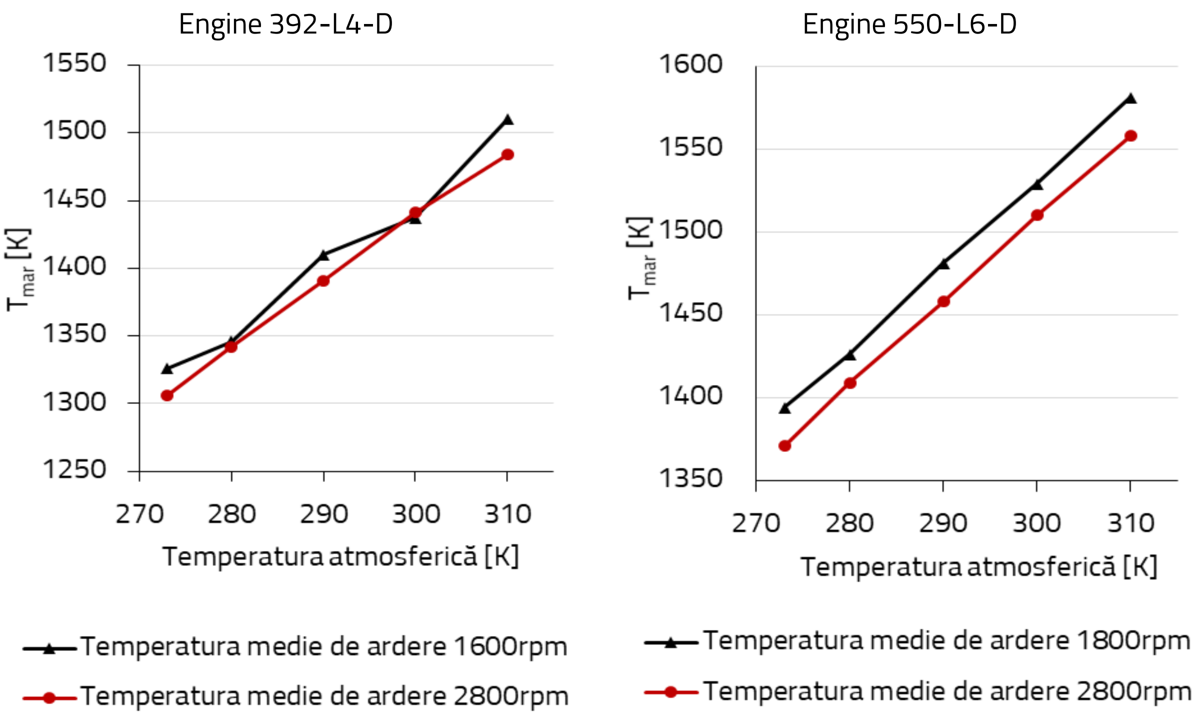

Fig. 4.2 Variation with *T0* of the average thermodynamic combustion temperature, T_{mar}

The heat developed by the combustion of fuel per unit engine cylinder volume, qar_{Vs}, proves to be relatively stable with increasing temperature T_0, registering higher values for the maximum torque speed, according to Figure 4.3.

The average indicated pressure, p_{mi} , undergoes minor variations with temperature, with higher values for the maximum torque speed than for the rated speed.

The heat of the exhaust gases Q_{ea} slightly increases with T_0. The indicated efficiency, η_i, decreases very slightly with increasing temperature (Figure 4.4).

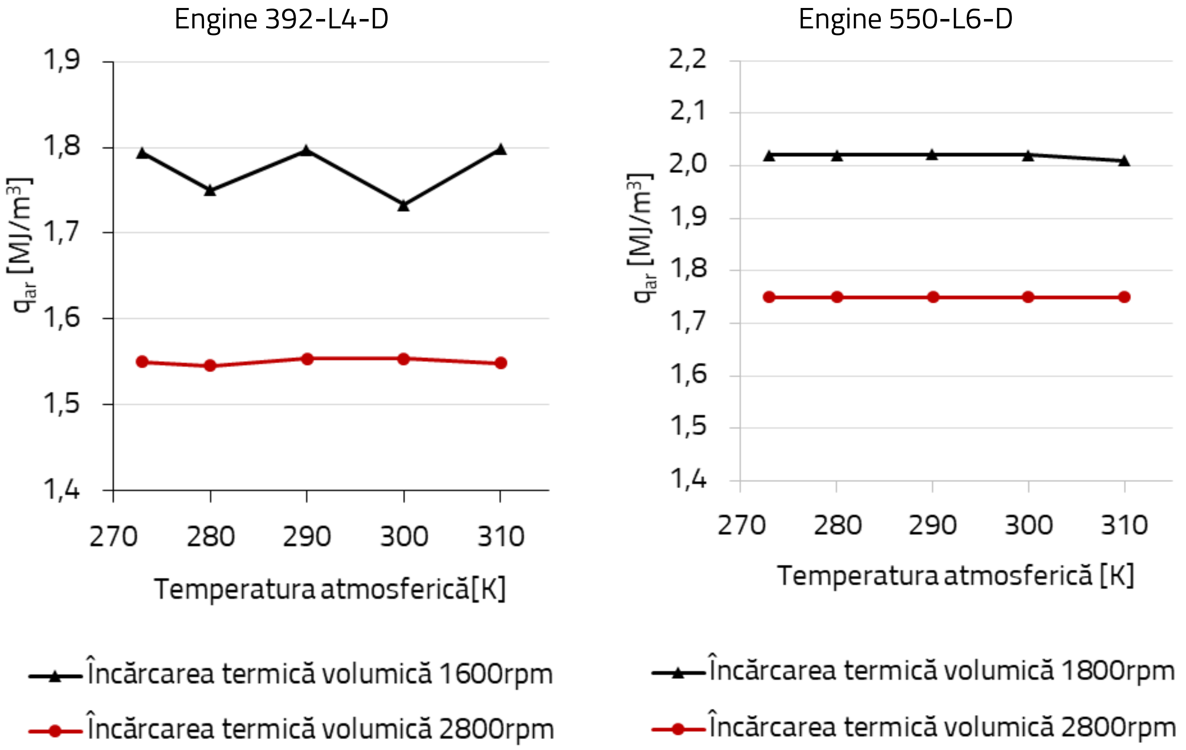

Fig. 4.3**Error! No text of specified style in document.** Variation with T_0 of *qarVs*

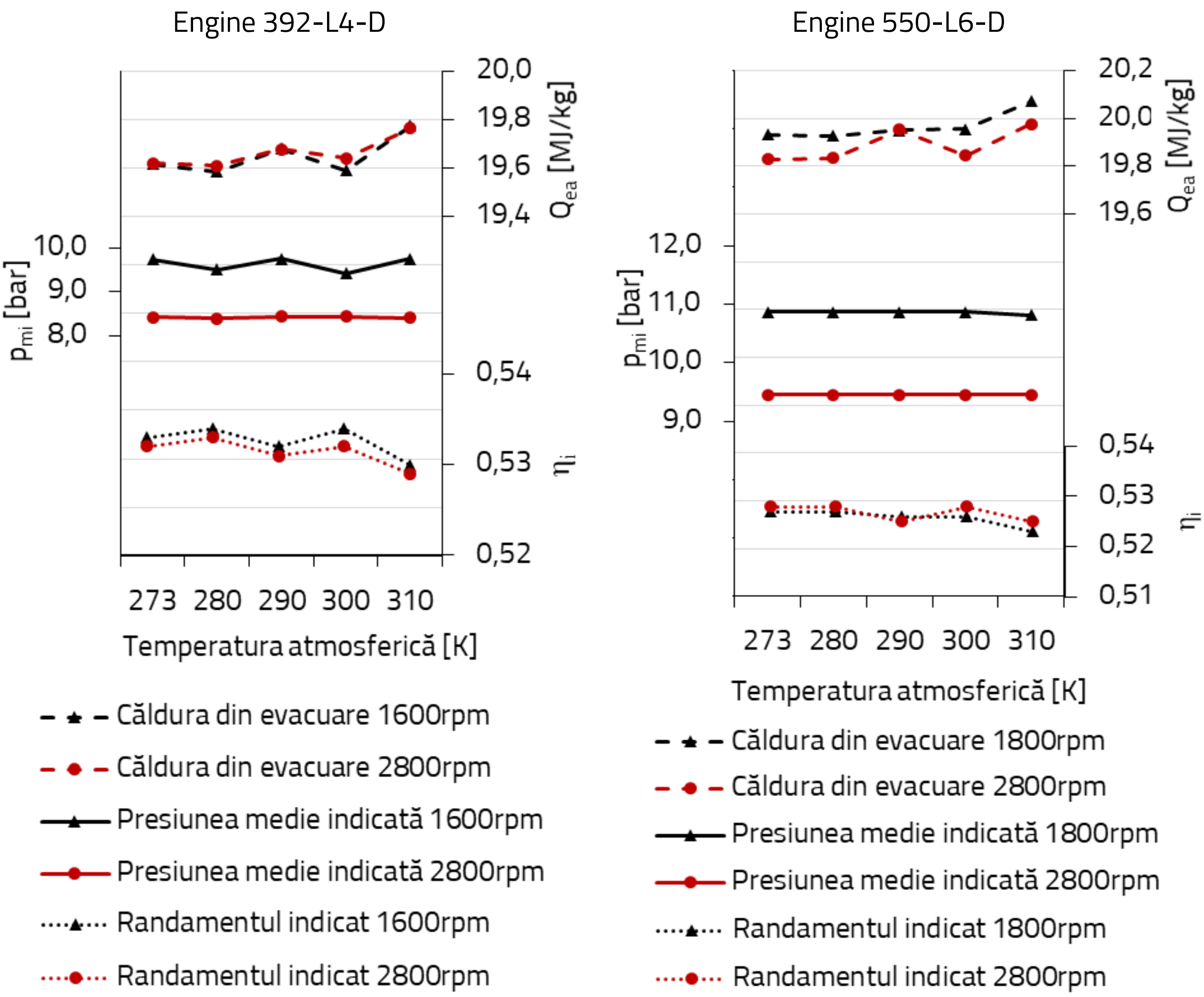

Fig. **Error! No text of specified style in document.** Variation with T_0 of p_{mi}, η_i, Q_{ea}

The irreversibility of combustion π_{irar} increases slightly, the exergy loss of exhaust gas heat to the environment π_{Qea} increases with T_0, and the loss caused by the irreversibility of exhaust processes is almost invariable with T_0.

By increasing **the compression ratio** (Figure 4.5), the heat evacuated by the exhaust gases Q_{ea} decreases, more significantly for the rated speed, and the indicated efficiencies and indicated mean pressures increase. From a quantitative point of view, for the 392-L4-D engine at a speed of 2800 rpm, it can be observed that by increasing the compression ratio from 18,5 to 21,5, the pressure increase ratio in isochoric combustion, λ, decreases by 18%, the volume increase ratio in isochoric combustion, ρ, increases by 15%, and the indicated efficiency increases by 1,9%.

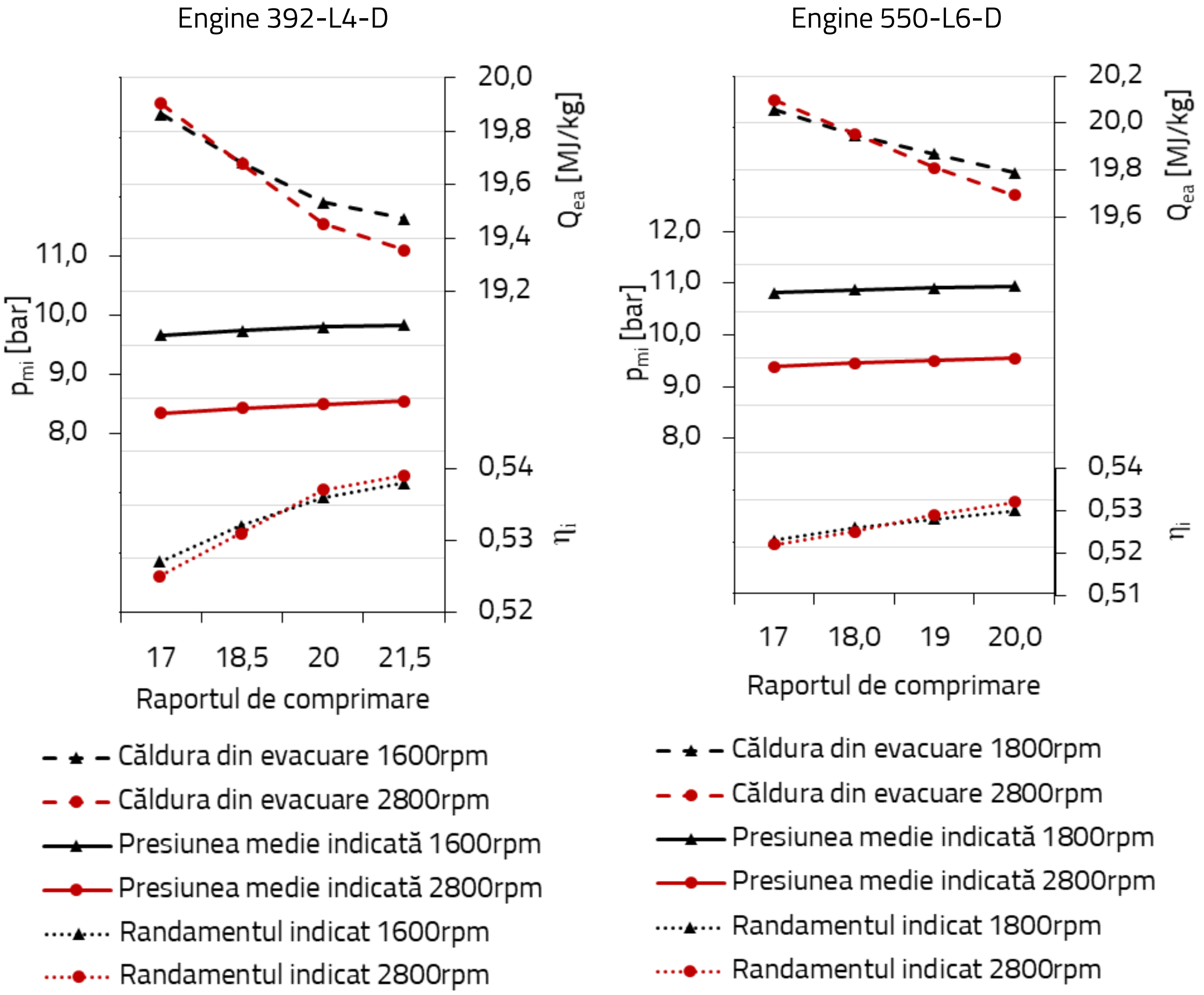

Fig. 4.5 Variation with the compression ratio of p_{mi}, η_i, Q_{ea}

Although the reductions in exergetic losses are not notable, the increase in the compression ratio leads to the simultaneous decrease of the two important terms π_{irar} and π_{Qea} (Figure 4.6).

Numerically, for the case of the 392-L4-D engine at a speed of 2800 rpm, π_{irar} decreases by 1,6%, and through heat exchange π_{Qea} decreases by 4,5%; at a speed of 1600 rpm, π_{irar} decreases by 1%, and π_{Qea} decreases by 3,4%.

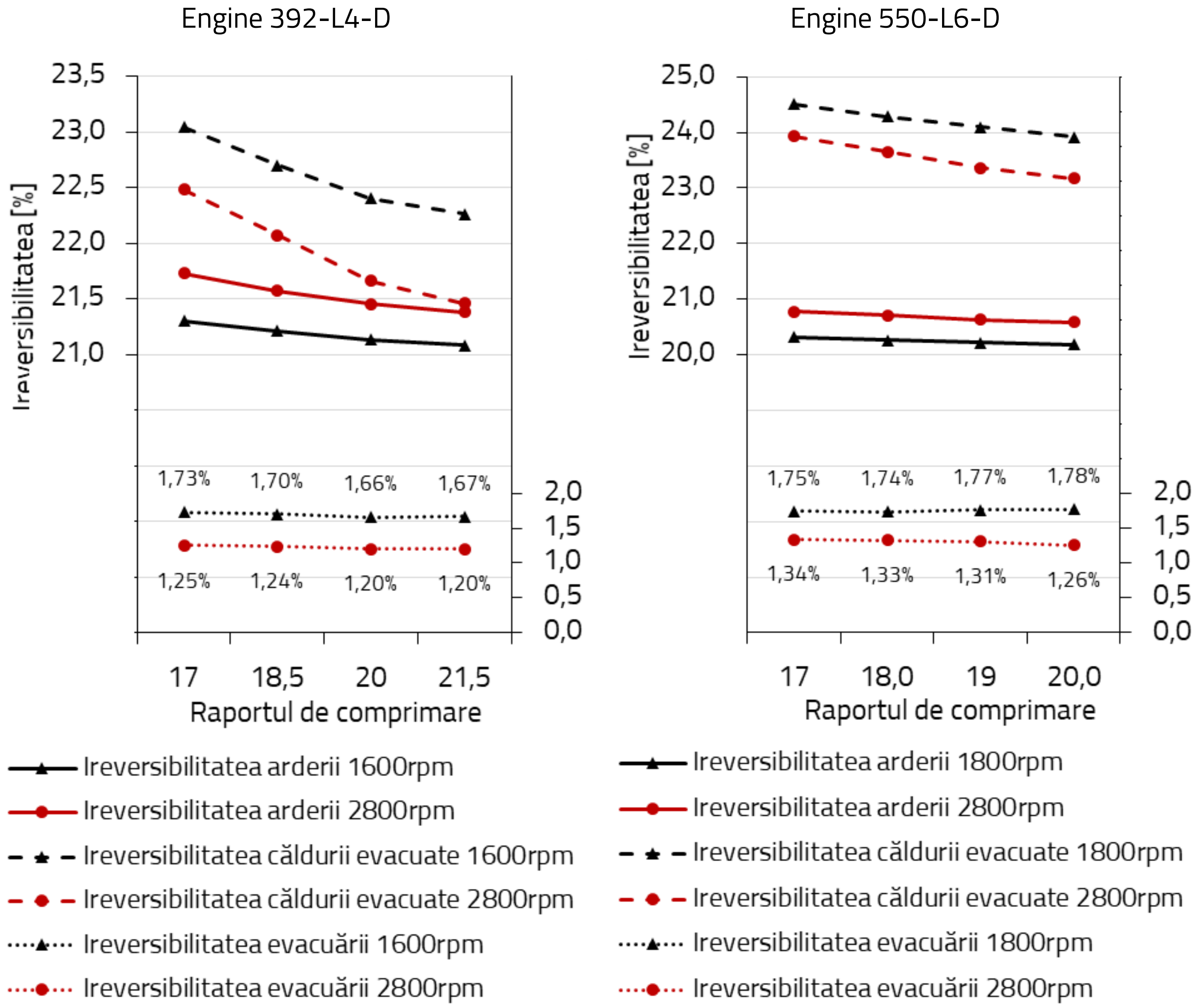

Fig. 4.6 Main exergy terms sensitive to compression ratio variation

Average thermodynamic combustion temperature, T_{mar} decreases considerably with an **increase in excess air**, more pronounced at high engine speeds, which predicts a decrease in the combustion exergetic efficiency and implicitly an increase in combustion irreversibility π_{irar}. This also causes a notable decrease in the qar_{Vs} parameter.

Figure 4.8 shows the considerable reduction in p_{mi} and the heat evacuated by the exhaust gases Q_{ea}, concurrently with the increase in indicated efficiency. By decreasing T_{mar}, the exhaust gas temperature also decreases, a fact which anticipates the decrease in exhaust gas exergy losses. The variation of the excess air ratio over the entire range of values 1,3-2,2, considerably decreases the volumetric heat load qar_{Vs} and the indicated mean pressure, and the indicated efficiency increases by about 2%.

With the increase of the excess air coefficient, the exergetic loss due to the irreversibility of combustion π_{irar} increases significantly, the exergy loss of heat from the exhaust π_{Qea} decreases significantly, and the irreversibility of the exhaust processes assessed by the term π_{ire} has a decreasing tendency with the increase of the excess air coefficient (Figure 4.9).

The trends of variation of exergetic parameters and terms are consistent with the literature.

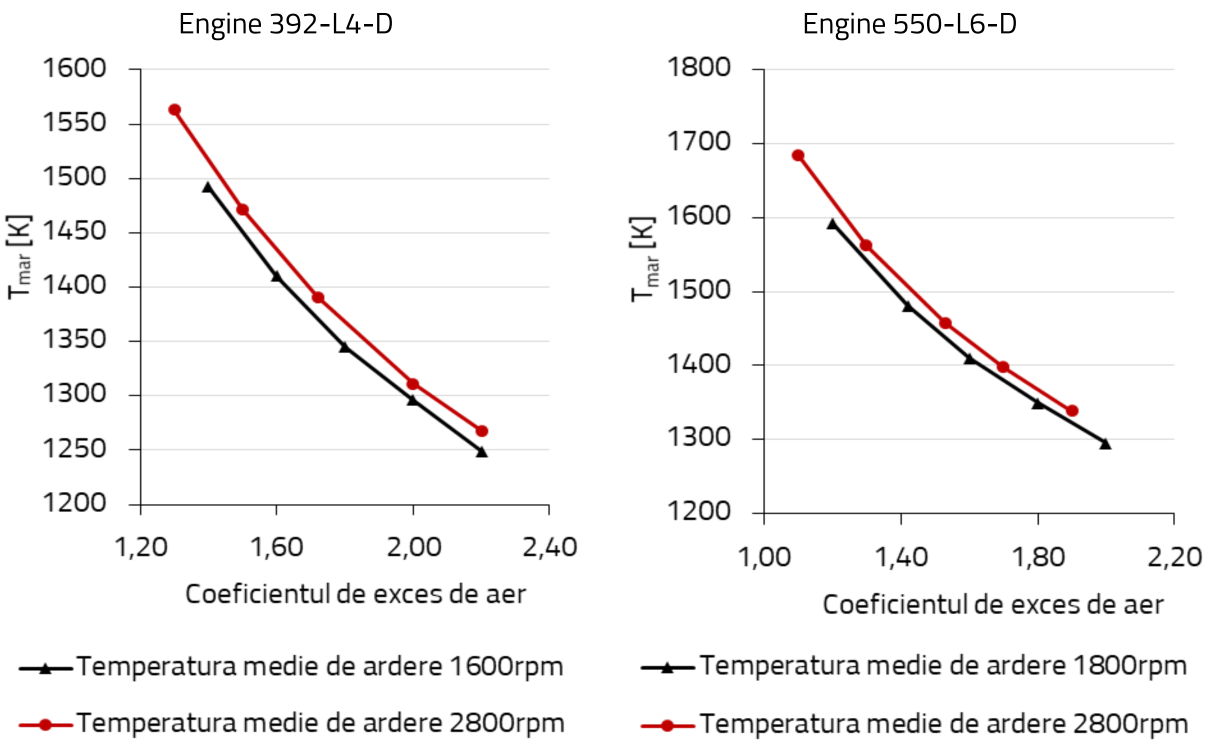

Fig.4.7 T_{mar} variation with α

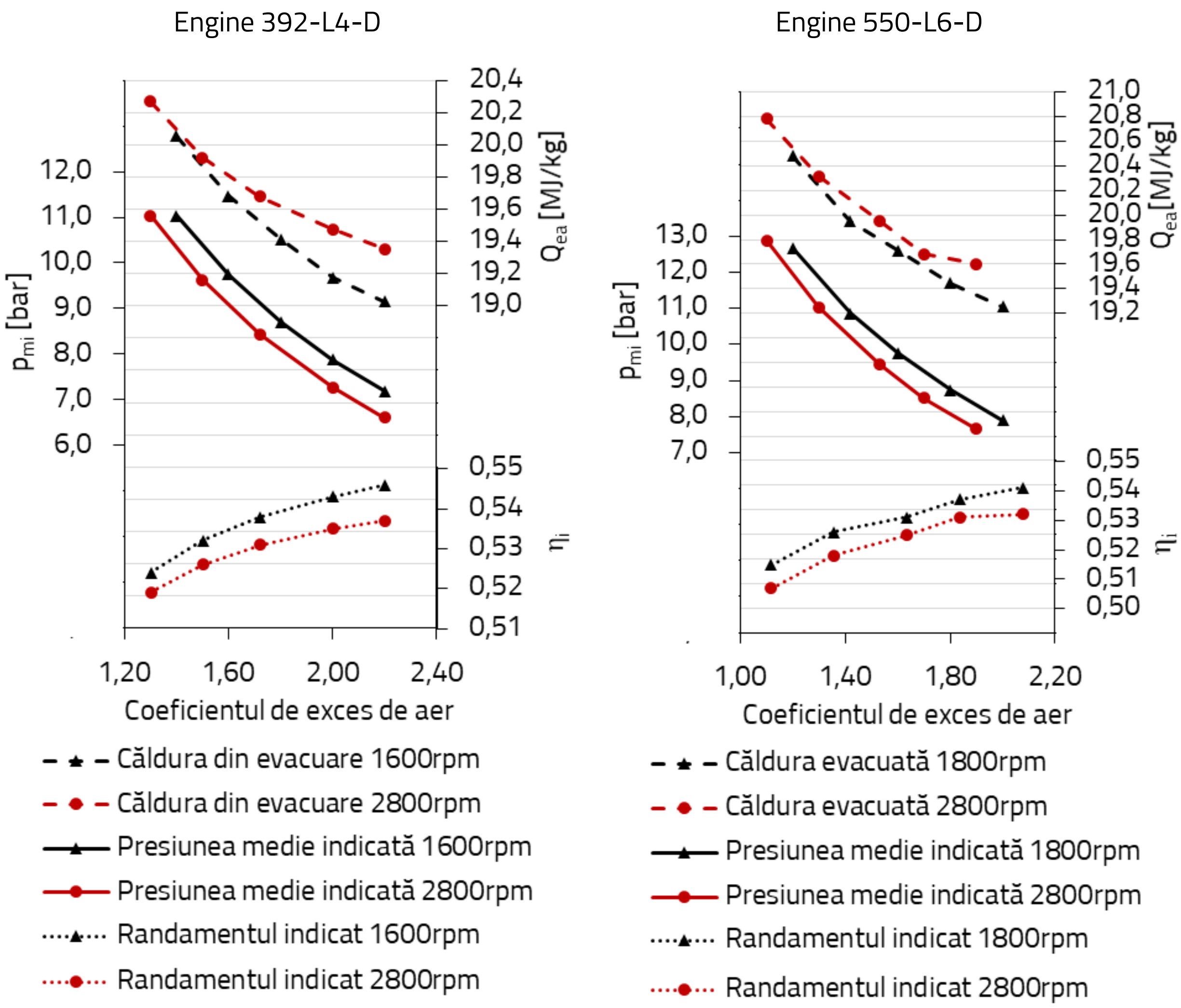

Fig. 4.8 Variation with α of p_{mi}, η_i, Q_{ea}

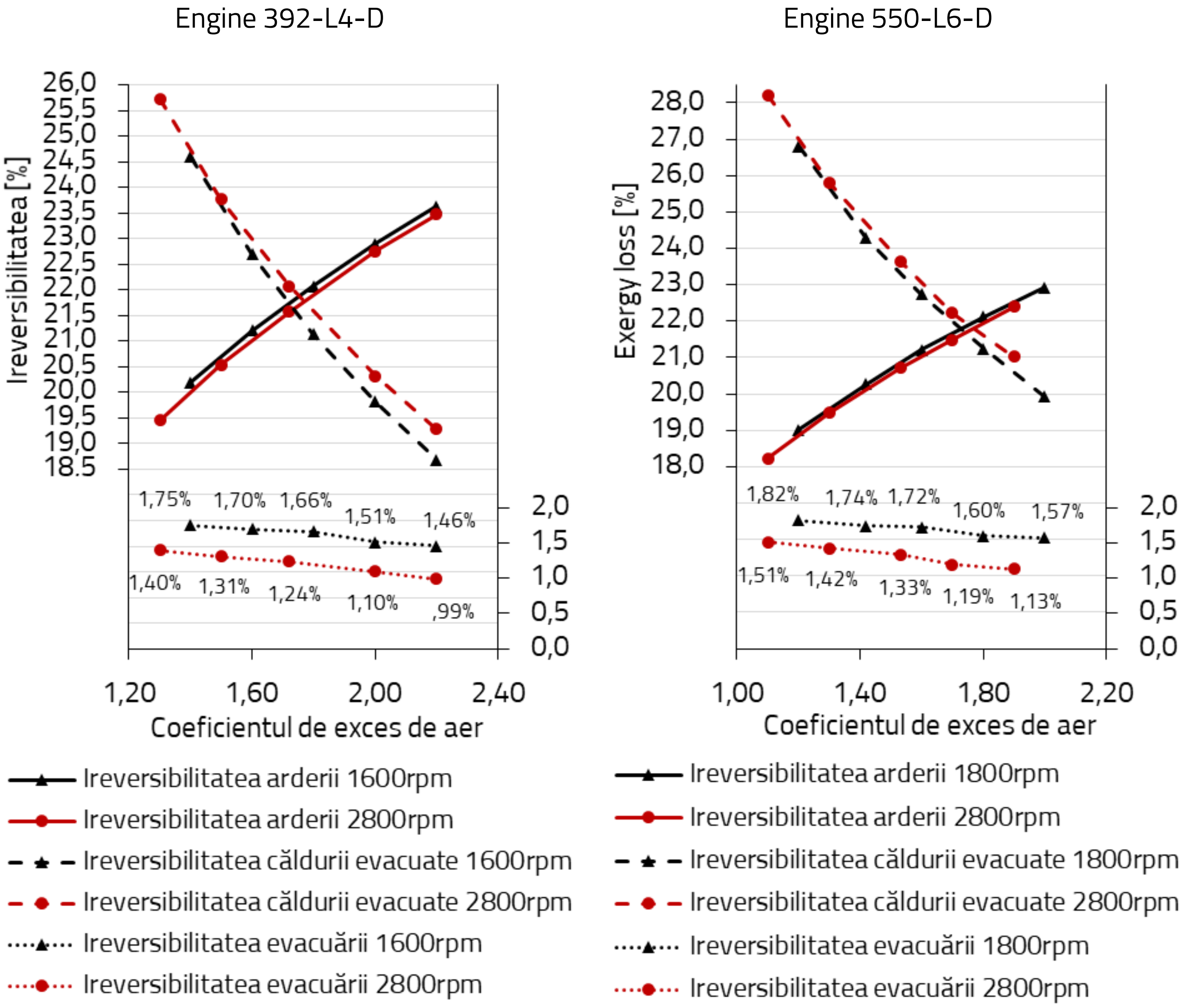

Fig. 4.9 The main exergetic terms sensitive to the variation of α

The compression ratio seems to be the only "win-win" parameter, simultaneously improving energy and exergetic performance. The excess air coefficient can simultaneously influence three exergetic terms, and the increase in speed influences Q_{ea} and π_{Qea}, important terms for the energy recovery from the exhaust gas.

For the case of **turbocharged engines**, the influence of factors on engine exergy follows the form presented for the case of naturally aspirated engines, with the necessary additions and modifications. Atmospheric factors - temperature, atmospheric pressure, and humidity - are reduced to atmospheric temperature, with atmospheric pressure being replaced by the boost pressure p_s. The quantities investigated were: T_{mar} - the mean thermodynamic temperature of combustion, the volumetric heat load of the cylinder q_{ar}, the heat rejected by the exhaust gases from the turbine during an isobaric cooling process, Qe_T, the indicated efficiency η_i, the indicated mean pressure, p_{mi}.

The main terms in the exergy balance investigated were the loss caused by the irreversibility of combustion π_{irar}, the loss with heat exergy π_{QeT}, the losses caused by the irreversibility of the compression process in the compressor π_{irs}, the irreversibility of the expansion process in the turbine π_{irT}, as well as the irreversibility of the exhaust process π_{ire} .

The study of these influences is based on the results of the numerical analysis of two turbocharged engines, presented in parallel, 550-L6-DT and 1240-V8-DT, based on experimental determinations at full load for two revolutions.

The increase in T_0 increases the cycle temperatures and the average thermodynamic combustion temperature, T_{mar}, having as in the case of naturally aspirated motors higher values for maximum torque speed, as shown in Figure 4.10.

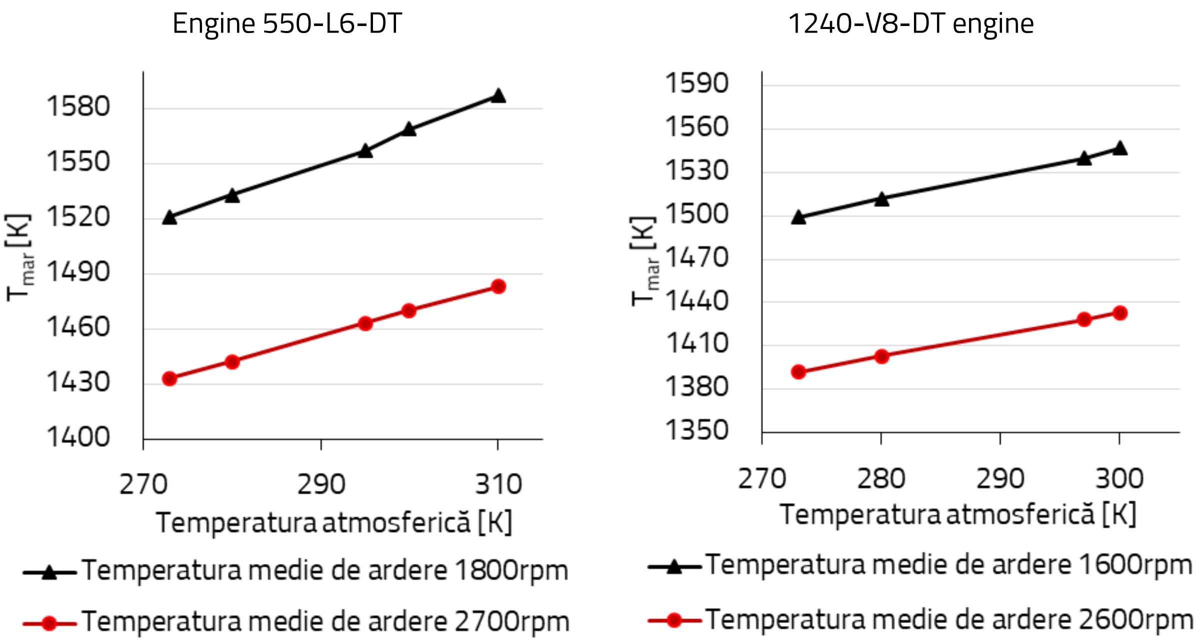

Fig. 4.10 Variation of T_{mar} with T_0

The heat developed by the combustion of fuel per unit engine cylinder volume, qar_{Vs}, also called volumetric heat load, slightly increases with temperature, registering higher values for the maximum torque speed; the heat at the turbine outlet Q_{eT} depends on the difference between the temperature at the turbine outlet ($T_{eT}=T_3$) and T_0; as T_0 increases, the temperature difference relative to the environment decreases, and Q_{eT} decreases, as can be observed in Figure 4.11.

There is an increase in the indicated mean pressure p_{mi} with the increase of T_0, which implies an obvious increase in the indicated efficiency η_i , valid for both engine speeds and shown in Figure 4.12.

The engine exergy losses, illustrated in Figure 4.13, show a slight increase in combustion irreversibility π_{irar} with the increase of T_0.

Although T_{mar} increases, in the expression that defines π_{irar}, (1-T0/T_{mar}), the increase in $T0$ is more important, and the trend is in line with the observations in the reference [36].

At the same time, the losses with the exergy of the rejected exhaust heat π_{QeT} are reduced.

With the increase of T_0, the exergy losses in the compressor π_{irS} decrease significantly, while the irreversibility of the exhaust process π_{ire} and irreversibility in the turbine π_{irT} remain quasi-constant.

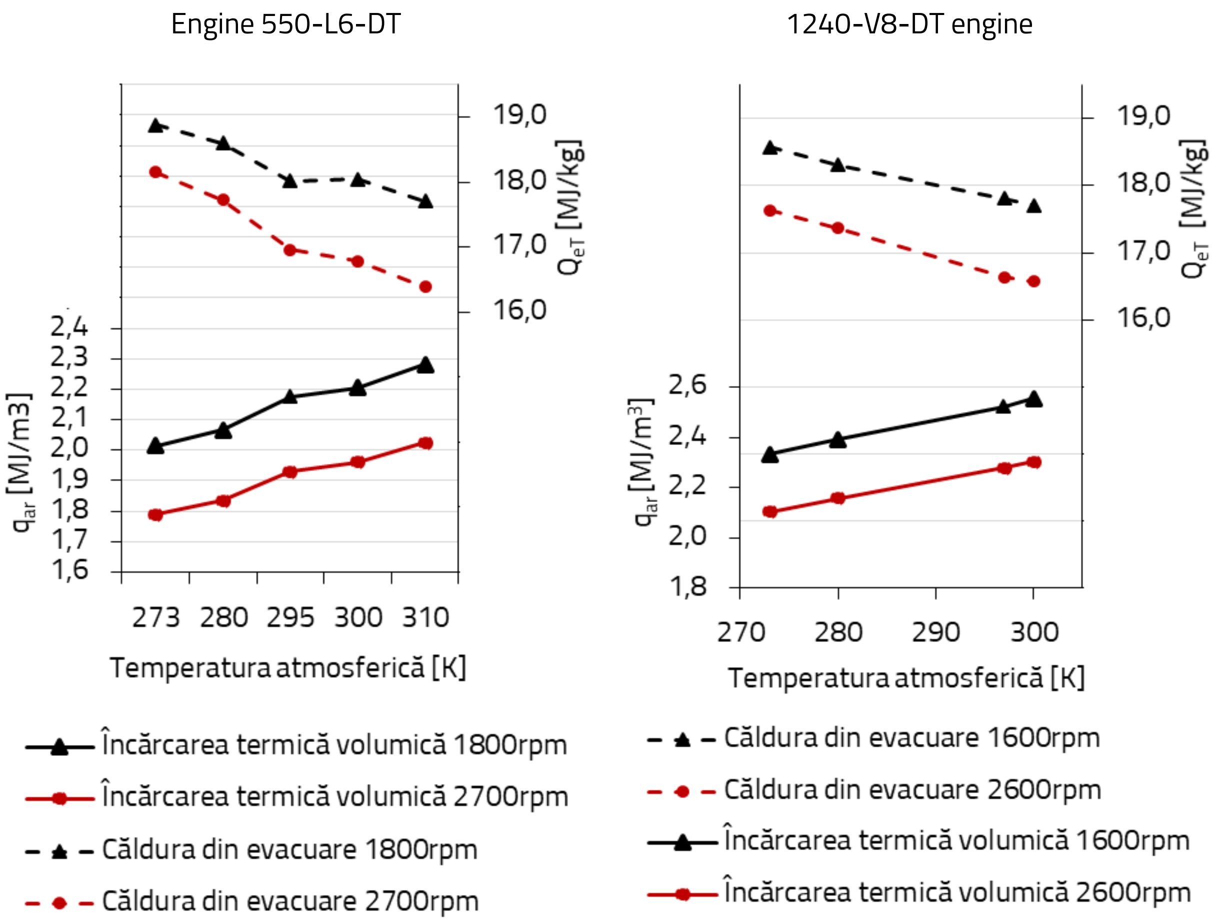

Fig. 4.11 Variation of qar_{Vs} and Q_{eT} with T_0

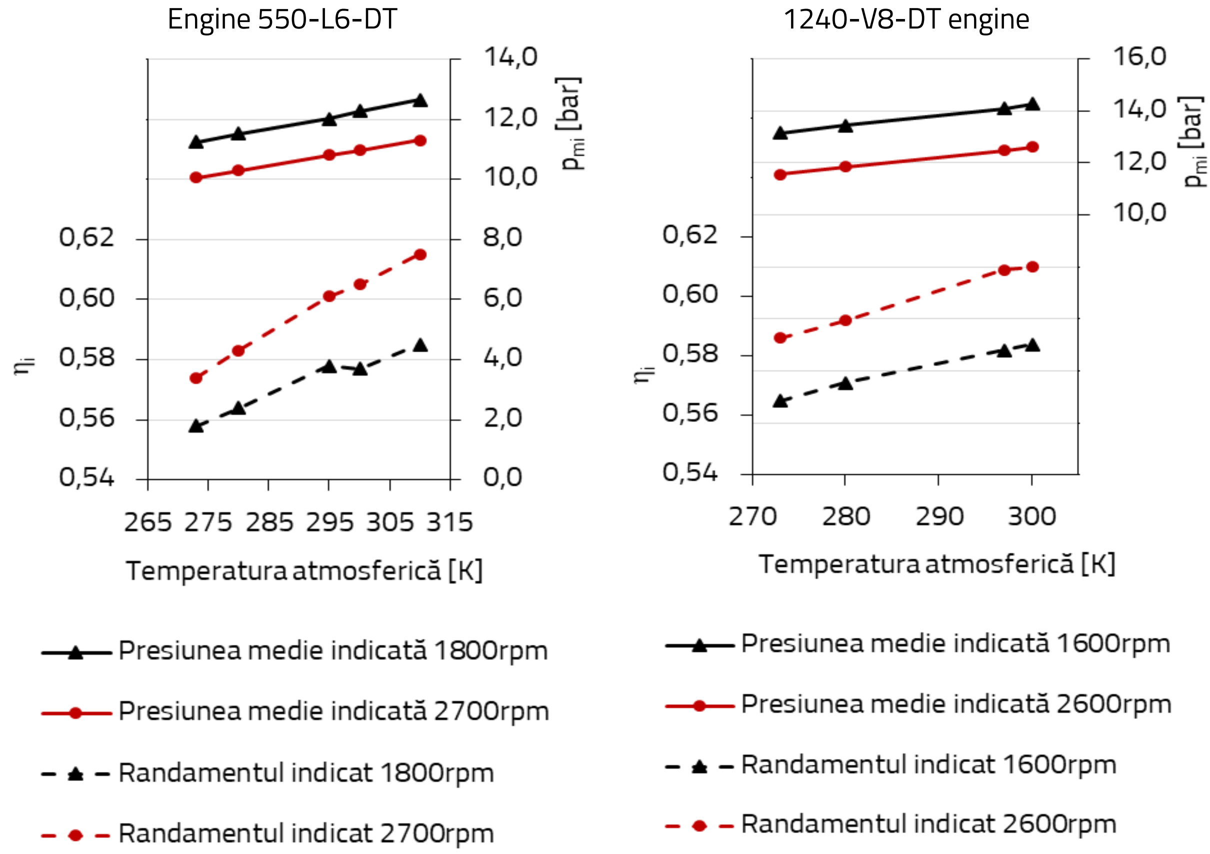

Fig. 4.12 Variation of p_{mi} and η_i with T_0

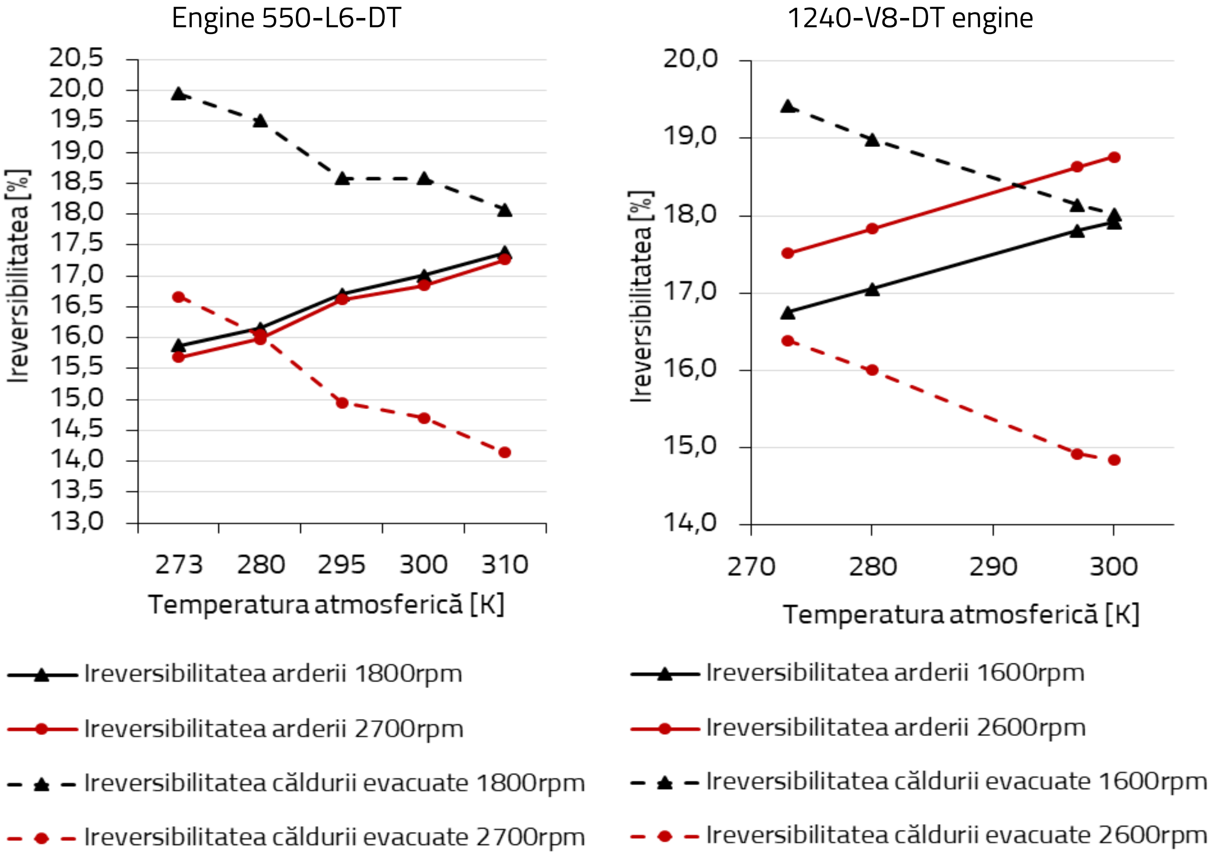

Fig. 4.13 Variation of π_{irar} and π_{QeT} with *TO*

Regarding the variation **of the boost pressure** p_s, the volumetric thermal load registers notable increases with *the increase* p_s , more pronounced for the low engine speed, but the heat released into the environment, Q_{eT}, remains rather constant (Figure 4.14). Increasing engine speed decreases qar_{Vs} and Q_{eT}.

The average indicated pressure increases, while the indicated efficiency increases very little for the rated speed and remains almost constant for the maximum torque speed (Figure 4.15). The increase in rpm decreases p_{mi} and increases η_i .

The p_s variation of the two important terms, π_{irar} and π_{QeT}, is limited. The combustion irreversibility π_{irar} increases very little with p_s.

Regarding the specific processes of supercharging, Figure 4.16 shows the evolution of the irreversibilities in the compressor and turbine.

The increase in p_s leads to a decrease in irreversibility in the compressor, π_{irs}, more pronounced at rated speed, while the irreversibility in the turbine, π_{irT}, are not influenced at all. The irreversibility of the exhaust process π_{ire} increases with p_s, more intensely at maximum torque speed.

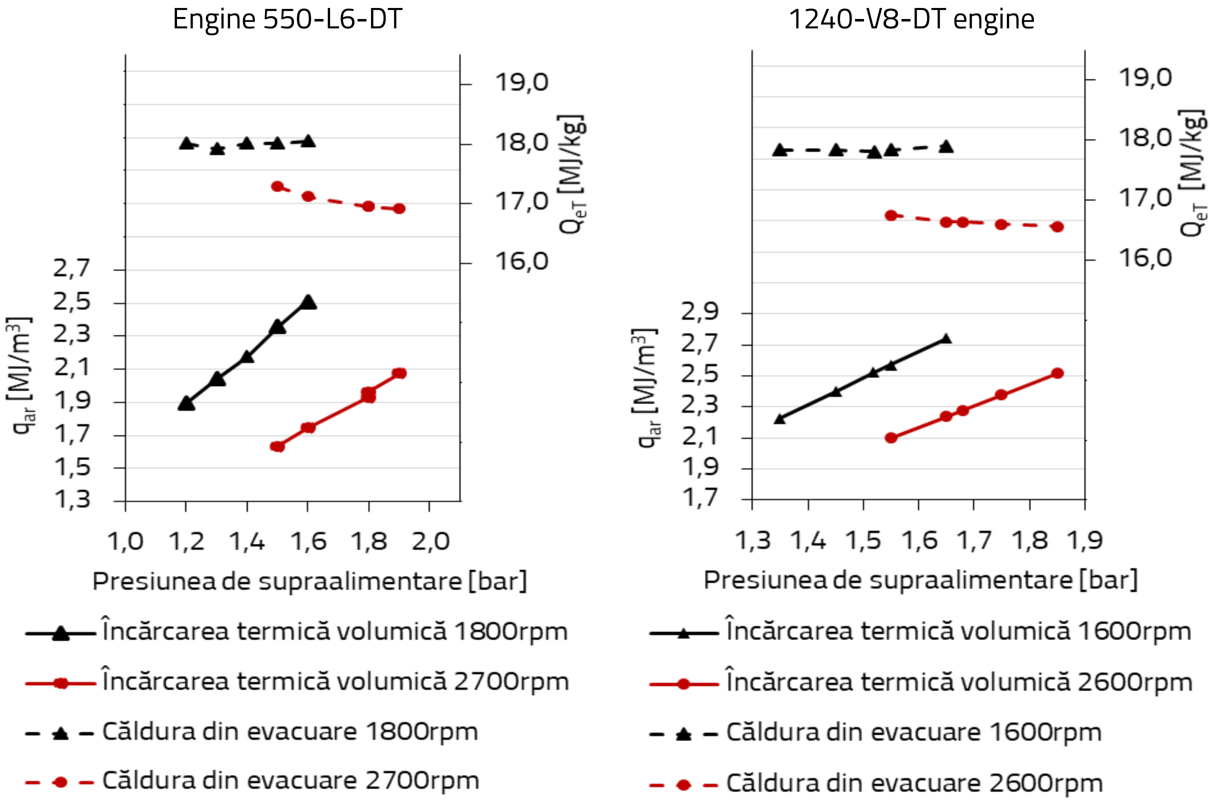

Fig. 4.14 Variation *qarVs* and *QeT* with the boost pressure *Ps*

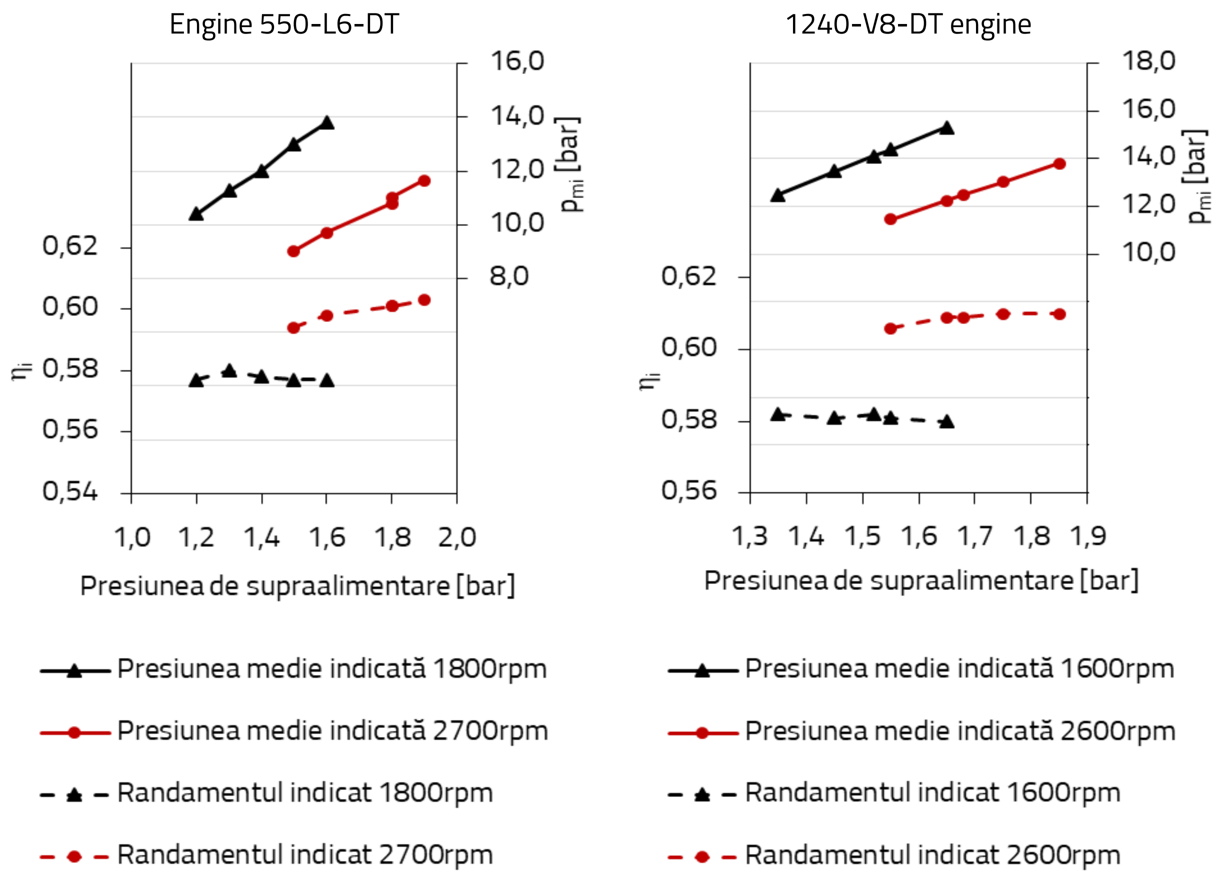

Fig. 4.15 Variation of p_{mi} and η_i with the boost pressure p_s

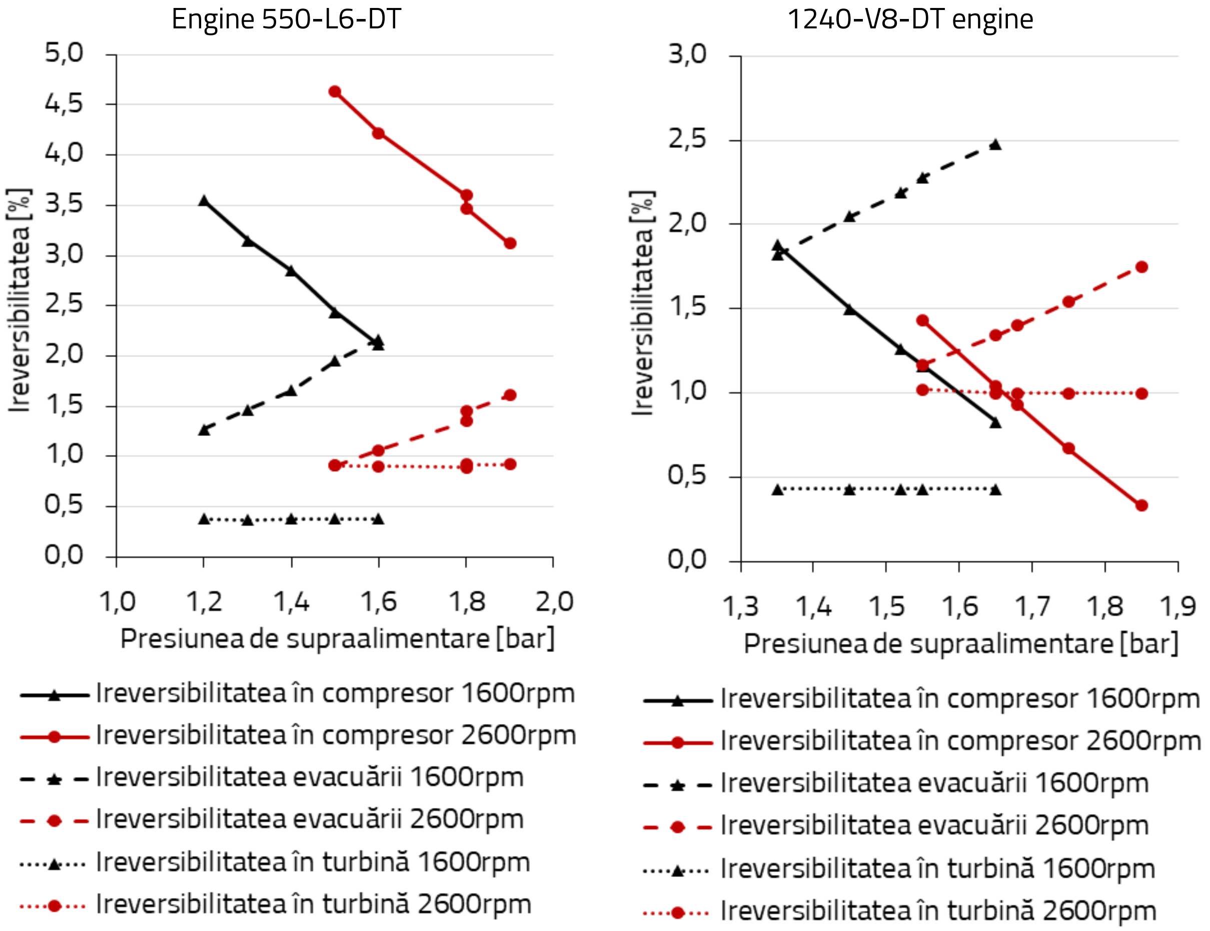

Fig. 4.16 Variation of π_{Irs} , π_{irT} and π_{Ire} with the boost pressure p_s

Increasing **the compression ratio** leads to an increase in the pressure and temperature in the cylinder, as well as in the indicated efficiency, η_i . The increase in the temperature level in the cycle is best described by the evolution of the T_{mar} parameter, shown in Figure 4.17.

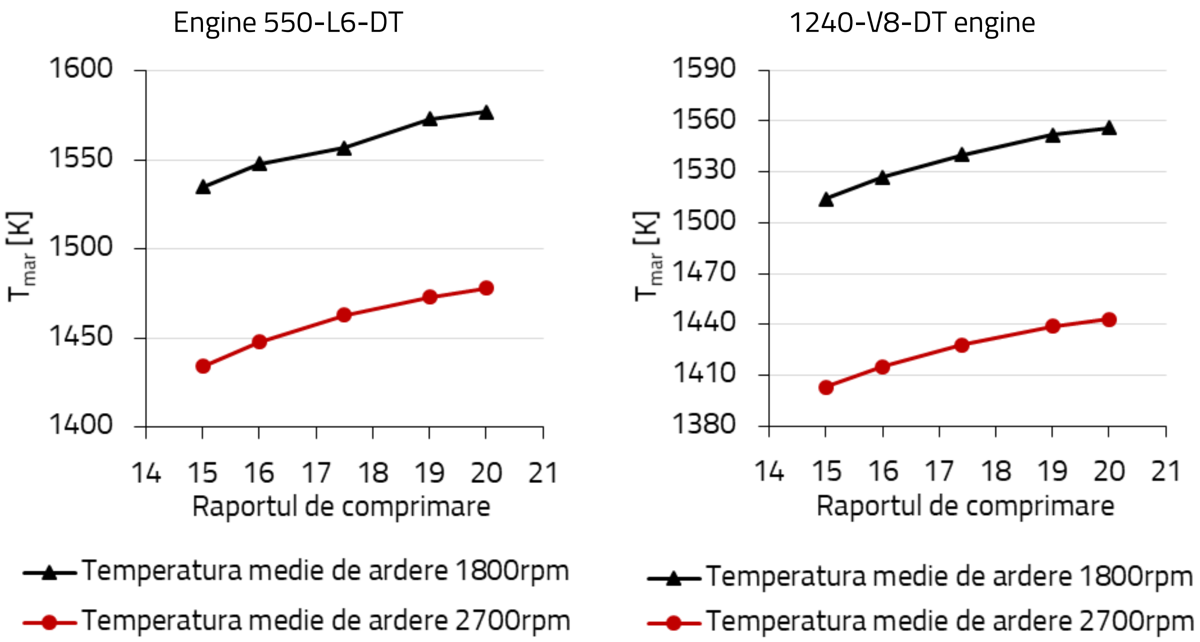

Fig. 4.17 Variation of T_{mar} with the compression ratio

The volumetric heat load, qar_{Vs}, remains constant with the variation of the compression ratio, and the heat evacuated to the environment Q_{eT} has a very slight decreasing tendency, both quantities registering lower values at nominal speed. By increasing the compression ratio, the indicated efficiencies and indicated mean pressures slightly increase. From an exergetic point of view, the two significant terms in the balance π_{irar} and π_{Qea} undergo a small simultaneous reduction, along with the increase in the compression ratio. The irreversibilities in the turbocharger, π_{irs}, π_{irT}, as well as the exhaust irreversibilities π_{ire}, are not influenced by the variation of the compression ratio.

Regarding the variation of exergy terms with **increasing excess air ratio** α , T_{mar} decreases, which leads to an increase in combustion irreversibilities, π_{irar}. In contrast, π_{QeT} evolves in the opposite direction as a result of decreasing temperatures at the turbine outlet (Figure 4.18), and the effect of engine speed is decreasing for both quantities.

The irreversibility in the compressor increases significantly with the increase in the excess air coefficient, and that in the turbine increases very little. On the other hand, the irreversibility of the exhaust process has a quasi-constant, slightly decreasing variation.

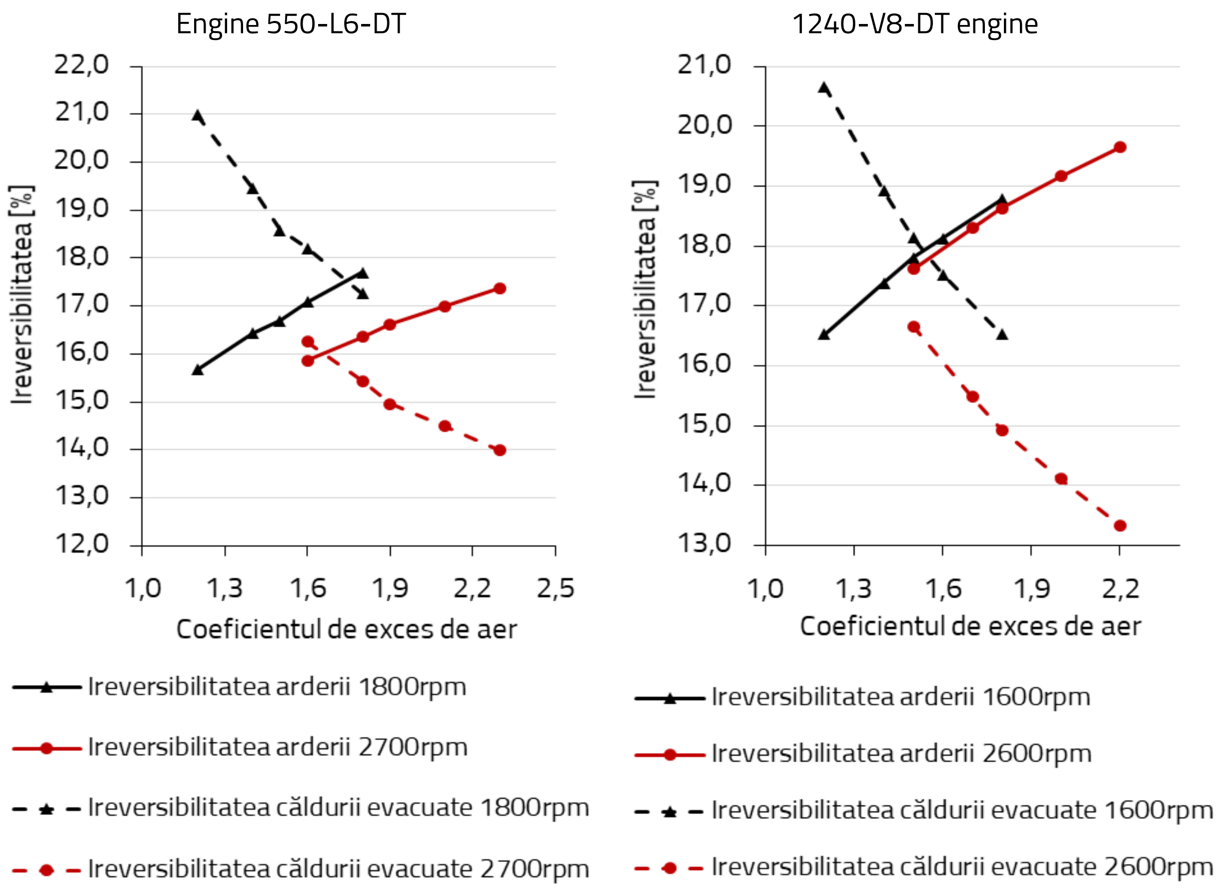

Fig. 4.18 Variation of π_{irar} and π_{QeT} with the excess air coefficient

Increasing **the maximum cycle pressure** p_{max} has the effect of decreasing slightly, simultaneously, the irreversibility π_{irar} and π_{QeT} (Figure 4.19). The increase in engine speed increases π_{irar} and decreases π_{QeT}.

The terms in the exergy balance associated with the turbocharger and exhaust indicate almost constant values, which are not significantly influenced by the variation p_{max} .

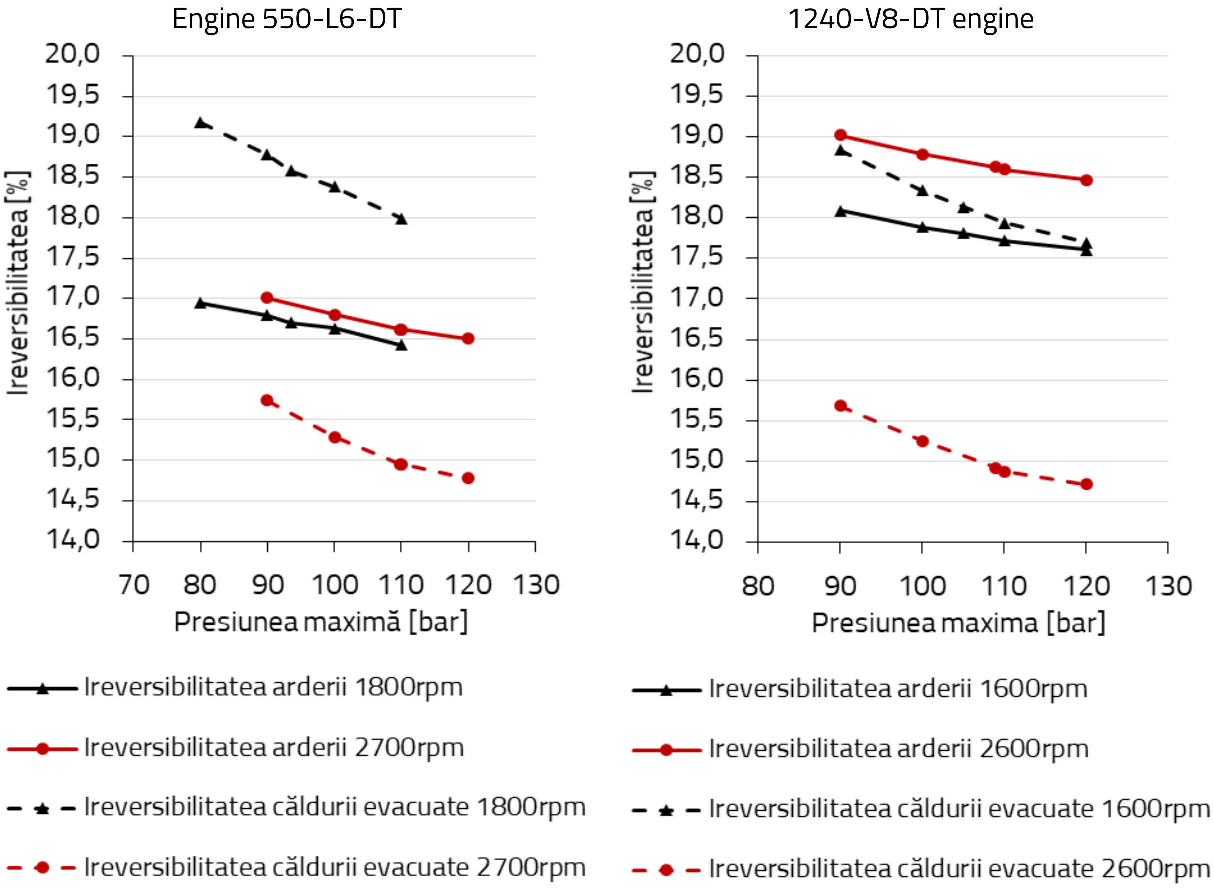

Fig. 4.19 Variation of π_{irar} and π_{QeT} with the maximum pressure in the cycle p_{max}

The analysis of turbocharged engines showed a good correlation of the variation of energy and exergy quantities with specialised studies. Turbocharging brings advantages such as increased indicated power and decreased exhaust heat. Operating optimisation can be achieved by increasing the compression ratio and the boost pressure, but with different influences on the exergy terms. Decreasing the excess air ratio increases p_{mi}, but also increases π_{QeT} .

The analysis of the influence of certain parameters on **turbocharged engines with intercooling** included the changes produced by the integration of the intercooler. Novelty in the calculation programme is related to cooling efficiency (τ), heat removed (Q_R), and air throttling in the cooler. The quantities investigated were: the mean thermodynamic temperature of combustion, T_{mar}, the volumetric heat load of the cylinder q_{ar}, the heat rejected by the exhaust gases from the turbine during the isobaric cooling process, Qe_T, the indicated efficiency, η_i, the indicated mean pressure, p_{mi}. The main terms from the exergy balance investigated were the loss caused by combustion irreversibility, π_{irar}, the loss with the exergy of the exhaust heat π_{QeT}, the losses caused by the irreversibility of the compression process in the compressor, π_{irs}, the irreversibility of the expansion process in the turbine, π_{irT}, as well as the irreversibility of the exhaust process, π_{ire}.

The supercharged and intercooled engines analysed were 550-L6-DTI and 1380-V8-DTI, presented in parallel, based on experimental determinations at full load for maximum torque speed and nominal speed.

Intercooling produces fewer effects than simple turbocharging, therefore some graphs show constant values, making it irrelevant to present them in full. The most important parameter of intercooling is the cooling efficiency (or degree of cooling), τ .

By increasing the efficiency of the cooling process in the cooler, the mean thermodynamic combustion temperatures, T_{mar} , decreases as a result of cooler air entering the engine cycle after the heating produced by compression in the compressor, Figure 4.20.

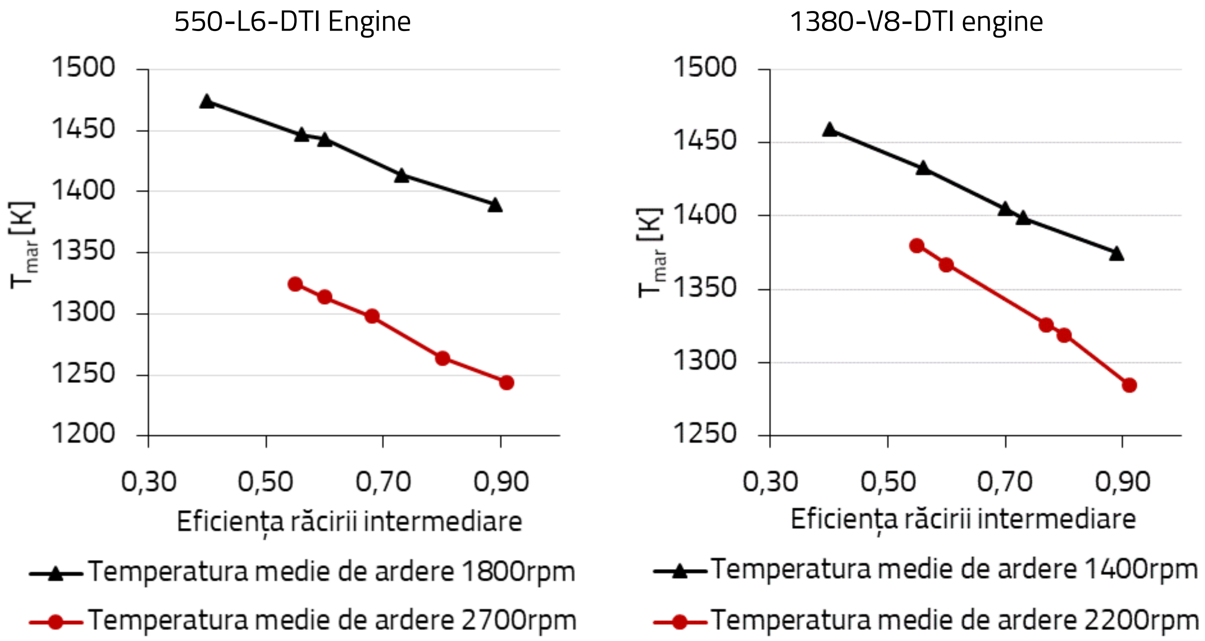

Fig. 4.20 Variation *Tmar* with τ

Better air cooling decreases the exhaust heat Q_{eT} and increases the volumetric thermal load, qar_{Vs}, both of which are inverse to that of the engine speed, as shown in Figure 4.21.

In the case of increasing the cooling efficiency, Figure 4.22 shows a slight increase in the indicated mean pressure, and the indicated efficiency shows a quasi-constant character. At the same cooling efficiency, increasing rpm gives lower p_{mi} values, but higher values of the indicated efficiency, η_i.

The variation of the exergy terms is presented in Figure 4.23, where a slight increase in combustion irreversibility and a moderate decrease in the irreversibility of exhaust heat at the turbine outlet are observed, along with the increase in intercooling efficiency.

Increasing engine speed significantly decreases the exergy loss of evacuated heat; in contrast, the effect of speed on combustion irreversibility is very reduced.

Figure 4.24 shows the terms of irreversibility in the turbocharging and exhaust processes in the engine. Irreversibility in the compressor and turbine does not exhibit sensitivity to variation of the cooling efficicency.

On the other hand, the irreversibility of the exhaust process increases slightly with the increase of the cooling efficiency. The increase in engine speed increases π_{irT} and decreases π_{ire} ; as far as π_{irs} are concerned, the two engines behave differently at the speed variation, with the observation that the respective percentages have low values, between 1-2% of the fuel energy, for both engines.

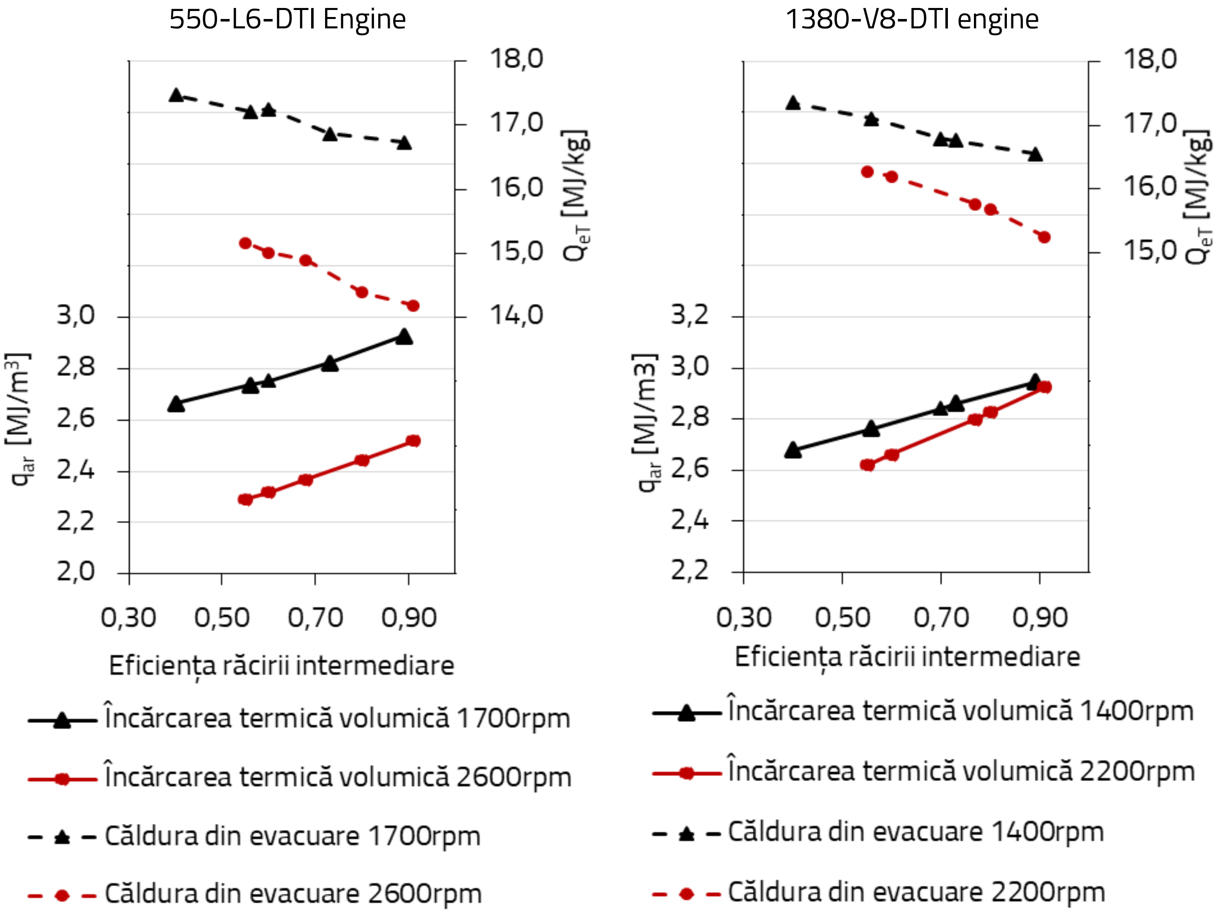

Fig. 4.21 Variation of qar_{Vs} and Q_{eT} with τ

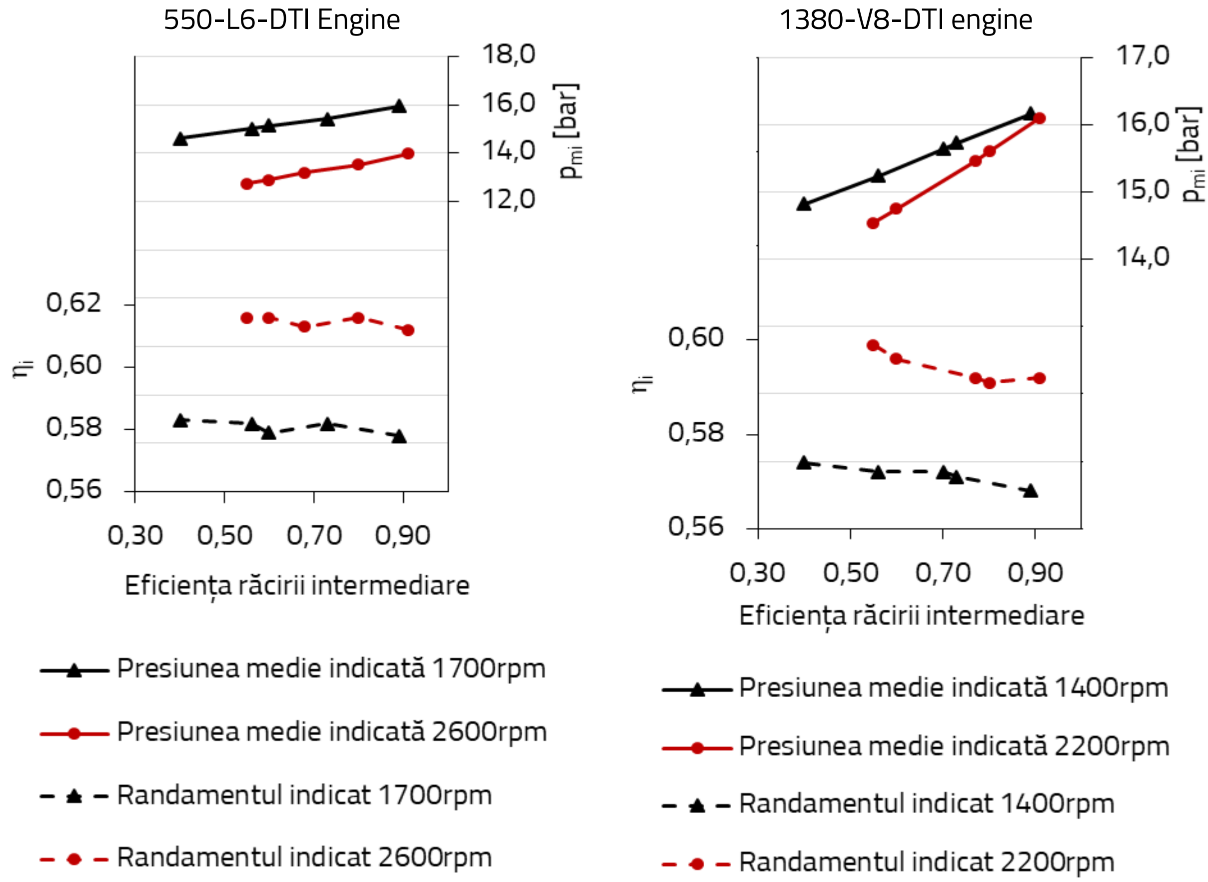

Fig. 4.22 Variation of p_{mi} and η_i with τ

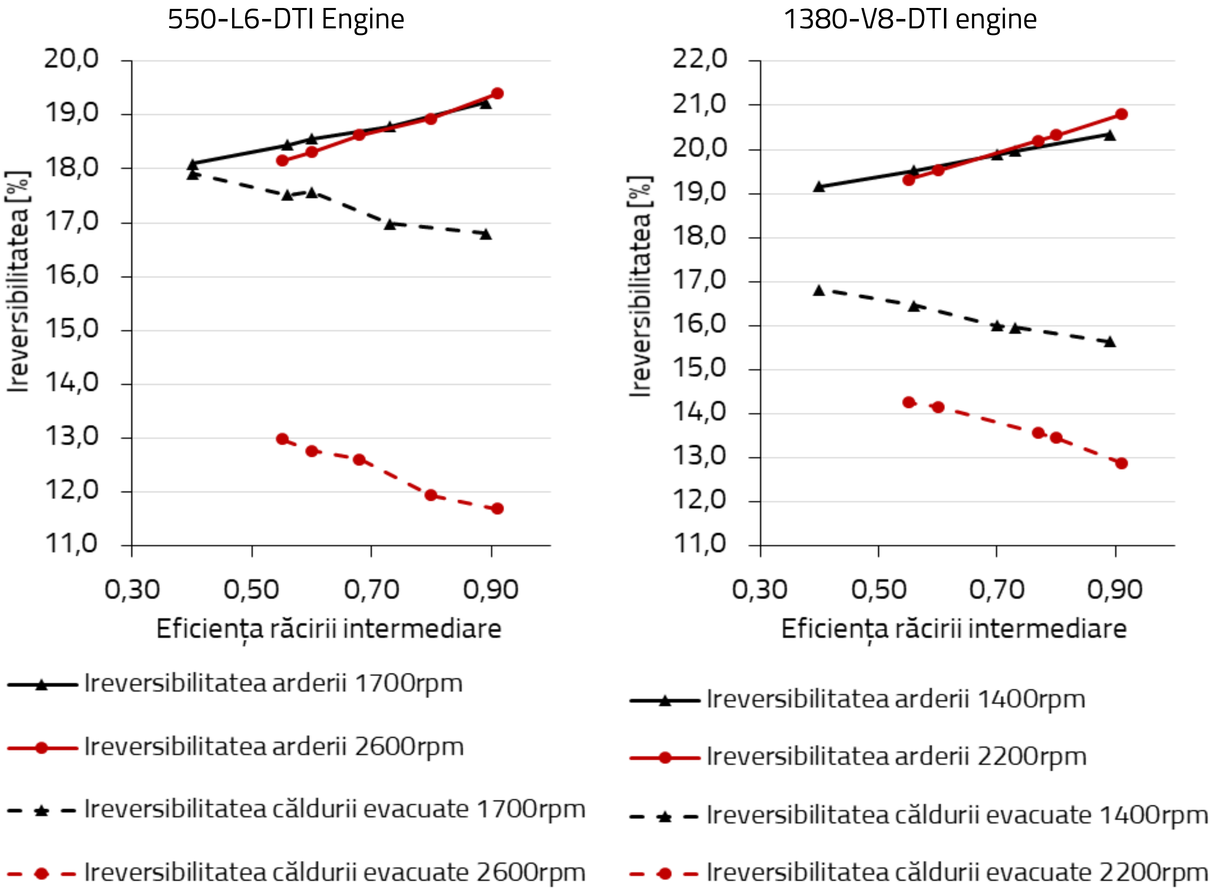

Fig. 4.23 Variation of π_{irar} and π_{QeT} with τ

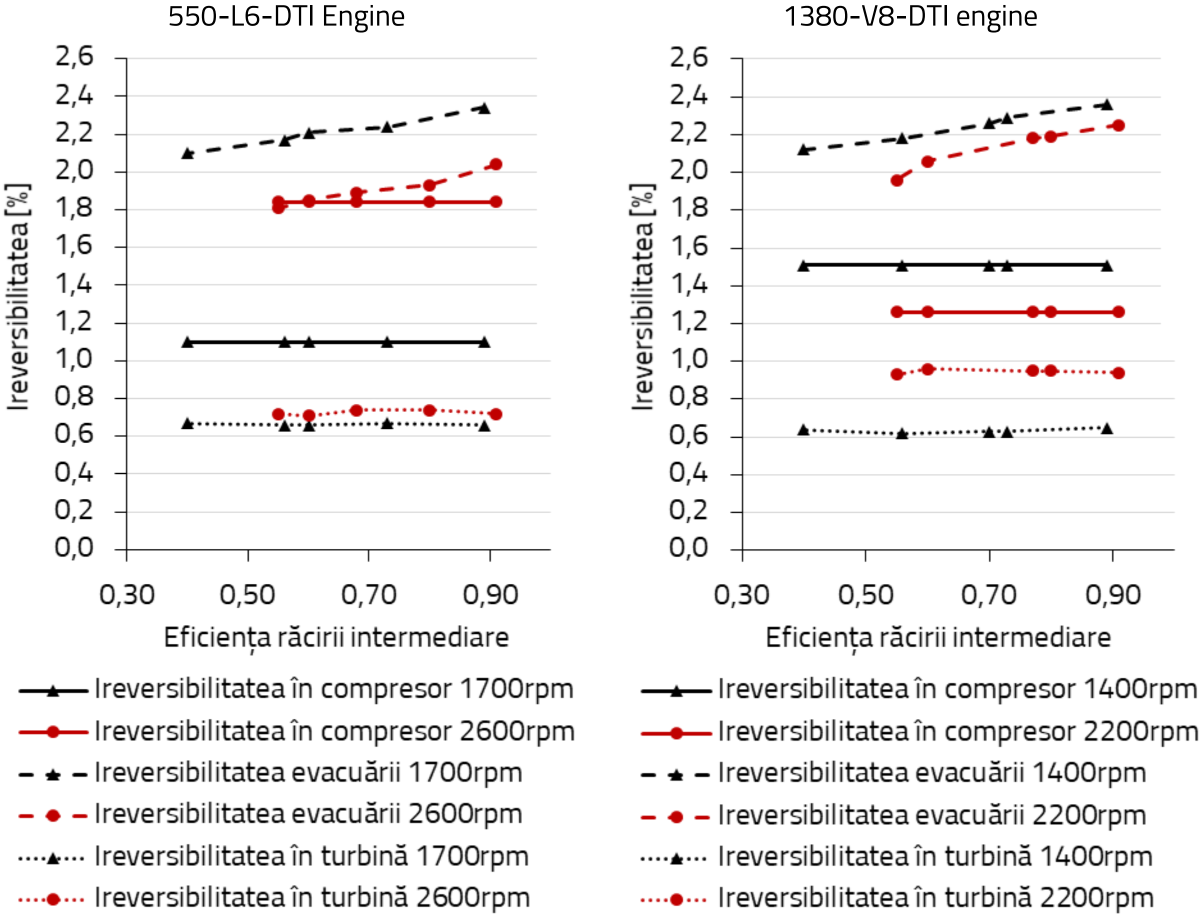

Fig. 4.24 Variation of π_{Irs} , π_{irT} and π_{Ire} with τ

The behaviour of the analysed RI engines registered a series of differences, justifiable by the different operating parameters and different ranges of working speeds. The results of the numerical study are in good agreement with the technical literature. Intercooling added an increase in indicated power compared to T engines. By applying RI, an increase in π_{irar} is observed concurrently with a decrease in exergy losses of heat released to the environment π_{QeT} . Parameter control is difficult, with energy optimisation often contradicting exergy optimisation. The quantities Q_{eT} and π_{QeT} are important for energy recovery from the exhaust gas heat, and increasing engine speed reduces them simultaneously.

The detailed study of the influence of parameters on the exergy terms offers a valuable perspective on optimising the operation of diesel engines from the point of view of both principles of thermodynamics. Although some constructive parameters (compression ratio) or environmental conditions (temperature, pressure) have predictable influences, functional control through parameters such as boost pressure and excess air ratio requires a multi-criteria approach to balance energy performance with exergy performance. Significant exergy losses through combustion and exhaust remain the main targets for future improvements.

5. IMPROVING ENERGY AND EXERGETIC MODELS

The first part focuses on the energy balance of the AVL 5402 engine, based on experimental data, with emphasis on the influence of speed on the main balance terms, the comparison between the naturally aspirated and turbocharged variants, and the evaluation of heat transfer through the engine surfaces. The AVL 5402 engine was tested on the stand in naturally aspirated (N) and turbocharged (T) operating variants, over a representative speed range (1600-3600 rpm) and at different loads (50%, 75%, 100%). The energy analysis focused on operating regimes above 50% load, because at low loads temperatures and flow rates are reduced, limiting the potential for energy recovery. The influence of engine speed on the balance terms was analysed for the AVL 5402 engine in naturally aspirated (N) configuration. For operation at the nominal regime, the proportions of these energy quantities per unit time are illustrated in Figure 5.1.

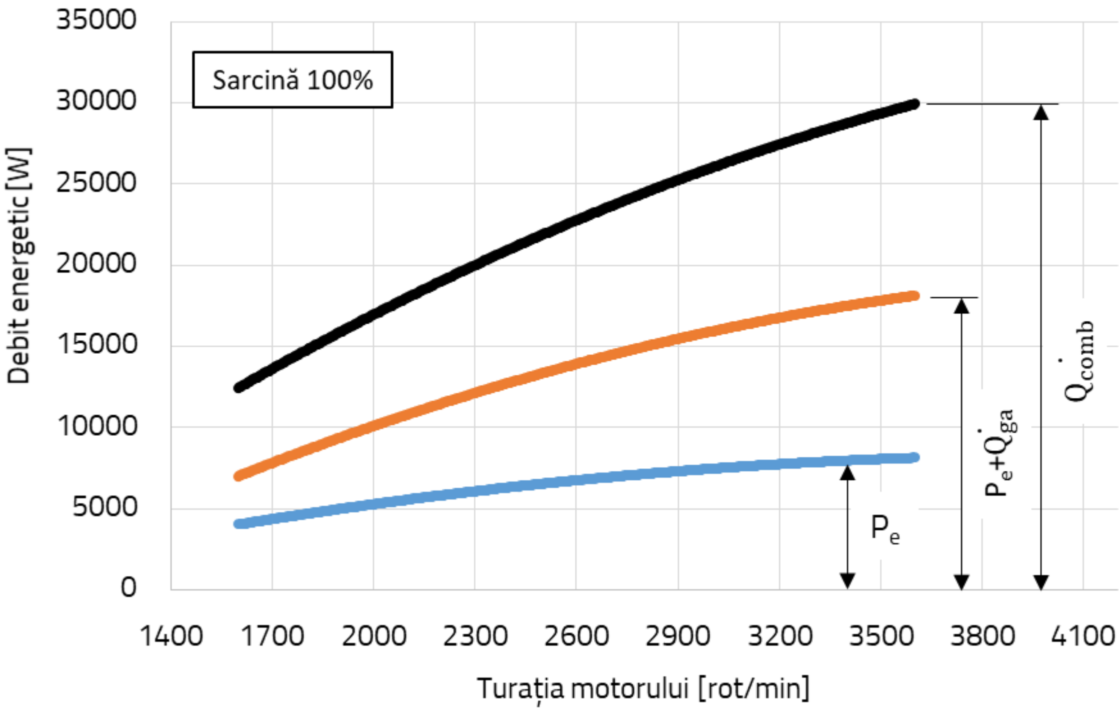

Fig. 5.1 Change in the main balance terms with speed, at full load

The term that represents the difference between the energy flow released by the complete combustion of fuel and the sum of the effective power and the heat flow evacuated by the exhaust gases is the extended cooling heat flow $\dot{Q}_{răce}$. At full load, the trends in the proportions of these quantities with increasing speed from 1600 to 3600 rpm, expressed relative to the energy of the fuel consumed per unit time, are the following: effective power, P_e decreases from 32,9% to 27,2% , the heat flow evacuated by the exhaust gases $\dot{Q}_{ga}$ increases from 25,1% to 33,1%, and the extended cooling heat flow, $\dot{Q}_{răce}$, decreases from 41,9% to 39,7%. Having the same balance terms considered previously in Figure 5.1, Figure 5.2 depicts the shape of the representative curves specific to turbocharged operation.

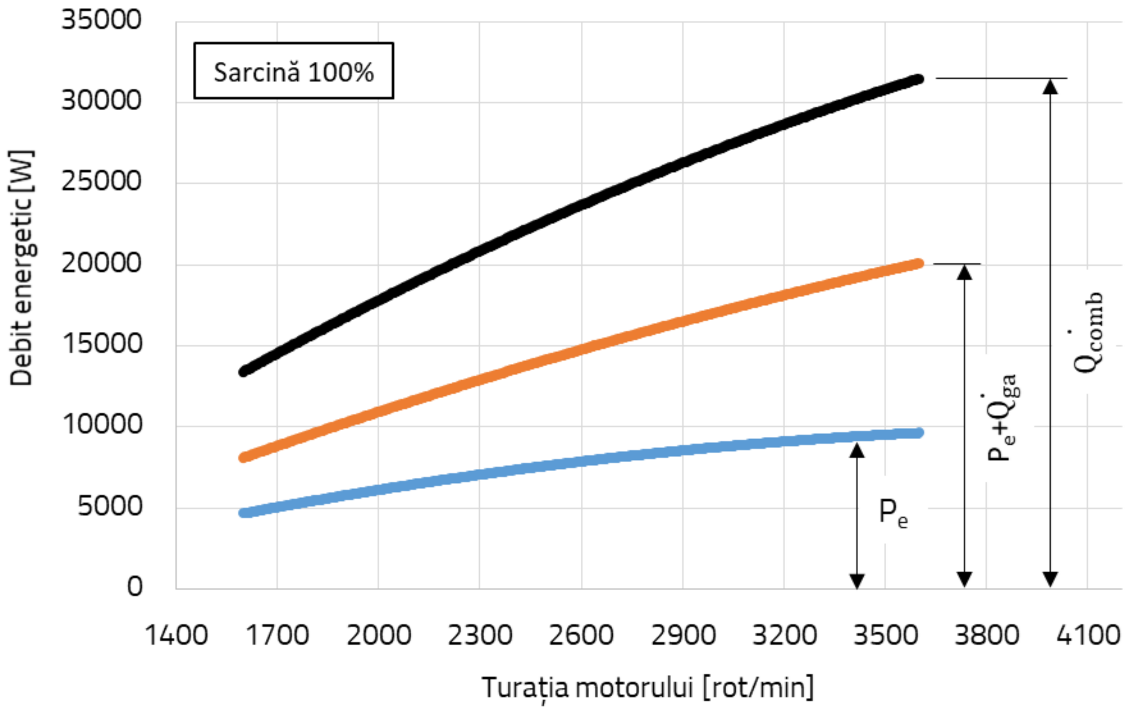

Fig. 2.2 Change in the main balance terms with speed, at full load

At full load, the evolution trends of the proportions of these quantities with increasing speed from 1600 to 3600 rpm, expressed relative to the energy of the fuel consumed per unit time, are the following: effective power, P_e decreases from 35,8% to 30,42%, the heat flow evacuated by the exhaust gases $\dot{Q}_{ga}$ increases from 25,3% to 33,4%, and the extended cooling heat flow, $\dot{Q}_{răce}$, decreases from 38,8% to 36,2%. Compared to the balance of the N variant, the T variant with increasing speed registers better utilisation of fuel energy, the averages of the percentages of the T terms compared to their N counterparts increasing by 3,2% for P_e and decreasing by 1,2% for $\dot{Q}_{ga}$ and by 2,4% for $\dot{Q}_{răce}$.

Heat transfer in combustion engines is a complex phenomenon that influences the effective efficiency, the thermal load of the components and the level of pollutant emissions.

According to the analysis of the energy balance terms (Chapter 2), the residual term, Q_{rez}, which closes the balance, has a proportion of the fuel energy estimated by different references, as follows: 2,6% [31], 6,8% [33], 8,16% [32, 105]. This term includes several constituents, of which **the heat transfer by convection and radiation from the engine surfaces to the environment $\dot{Q}_s$** is the most significant in energetic magnitude. The experimental evaluation of the heat transfer by convection-radiation from the engine surfaces to the environment , $\dot{Q}_s$, can be done starting from the data of the AVL 5402 engine, measured during the tests described in Chapter 3, and reported as a percentage of the fuel energy. The heat transfer from the engine surface to the environment $\dot{Q}_s$ has two components, one produced by thermal convection, $\dot{Q}_c$, and the other by thermal radiation, $\dot{Q}_r$.

$$\dot{Q}_c = \alpha_c(t_{pm} - t_f)A_{ef} \quad [W]$$

$$\dot{Q}_r = \varepsilon_r C_N \left[\left(\frac{T_{pm}}{100}\right)^4 - \left(\frac{T_f}{100}\right)^4\right] A_{ef} \quad [W]$$

$$\dot{Q}_s = \dot{Q}_c + \dot{Q}_r$$

in which α_c – the convective heat transfer coefficient, A_{ef} – the effective area of the engine block surface, ε_r - the energetic emission coefficient by radiation of the engine block surface (emissivity), C_N - the radiation coefficient of the absolute black body (Stefan-Boltzmann constant), and T_{pm} and T_f are the mean absolute temperatures of the engine block surface and the surrounding air, respectively. For the particular case of the engine speed of 2000 rpm at full load, the local temperature of the engine block was measured with an infrared thermometer at multiple points, the temperature varying between 85 and 91°C (Fig. 5.3).

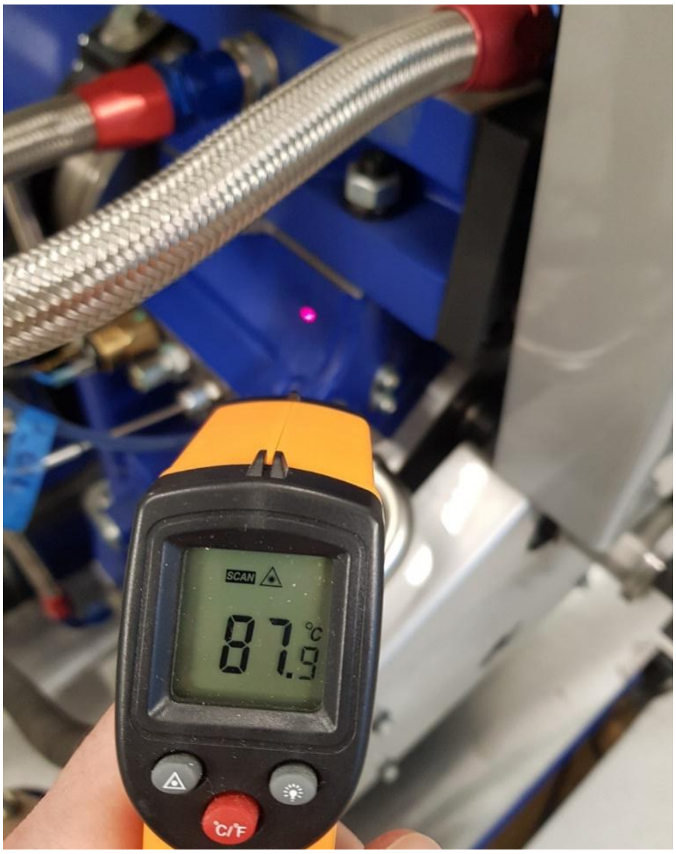

Fig. 2.23 Reading the exterior temperature of the AVL 5402 engine block

For the average surface temperature of 88°C, and the ambient temperature of the laboratory of 28°C, calculations were performed, resulting in the following conclusions:

a. The share of the radiant term in the heat transfer ($\dot{Q}_r/\dot{Q}_s$) is only 2.48%, the convective transfer being dominant.

b. Reporting $\dot{Q}_s$ to the energy flow corresponding to the fuel represents 6,6%, a value quite close to the range of values of the residual term, Q_{rez}, which includes $\dot{Q}_s$, according to the four references [31-33, 105].

A numerical evaluation of heat transfer through the surface of the exhaust manifold was performed for the D30 engine, using the COMSOL Multiphysics software. Modelling involved defining the manifold geometry, material and fluid properties, boundary conditions, and generating a finite element mesh. The simulation results (Figure 5.4) illustrated the distribution of temperature, velocity, and pressure of the exhaust gases in the manifold.

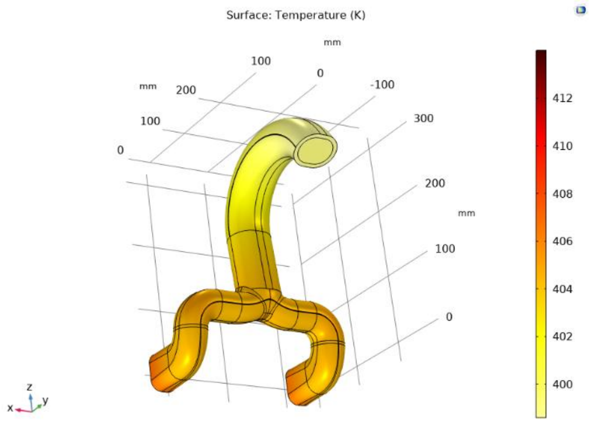

(a)

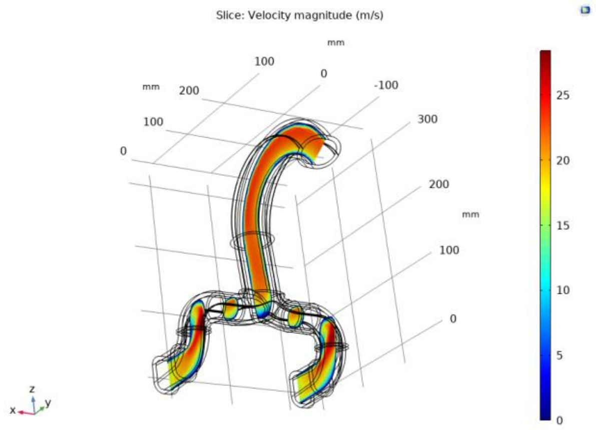

(b)

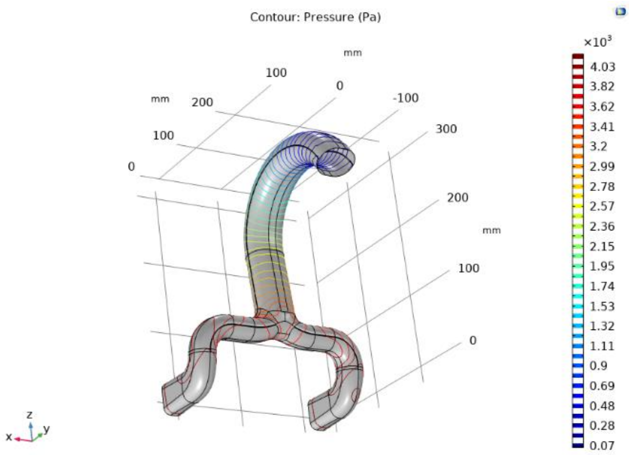

(c)

Fig. 2.24 Results of exhaust gas flow simulation through the exhaust manifold

A significant decrease in temperature was observed at each bend, attributed to the increase in local pressure and the favouring of heat transfer by convection. The increase in section at the intersection of the exhaust pipes also affected the cooling of the gases. Model validation was performed by comparison with experimental measurements (infrared thermal scanning).

Mechanical losses include losses due to friction between engine parts, losses from driving various auxiliary systems, as well as pumping losses; the prediction of these losses uses simple and fast calculations, with a few of the main engine variables, being expressed through the mean effective pressure of inherent resistances, p_{rp}, dependent on the mean piston speed, w_{pm}, the maximum pressure in the combustion chamber p_{max}, the speed n, and the compression ratio ε. A series of five empirical formulas were analysed comparatively with experimental data extracted from the INAR test bulletins, leading to **four new equations**, adapted to the characteristics of the engines investigated in this work**:**

$p_{rp} = 1{,}113 + 0{,}118 \cdot w_{pm}$ (1), in the bar

$p_{rp} = 0{,}749 + 0{,}1629 \cdot w_{pm} + 5 \cdot 10^{-8} x p_{max}$ (2), in the bar

$p_{rp} = -13600 + 29{,}4 \cdot n + 0{,}016 \cdot p_{max}$ (3), in Pa

$p_{rp} = 85{,}1 + 48 \cdot (\frac{n}{1000}) + 0{,}4 \cdot w_{pm}^2$ (5), in kPa

The chapter also explores the possibility of predicting mechanical losses for untested engines using global formulas calibrated based on data from the tested engines.

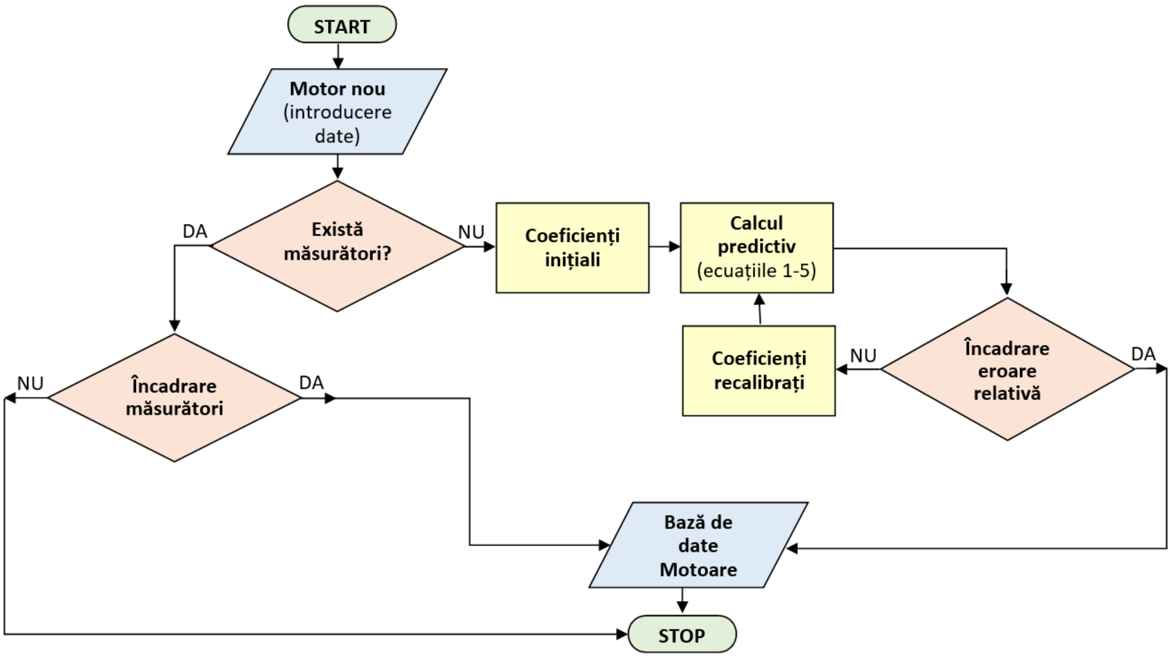

Fig. 5.5 Database operation algorithm

The proposed algorithm (Figure 5.5) involves the iterative application of empirical formulas and the calibration of their free term to minimize the error compared to the average mechanical losses of the tested engines. As a result of the analytical determination of these mechanical losses, a new exergy term was generated in the initial exergy balance, Π_m, which is calculated with the formula proposed in reference [36]. After normalising by the fuel exergy and subtracting the pumping losses, the loss due to the irreversibility of the friction processes results; this becomes $\bar{\pi}_f$:

$$\bar{\pi}_f = \bar{\pi}_m - (\bar{\pi}_{la} + \bar{\pi}_{le})$$

Table 5.1 includes, based on the calculations presented in the heat transfer evaluation, the situation of the analysed engines from the point of view of how the mechanical losses were calculated, as well as the percentage of mechanical losses due to the irreversibility of friction processes, $\bar{\pi}_f$, reported to the fuel exergy, a fact which was achieved by dividing the percentages from the energy balance by the previously calculated constant, 1,07.

Tab. 5.1 Losses associated with friction in the engine, $\bar{\pi}_f$

Engine	Intake Type	Method	$\bar{\pi}_f$[%]	
			At the rated speed	At maximum torque speed
D127	N	Prediction	12,10	7,83
	T	Prediction	12,97	11,02
392	N	Prediction	11,17	7,40
	T	Experimental	13,93	9,15

550	N	Experimental	10,26	7,38
	T	Experimental	11,48	8,48
	RI	Experimental	11,24	7,47
1035	T	Prediction	10,44	7,26
1070	RI	Experimental	10,68	7,03
1230	RI	Prediction	8,61	6,28
1240	T	Prediction	11,18	7,45
1380	T	Experimental	10,48	6,36
	RI	Experimental	10,25	7,02
D30	N	Prediction	9,49	-

Combustion efficiency can be calculated if the quantities of combustion products CO (carbon monoxide), HC (hydrocarbons), PM (particulate matter) are known. Carbon monoxide releases 10,16 MJ/kg through combustion; the released hydrocarbons are considered to be compositionally close to the hydrocarbons present in the fuel, therefore it is accepted that they have lower heating values close to those of diesel fuels and gasoline (42-44 MJ/kg). Particulate matter emitted by diesel engines has a more diverse chemical composition, however, it is accepted that 75% is represented by amorphous carbon, and 24% by heavy hydrocarbons [121]. A heating value of 32,8 MJ/kg is attributed to carbon, and for heavy hydrocarbons the heating value of fuel oil, of 40,9 MJ/kg. Thus, the efficiency of combustion or combustion η_c can be calculated with the following formula:

$$\eta_c = 1 - \frac{\sum g_i H_{ij}}{(\dot{m}_{cb}/(\dot{m}_{cb} + \dot{m}_a))Hi_{cb}}$$

where: j = CO, HC, PMc (carbonaceous particles), PMh (particles from heavy hydrocarbons), g_j – the mass fraction of component j in the exhaust gas, H_{ij} – the lower calorific value (mass) of component j or fuel, $\dot{m}_{cb}$ - the mass flow rate of fuel, $\dot{m}_a$ – the mass flow rate of air.

The results of two combustion efficiency calculations for two engines, technologically three decades apart, 1240-V8-DT and AVL 5402, based on the previously presented formula, are presented. The previously presented lower heating values were used, and for diesel fuel 42,5 MJ/kg was considered. Both engines were tested in the same 13 representative stationary regimes described by European Regulation No. 49 [125], a fact which allowed the comparison of the results. The calculation results are based on the pollutant emissions involved in the oxidation process of the two investigated engines and on the combustion efficiency formula, being presented in Table 5.2.

Tab. 5.2 Combustion efficiency and pollutant emissions

Engine	CO [g/kWh]	HC [g/kWh]	PM [g/kWh]	η_c
1240-V8- DT	3,82	0,76	1,93	0,982
AVL 5402	4,4	0,275	0,106	0,996

In conclusion, **according to the data in Table 5.2**, it is confirmed that the loss is about 2% as predicted by the reference [31], contemporary with the 1240-V8-DT engine.

The methodological novelty presented is the differentiation of the calorific value of particles based on their composition (carbon and heavy hydrocarbons), which improves the accuracy of the calculation of combustion efficiency.

Part 2 evaluates more precisely the influence of the fuel exergy, the quantity to which the exergy terms are normalised.

Diesel was considered to be mainly made up of carbon and hydrogen, neglecting impurities such as sulphur, nitrogen, and oxygen.

Compositional variation has led to a variety of exergy evaluation formulas, with approaches based on choosing a representative hydrocarbon (e.g., dodecane $C_{12}H_{26}$) or expressing the number of atoms with decimals ($C_{14,4}H_{24,9}$).

The most accepted approach, used in the thesis, expresses the chemical exergy of the fuel (A_{cb}) as a function of the lower calorific value (H_i) and the chemical composition in the form of $C_zH_yO_pS_q$:

$$A_{cb} = H_i \left(1{,}0401 + 0{,}01728\frac{y}{z} + 0{,}0432\frac{p}{z} + 0{,}2196\frac{q}{z}(1 - 2{,}0628\frac{y}{z})\right)$$

Although there is no scientific explanation, it is worth noting that the proportionality coefficient, which is valid for many liquid petroleum fuels: the value of 1.07 of the ratio Acb / H_i coincides with the ratio of the upper calorific value to the lower calorific value, H_s / H_i, which can lead to approximation of the fuel exergy with the upper calorific value $A_{cb} \approx$ Hs .

The exergetic study of **the heat transfer in the cylinder** during the compression, expansion and combustion process generated **three new exergetic terms** $\bar{\pi}_{Q_{ar}}$ through the walls of the combustion chamber and the cylinder during the combustion processes, $\bar{\pi}_{Q_c}$ in the compression process and $\bar{\pi}_{Q_d}$ in the expansion process.

The extension of the exergy balance involved normalising the existing terms to the fuel exergy, using a correction factor of 1,07, and the addition of the exergy term for the mechanical losses of the engine $\bar{\pi}_f$, as well as the three exergy terms for the heat losses from the cylinder, $\bar{\pi}_{Q_{ar}}$, $\bar{\pi}_{Q_c}$, $\bar{\pi}_{Q_d}$.

It is worth mentioning that in the new Sankey diagrams, the representation of the loss associated with combustion efficiency η_c was neglected, being estimated as being less than 1%.

A new term is added to the four distinct terms described above, $\bar{\pi}_x$, which designates indeterminate exergy losses that are not explicitly included in the exergy balance.

In conclusion, compared to the initial exergy model, by adding **the four new exergy terms**, the engine loss profile becomes clearer, more detailed, as can be observed in Figure 5.6 for the analysis of the 550-L6-DTI engine at full load regimes corresponding to maximum torque speed and nominal speed.

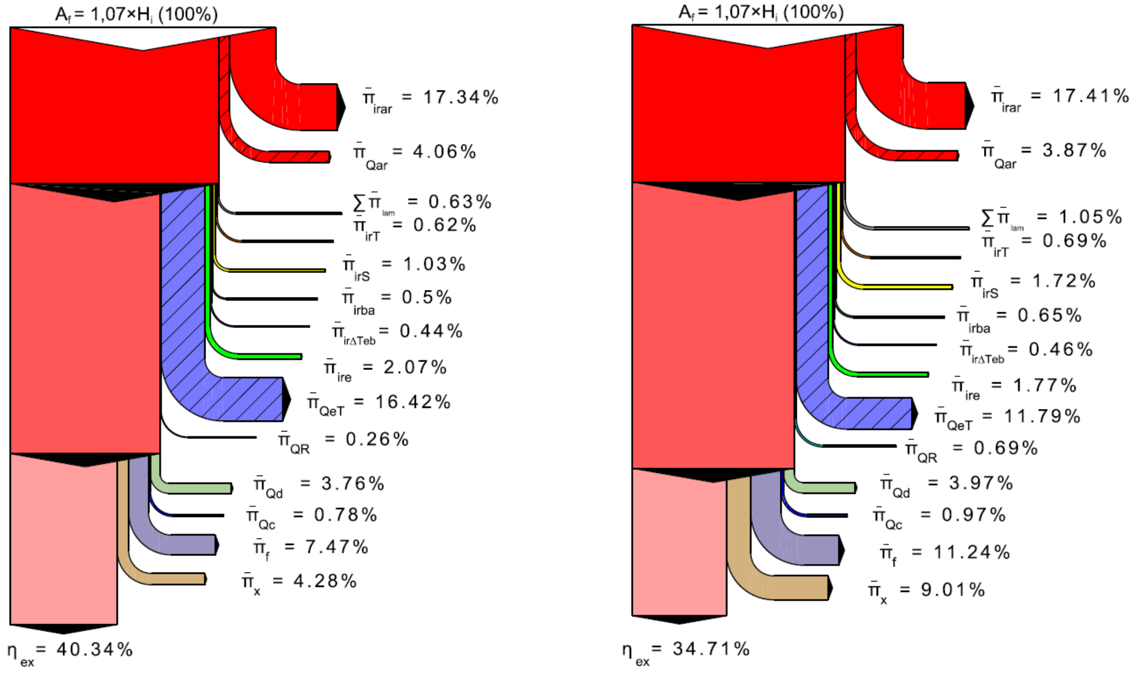

a. Maximum torque speed - 1700 rpm b. Rated speed - 2600 rpm

Fig. 5.6 Extended exergy balance of the 550-L6-DTI engine

6. ENERGY RECOVERY FROM THE EXHAUST GASES

6.1. Energy recovery methods

To harness the full energy potential of internal combustion engines, the principle of "Waste Heat Recovery" (WHR) has become increasingly known, making it possible to improve the overall efficiency of the internal combustion engine by converting wasted heat into ordered energy. Evidently, not all the energy released from the combustion of fuel in the engine cylinders can be recovered, but even a tiny fraction of it can contribute significantly to conserving the planet's energy resources. Exhaust gases that are released into the atmosphere through the exhaust system or gases recirculated through the EGR system, heat losses from the engine's cooling and lubrication systems, or even radiation emitted from its surface, all can be considered sources of waste heat in the internal combustion engine [134]. Figure 6.1 presents conventional methods for recovering waste heat from internal combustion engines. These technologies can be classified as passive or active technologies, depending on whether the heat is used directly at the same or a lower temperature, or is transformed into another form of energy or to a higher temperature [135]. Heat exchangers and Thermal Energy Storage (TES) systems are among the most used passive technologies for heat recovery, being capable of constantly transferring energy, either by storing it and/or releasing it on demand. Turbocompound systems, heat pumps, thermal power cycles, and thermoelectric generators are considered active technologies.

The dotted connections in the figure represent the possibility of bypassing certain technologies in the process of obtaining mechanical work or electrical energy.

These technologies are useful not only in the transport sector, but also in the industrial sector, each with its advantages related to available space, the recoverable energy source depending on temperature and heat flow, as well as costs [136].

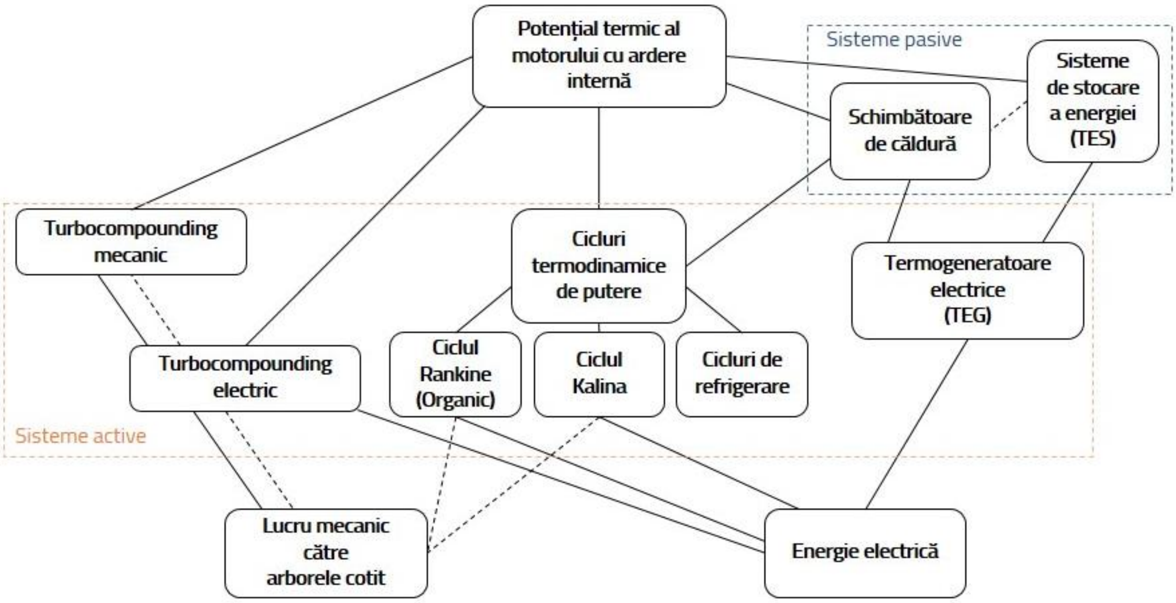

Fig. 6.1 Waste heat recovery technologies (Adaptation after [135, 136])

Table 6.1 shows the advantages and disadvantages of the main energy recovery systems, adapted according to the [163], [162].

Tab. 6.1 Energy recovery technologies. Advantages and disadvantages

	Advantages	Disadvantages
Thermoelectric generator (TEG)	- Operational safety - They do not produce noise - They do not produce harmful emissions - Do not depend on the type of the heat source - They can be mounted and oriented in any direction - Direct heat conversion - Compact size	- Low conversion rate (4-10%) - Cost per watt generated (€8.4/W) [141] - Dependent on system construction
The Rankine Cycle applied to M.A.I.	- Operating range (100-500 °C) according to internal combustion engines - Considered to perform better than other power cycles such as Kalina or conventional Rankine - Simplicity of design - Conversion rate 10%-46% [151]	- Requires operational safety measures due to working fluids with potential for environmental pollution - Overall dimensions and weight

Turbocompounding	- Low specific fuel consumption - Simple design - Suitable for operation at high speeds and loads [163] - Conversion yield 68-88% [175] - Low volume	- Considerably increases the resistance to the exhaust gas flow - At low loads, specific fuel consumption is worse than the non-turbocompound configuration
Energy storage devices	- High energy storage capacity - Long energy storage period - Reduces engine operation at high load by using stored heat and reduces heat released to the environment - Can be used concurrently with other energy recovery systems	- Desynchronization between energy demand and energy availability - Design complexity - High upfront and maintenance costs - Increased wear according to charge-discharge cycles - Long charging and discharging time for latent heat storage.

6.2. Sources of energy recovery. The case of internal combustion engines

The main energy sources of the heat engine that could be used for recovery are exhaust gases, recirculated exhaust gases (EGR), boost air, coolant, lubricants and the outer surface of the engine, which during operation can reach a considerable temperature of over 90°C.

Energy recovery is greater the higher the temperature of the hot source, therefore the recovery sources of thermal engines are divided into two categories, high potential and low potential, the former being much more efficient and comprising only the exhaust gases themselves and the exhaust gases recirculated through the EGR system.

The heat transformation factor is associated with the theoretical degree of energy recovery (1-T0/T), having values for an ambient temperature T_0 of 20°C, included in Table 6.2.

It can be observed that there is a similarity of data for the same type of source, as well as a clear separation of the sources based on the level of energy potential.

For the three detailed engines, the exhaust gases themselves and the recirculated ones reach high recovery potential values of 0,39-0,67 by combination, while the low potential sources cover the range (0,09-0,22) by combination.

On average, hot sources have 3,42 times greater energy recovery potential than less hot sources, a fact which is decisive in the selection process of the recovery procedure.

Tab. 6.2 Thermal characteristics of the heat sources in diesel engines [122, 160, 176]

Hot source	Burnt gases	Recirculated exhaust gas (EGR)	Lubricant	Coolant	Boost air	Engine surface
6-cylinder diesel engine, 243 kW [160]						
T hot source, K	479-744	555-867	363-373	347-357	330-426	-
Factor (1-T0/T)	0,389-0,606	0,472-0,662	0,193-0,214	0,156-0,179	0,112-0,312	-
1240-V8-DT diesel engine, 265 kW [122]						
T hot source, K	453-833	-	358-375	349-354	-	-
Factor (1-T0/T)	0,353-0,648	-	0,182-0,219	0,160-0,172	-	-
Diesel engine 392-L4- DTI, 93kW, [176]						
T hot source, K	490-803	-	351-373	351-368	322-375	-
Factor (1-T0/T)	0,402-0,635	-	0,165-0,214	0,165-0,204	0,09-0,219	-
AVL 5402 diesel engine, single-cylinder, 8 kW						
T hot source, K	632-771	-	362-364	344-377	-	330-364
Factor (1-T0/T)	0,568-0,620	-	0,190-0,195	0,148-0,223	-	0,112-0,195

In the situation of engines or other industrial systems with large installed capacities, the selection of energy recovery procedures could also lean in favour of colder sources, if the flow rates of the thermal agents were large enough to ensure the profitability of the recovery. For systems recovering unused energy from fuel combustion (WHRS), in an internal combustion engine there are two main sources that can be exploited: the exhaust gases and the other hot sources (Table 6.2). The former are considered to have high potential for recovery due to the larger temperature differences compared to that of the ambient environment, but because the exhaust system contains emission reduction devices (oxidation catalysts, selective catalytic reduction systems for NOx, particulate filters) which reach their maximum efficiency at high temperatures, the use of WHRS could interfere with their functioning. For road vehicles, energy recovery from exhaust gases depends on the engine operating regimes, and the evaluation of the potential for recovering lost heat can be best performed starting from experimental data collected from an engine test stand.

6.3. Evaluation of exhaust gas exergy

The exergy of a thermal agent in continuous flow and steady state is considered as a sum of the physical exergy, the kinetic exergy, the potential exergy, and the chemical exergy. Kinetic and potential exergy have formulas identical to those of the respective energies; usually these have very low values and are neglected. Chemical exergy is the specific exergy of the fuel.

Physical exergy is given by the relationship [177]:

$$E = (I - I_0) - T_0(S - S_0)$$

The quantity $(I - I_0)$ is the difference between the enthalpy of the thermal agent at the state characterised by parameters (*p, T*) and the enthalpy of the thermal agent at equilibrium with the ambient environment (p_o, T_0), and $(S - S_0)$ is the difference of analogous entropies. The calculation of the quantity *E* is dependent on the specific values of the agent, available in thermodynamic tables. In this chapter, the subscript *g* will be used instead of *ga* for exhaust gases to be in accordance with already published formulas and graphs. By normalising the equation to unit time and to the specifics of the exhaust gases, the equation is obtained::

$$\dot{E_g} = \dot{m_g}\left[c_{pg}(T_g - T_0) - T_0(s_g - s_0) + \frac{v_g^2}{2} + gh\right]$$

in which $\dot{m_g}$ is the mass flow rate of the exhaust gases, T_g is the absolute temperature of the gases, *s* is the specific entropy, *v* is the gas velocity, *h* is the height of the system relative to the ground surface, and *g* is the gravitational acceleration. Particularising for the entropy variation, the exergy flow rate $\dot{E_g}$ can be written as follows:

$$\dot{E_g} = \dot{m_g}\left[c_{pg}(T_g - T_0) - T_0\left(c_{pg}\ln\left(\frac{T_g}{T_0}\right) - R_g\ln\left(\frac{p_g}{p_0}\right)\right) + \frac{v_g^2}{2} + gh\right]$$

In literature there is a series of derived indicators of this quantity which allow normalising to the energy flow from the exhaust gases or to the exergy flow of the fuel; the first quantity, δ, is called the exhaust efficiency, first defined in work [38] as the ratio between the exergy of the exhaust gases E_g and the thermal energy of the exhaust gases Q_g. This ratio shows the percentage of exhaust gas energy that can be transformed into useful mechanical work in an ideal energy recovery system, being recognised and intensively used in articles dedicated to energy recovery [166]:

$$\delta = \frac{\dot{E_g}}{\dot{Q_g}}$$

The second indicator, ε, compares $\dot{E_g}$ in relation to the chemical exergy introduced into the engine by the fuel, being relevant in determining the amount of energy possible to be extracted using an ideal energy recovery system, from the exergy of the fuel used:

$$\varepsilon = \frac{\dot{E_g}}{A_{cb}\dot{m_{cb}}}$$

6.4. Evaluation of the energy recovery potential of the AVL 5402 engine in relation to engine operating cycles

The conversion of heat into mechanical work depends on the Carnot cycle efficiency, which is defined as the maximum efficiency of a thermal engine operating in a completely reversible cycle between two temperatures of the hot source and the cold source. The variation of the cold source, usually the atmospheric temperature, is quite small, so the Carnot cycle efficiency depends mainly on the highest temperature in the cycle. This explains why waste heat recovery applied to exhaust gases at 450-600°C is 2-4 times greater than that of waste heat recovery from the coolant or lubricant, i.e., 80-90°C, the calculation being done in the absolute Kelvin temperature scale. For the operation of the naturally aspirated AVL 5402 engine, at full load, the temperature curves of the exhaust gases, coolant, and lubricant are represented in Figure 6.2.

The considerable difference between the temperatures of the combustion gases compared to those of the coolant and lubricant explains the disadvantageous recovery potentials of the latter.

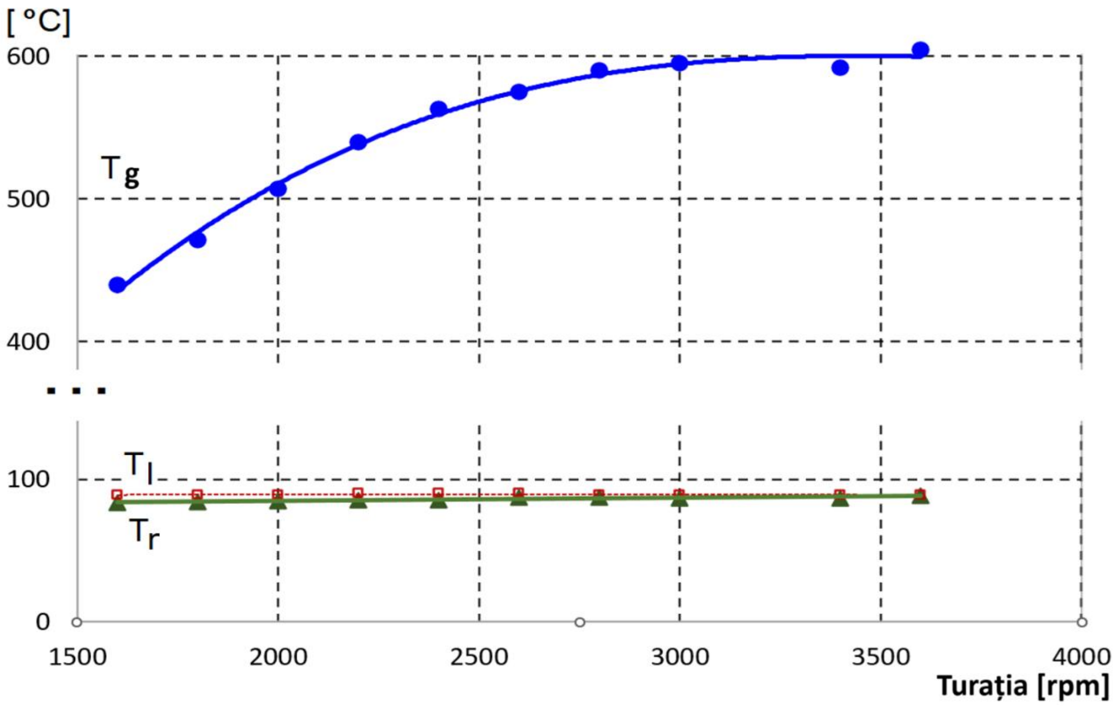

Fig. 6.2 Variation of exhaust gas (T_g), lubricant (T_l), and coolant (T_r) temperatures at full load

The operating conditions of the investigated engine and the corresponding calculations correspond to those described in the analysis of the experimental data resulting from the testing of the naturally aspirated (N) AVL-N engine, for all operating regimes, at speeds in the range 1600-3600 rpm and at loads of 25%, 50%, 75%, and 100%, for each speed.

The calculation of the exergy $\dot{E_g}$ is based on the following equation, with the kinetic and potential energy terms being neglected:

$$\dot{E_g} = \dot{m_g}\left[c_{pg}(T_g - T_0) - T_0\left(c_{pg}\ln\left(\frac{T_g}{T_0}\right) - R_g ln\left(\frac{p_g}{p_0}\right)\right)\right]$$

Exhaust gas temperature has a determining contribution in both energy analysis and exergy analysis. By applying the previously presented equations, as can be observed in Figure 6.3, for the nominal regime the increase in temperature leads to a tripling of the transferred energy flow rate $\dot{Q}_g$, as well as the exergy flow rate $\dot{E_g}$.

Technical literature has noted that exhaust gas temperature increases significantly with speed, being reported in numerous references in the field, such as [180] for diesel engines normally used in trucks under maximum load conditions and [181] for driving cycles of heavy-duty vehicles.

Regarding speed and load, as represented in Figure 6.4, the energy flow rate of the exhaust gases increases with both parameters, the influence of speed being greater than that of load [91].

For a speed range between 1600-3600 rpm, reported relative to the initial values, $\dot{Q}_g$ increases on average by 2,7 times, for all loads; for the load range 25-100%, $\dot{Q}_g$ increases on average by 1,9 times, at all speeds.

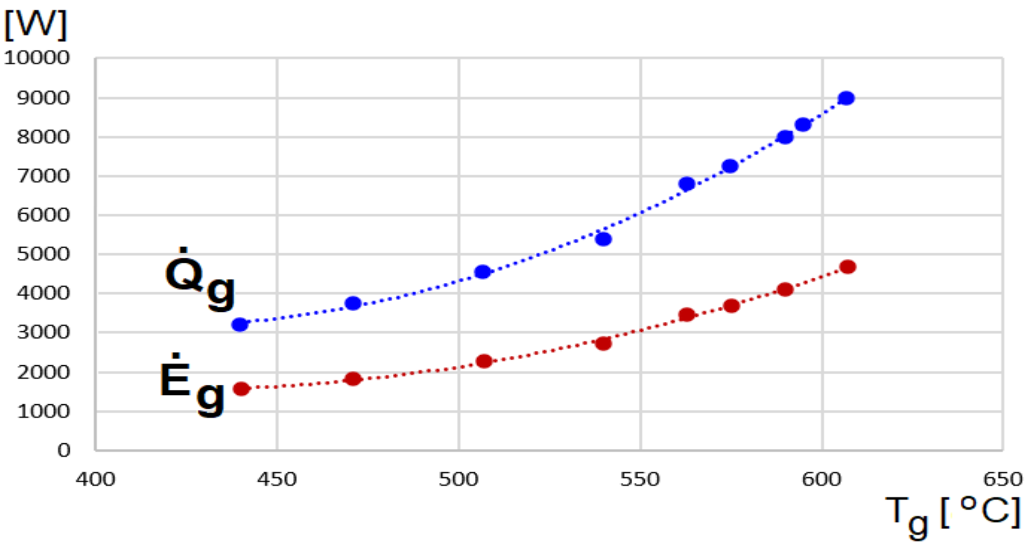

Fig. 6.3 Energy flow rate $\dot{Q}_g$ and exergy flow rate $\dot{E}_g$ as a function of temperature T_g

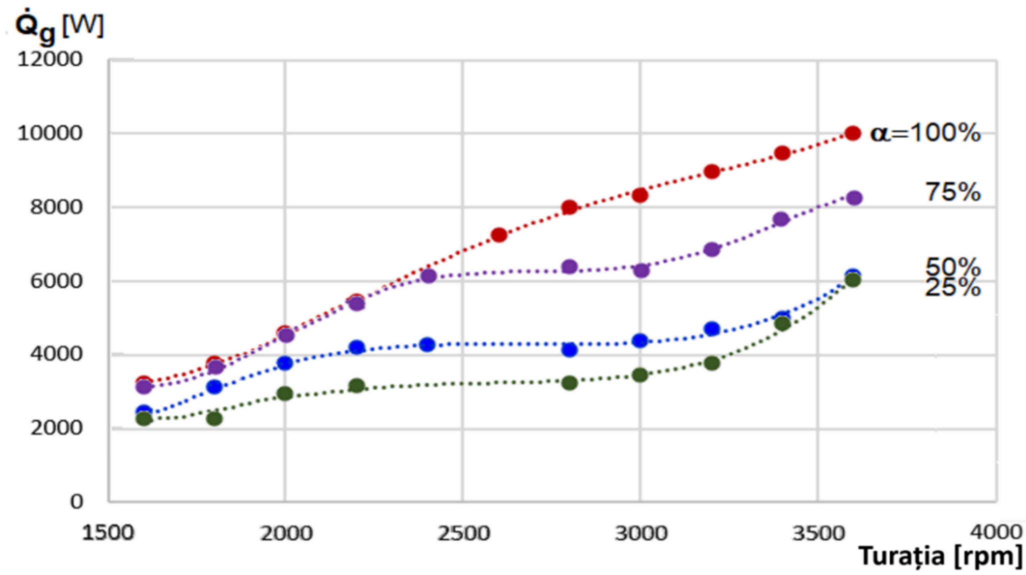

Fig. 6.4 Exhaust gas energy flow rate $\dot{Q}_g$ as a function of speed and load

The values of the exergy flow rate, $\dot{E}_g$, present profiles quite similar to those of the graph for $\dot{Q}_g$, as can be observed in Figure 6.5, but with lower values. The influence of speed and load on the exergy flow rate is quite similar to that of $\dot{Q}_g$. Similar to previous results, $\dot{E}_g$, increases on average by 2,8 times with increasing speed for all loads; for the load range 25-100%, $\dot{E}_g$ increases on average by 2,1 times for all speeds.

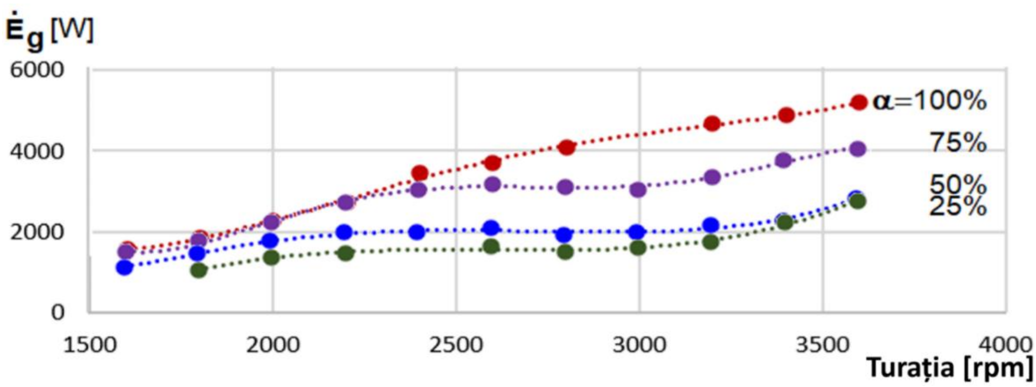

Fig. 6.5 Exergy flow rate $\dot{E}_g$ as a function of speed and load

The exhaust gas temperature was taken from the data generated by the AVL PUMA software. A graphical representation of the temperature evolution as a function of mean effective pressure and speed is presented in Figure 6.6. The increase in exhaust gas temperature with increasing mean effective pressure in the cylinder and engine speed can be observed.

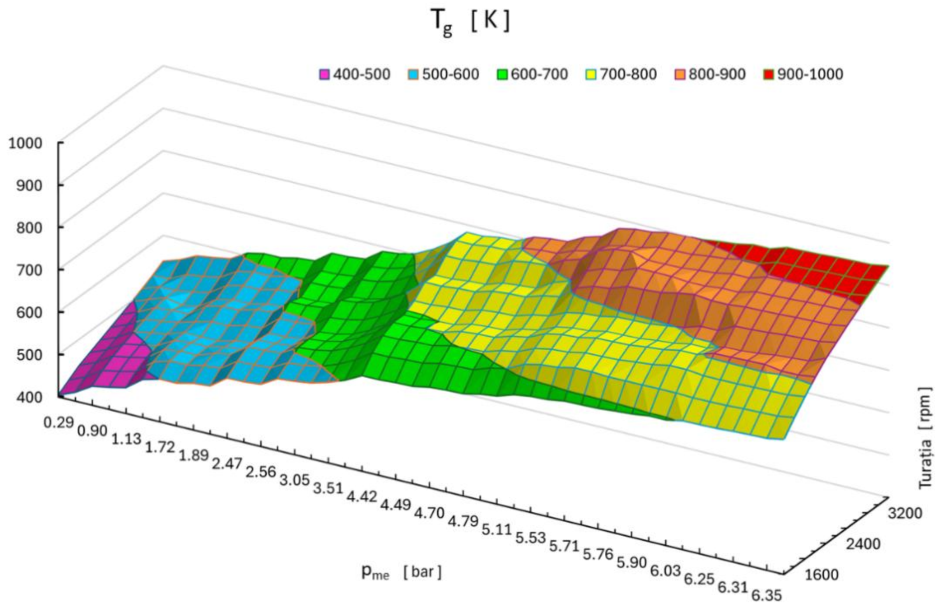

Fig. 6.6 Exhaust gas temperature depending on the average speed and effective pressure

The ratio between $\dot{E}_g$ and $\dot{Q}_g$, symbolised δ, shows the part of the exhaust gas energy that can be transformed into a convertible form of energy or exergy. It varies between (0,45-0,52), having lower values in the range of low loads and speeds. The value 0,5 is reached at maximum load and at speeds over 2400 rpm. The magnitude ε indicates how much of the fuel exergy survives the engine cycle and can be recovered. This percentage is quite small, between 11-20%, with the low values in the range being dominant for high loads – Figure 6.7.

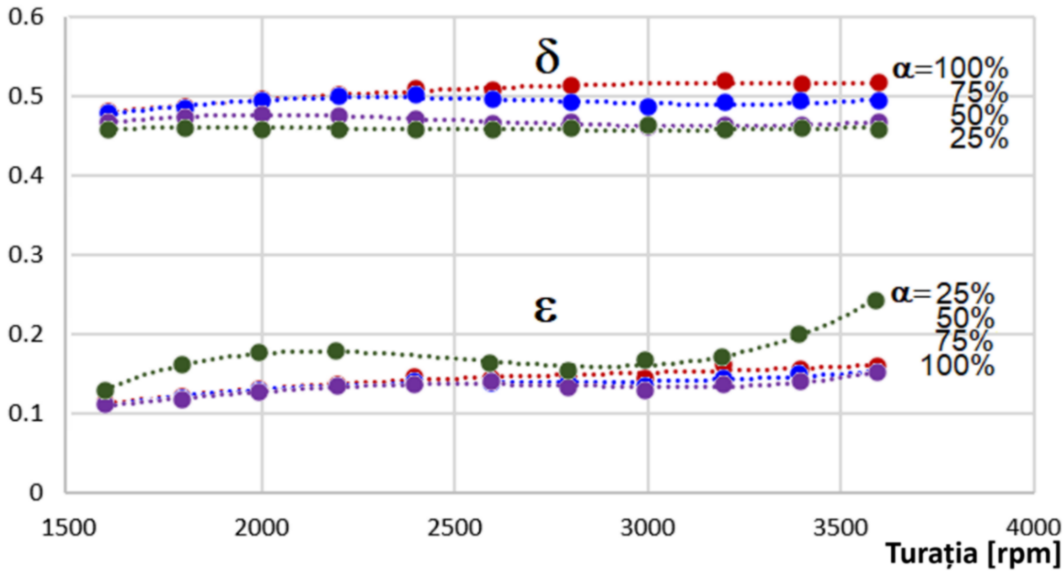

Fig. 6.7 Exergetic indicators by speed and load

The recovery of energy from the exhaust gases depends to a large extent on the flow rate and temperature level.

The maximum flow rate is registered at the highest speed, while the highest temperatures are influenced by speed and load. Through an ideal heat recovery system, the maximum energy recovered could be around 50% of the exhaust gas energy or the approximate equivalent of 11-15% of the fuel exergy.

6.5. Study of energy recovery potential in relation to engine operating cycles

For the case of thermal engines used for vehicle propulsion, the potential for energy recovery depends on the structure of the operating cycles, on the load and speed regimes. Limiting the object of the research to the case of road vehicle engines - primarily freight or passenger transport vehicles - the effect of the composition of different operating cycles on energy recovery is analysed below.

In this work, **two existing operating cycles established by European organisations** for measuring pollutant emissions were used, as well as **three representative cycles studied through regime monitoring in the operation of vehicle engines in Romania**, proposed by the Road Vehicle Institute Brașov [182]. The operating cycle of a vehicle is associated with its destination and refers to the type of service it performs. By performing load and speed measurements and applying regime monitoring, the temporal distribution of operating regimes for a specific route and type of service can be identified, establishing performance, pollution level, as well as **evaluating the potential for energy recovery**. The cycles used are the stationary cycle included in CEE-ONU Regulation No. 49 [125], the European test cycle ESC [184], as well as three cycles developed based on regime monitoring from Romania in urban traffic, traffic on mountain roads, and on highways [182]. In urban traffic, low speeds and low loads corresponding to idling and engine braking predominate as a result of frequent speed changes. On highways, high loads and speeds are predominant. On mountain roads, medium speed regimes around maximum torque are dominant, with loads towards the upper limit, corresponding to starts from full stop, alternating with low loads corresponding to idling and engine braking. Based on the defined cycles mentioned, their application to the data collected on the dynamometric stand for the 392-L4-DT engine [70] was carried out. The results demonstrated that energy recovery is more efficient when the engine operates at high loads and at medium and high speeds. The averaging of temperatures according to their temporal weight generated a representative value for each test cycle, illustrated in Figure 6.8.

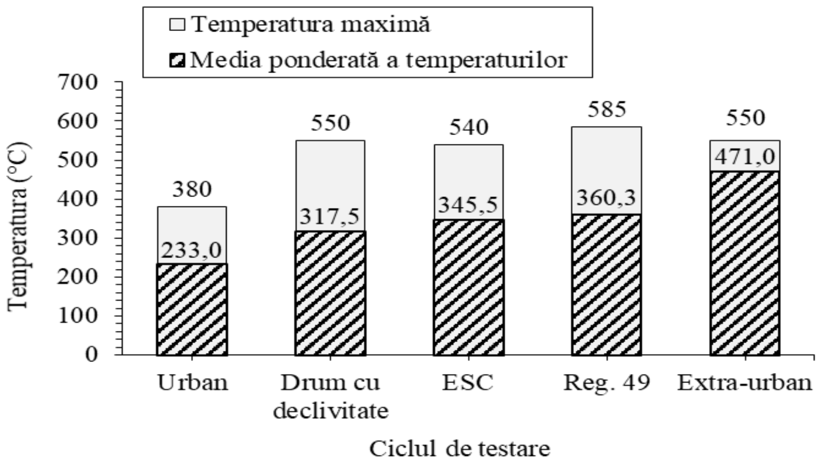

Fig. 6.8 Maximum and average exhaust gas temperature as function of the test cycle

The potential for energy recovery from exhaust gases depends on both average temperature and flow rate. The formulas used for determining the recovery potential are identical to those from section 6.4. A comparison of driving cycles based on the averaged exergy value (Figure 6.9) indicates their ranking based on the intensity of using high load and speed regimes. The extra-urban regime, specific to highway driving, proves to be the best performer in terms of energy recovery resource, being followed with a large difference by the other regimes. The most disadvantageous proves to be the urban regime, about 6 times lower.

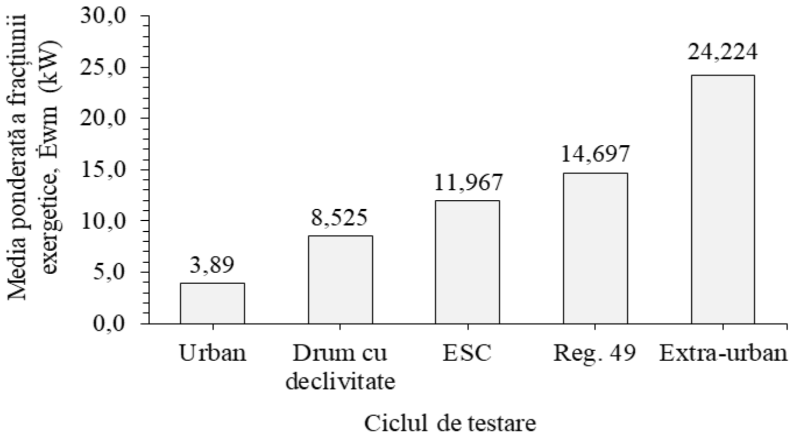

Fig. 6.9 Weighted average exergy rate in driving cycles

This ranking is maintained for the quantities δ and ε (Figure 6.10), for which the theoretical potential for energy recovery can reach 40% of the exhaust gas energy or over 12% of the fuel energy.

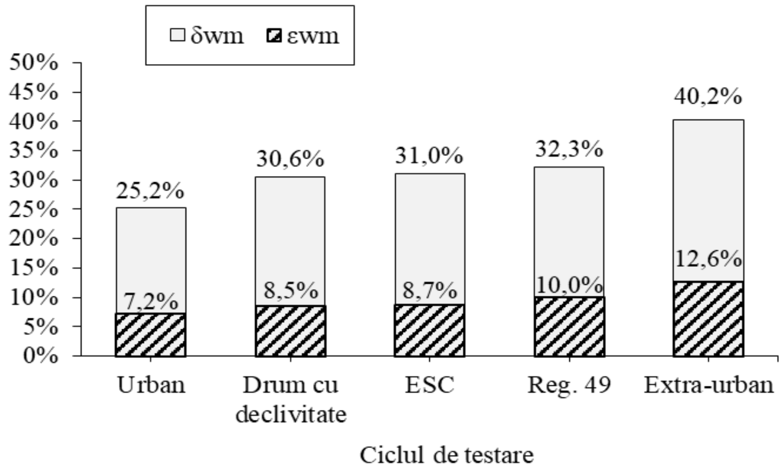

Fig. 6.10 Exergy normalised to exhaust gas energy (δ) and to fuel exergy (ε)

The control of engines using exergy-oriented techniques can be done by defining an exergy maximisation function, which is based on the detailed results of the study on the influence of parameters on the terms in the exergy balance (Chapter 4). The averaged ranking of the terms of the exergy balance for the most general case, of two turbocharged and intercooled engines from the INAR database, led to the following distribution of the terms:

Tab. 6.3 Hierarchy of exergetic terms - turbocharged and intercooled engines

	π_{irar}	π_{QeT}	π_f	π_{Qd}	π_{Qar}	π_{ire}	π_{irS}	Sum of laminations	π_{irT}	π_{irba}	π_{QR}	$\pi_{\Delta Teb}$
[%]	18,05	13,96	8,99	3,99	3,94	2,00	1,34	0,74	0,70	0,59	0,53	0,52
Order	1	2	3	4	5	6	7	8-11	12	13	14	15

It is observed that the first three terms have the largest weights, summing to 41% of the fuel exergy. Terms 4-7 follow, summing to 11,27%, then terms 8-15, under 1% each, summing to 3,08%.

Techniques for simultaneous reduction should be sought and applied to the first three terms. By defining a minimisation function for exergy losses $F = min(\pi_{irar} + \pi_{QeT} + \pi_f)$, the operating regimes (load, speed, compression ratio, etc.) that generate the local minimum values can be sought and found. The variation of the first two terms was specified in Chapter 4; the variation of the term π_f is predictable as a function of load if the influence of the excess air ratio, already investigated, is known, and π_f increases with increasing engine speed. These correlation functions of the parameters studied in Chapter 4 together with the minimisation function can generate individual correlation curves for each engine, which can be introduced as a supplementary function of the engine's central control unit (ECU) to prepare the engine to operate in those regimes with minimal exergy destruction and maximum energy recovery. The success of this method is predictable because the variations of the quantities π_{irar} and π_{QeT} are inverse to the variation of load, speed, and the air cooling degree in the intercooler.

7. CONCLUSIONS, CONTRIBUTIONS, RESEARCH DIRECTIONS

The main conclusions formulated follow the objectives of the thesis:

1. The effective efficiency of diesel engines resulting from the literature analysis, particularised for the case of heavy-duty vehicles used for freight transport, currently varies between 42-47%, in rare cases even exceeding 50%. By adding WHR systems, these engines gain approximately 5% on top of the effective efficiency without WHR. An increase of at least 10% in effective efficiency compared to those recorded in classical literature has been achieved over the last four decades.

2. There is a very good correspondence between the results reported in this work and the specialised literature, concerning the weights of the terms in the energy and exergy balances of the engines, which reinforces confidence in the numerical models, while confirming the variability of these terms with changes in environmental factors and constructive and functional factors.

3. Based on the data interpreted in detail in Chapter 4 and in accordance with Objectives 1.1-1.4, the following aspects regarding the variation of the engine's energy and exergy quantities with the modification of functional, constructive, and environmental parameters can be synthesised, while simultaneously considering the type of air intake system (N, T, RI):

- **Increasing the excess air ratio** has the same effect for all engine categories (N, T, RI) of decreasing the exergy loss of exhaust gases (π_{Qea}or π_{QeT}), concurrently with the increase of combustion irreversibility (π_{irar});

- **Increasing engine speed** has the same effect of simultaneous decrease of the heat evacuated by exhaust gases Q_{ea} or Q_{eT}, as well as the exergy loss associated with this heat, π_{Qea} or π_{QeT};

- **Increasing the compression ratio** is very efficient for naturally aspirated engines, registering significant and simultaneous reductions of Q_{ea}, π_{Qea}, π_{irar}; for turbocharged engines the same trends for Q_{eT}, π_{QeT}, π_{irar} are maintained, but with more modest reductions; for turbocharged and intercooled engines, the trends persist, but the reductions of the same terms are negligible.

- **Increasing the maximum cylinder pressure** $\boldsymbol{p_{max}}$ largely produces similar effects to increasing the compression ratio, by a simultaneous but modest reduction of both important quantities π_{irar} and π_{QeT} for N, T, RI engines. The adjusting of this parameter depends on the quantity of fuel injected corresponding to the isochoric combustion phase, a quantity that cannot be experimentally determined.

- **Atmospheric factors** influence through the variability of ambient temperature T_0 and pressure p_0; for N engines, by increasing atmospheric temperature T_0 there is an increase in π_{irar}, with π_{Qea} remaining almost constant; while for T engines, there is an increase in π_{irar}, with a decrease in π_{QeT}. Increasing atmospheric pressure leads in the case of N engines to an increase in π_{irar}, simultaneously with a decrease in π_{Qea}.

- **Increasing boost pressure,** $\boldsymbol{p_s}$, improves energy performance but does not produce notable effects on exergy terms.

- **Increasing the intercooling efficiency**, $\boldsymbol{\tau}$, decreases the loss of exergy from the exhaust gases π_{QeT}, increasing the combustion irreversibility π_{irar} to a lesser extent.

4. The level of knowledge of the terms in the energy and exergy balances was qualitatively and quantitatively increased, and the ranking of magnitude variations was done in accordance with Objectives 1.3, 1.5, and 2.3. New exergy terms were added, and the undetermined exergy term $\bar{\pi}_x$, which closes the exergy balance, had an average value for the 12 operating regimes detailed in Annex A.5.2 of 6,27%.

5. In accordance with Objectives 1.2 and 1.5, Chapter 5 presents the estimation of heat transfer from the cylinder, which follows the formalism of the established Nusselt-Reynolds equation and introduces an adapted proportionality coefficient for the studied engines. For the compression, combustion, and expansion processes, additional terms were added, which were quantified and included in the exergy balance. The evaluation of the engine's mechanical losses, based on data extracted from test reports (in cooperation with INAR), was confirmed with the help of a set of four numerical equations that determine with good precision, as well as a selection algorithm by comparison, generating a new exergy term. In total, **the proposed extended model added five new exergy terms**.

6. For five specific testing cycles depending on the category of the road, the energy and exergy flow rates of the exhaust gases were calculated for the engine tested at INAR Brașov. Both evaluations were convergent, demonstrating that high load and speed regimes have the highest energy recovery potentials, and the favourable cycle is the highway operation cycle, being followed in descending order by the cycle from CEE Regulation 49, the ESC cycle, the cycle on grade roads, and the urban cycle.

7. The complexity of processes in internal combustion engines affects the possibilities of energy recovery, only within a limited interval. For the case of the AVL 5402 engine that was tested, this potential for energy recovery from exhaust gases represented only 11-20% of the fuel energy.

For the case of engines with variable operating regimes with load and speed, such as engines used in the transport sector, regime optimisation functions included in the ECU are necessary to favour regimes with high recovery potential.

For the case of engines with stationary operating regimes (cogenerating units, motor pumps), the problem of energy recovery simplifies, with the stable regime that has the highest recovery potential being preferred, typically the nominal regime. Furthermore, these engines have the advantage that they can integrate energy recovery systems more easily, without having the weight and size limitations that engines for road vehicles have..

The main contributions made within the doctoral research, presented extensively in the thesis and capitalised on, mostly through publications in specialised journals and volumes of international conferences with a review committee, are the following:

- Development of **the thermodynamic, energetic and exergetic model of internal combustion engines**, through an extensive study of the current state of research in the field. Establishing the parameters of the model and related systems of equations – Chapter 2 [in accordance with Objective 1.1].

- Development **of an integrated calculation program** that incorporates in a computational structure the specific thermodynamic equations, energy and exergy models, developed in Chapter 2 [in accordance with Objective 1.2].

- Creation of a **database** consisting of the characteristics of vehicle engines developed by the INAR Research Institute of Brașov and manufactured at S.C. Roman S.A. This database, which became the documentary basis of the doctoral research regarding process irreversibilities in engines, was consolidated by extracting technical information from industry technical standards, from studies and test reports from the INAR archive. The information extracted from these test reports was essential for the in-depth critical study of energy models and their validation through detailed evaluation of energy and exergy terms.

- The result of running the integrated calculation program was **the generation of a first series of Sankey diagrams** that quantify the main terms of the exergetic analysis for the engines in the database; the generation of the diagrams was parameterized by using the Design Table module in the Catia v5 format that allows the association of multiple variables from the CAD system with a Microsoft Excel spreadsheet.

- **Instrumental integration of the test stand** for the energy analysis of the AVL 5402 motor, within ICDT – Research and Development Institute of Transilvania University. The experimental configuration was adapted to the requirements of the thesis which also required atypical measurements, in addition to the established engine tests, such as the measurement of engine surface temperature and air velocity near the engine surface [in accordance with Objectives 2.1 and 2.2].

- **Development of a test stand program** and structured acquisition of experimental data under the control of Puma Open software, AVL instrumental informatics system [in accordance with Objective 2.2].

- The integrated calculation program was also exploited by applying the method of small variations - of the main engine parameters - to study their influence on energy and exergy quantities, in Chapter 4. The results of these multi-variable investigations were structured according to the classification of engines into naturally aspirated (N), turbocharged (T), and turbocharged and intercooled (RI) engines. **The contributions consisted of determining the influences of environmental and constructive-functional factors on established engine quantities and on energy and exergy balance terms**. Thus, a ranking of the magnitude of exergy losses was also performed, which is very useful in the strategy for controlling energy recovery [in accordance with Objective 1.3].

- The dependence between the flow regime of the thermal agent and heat transfer from the cylinder was validated in Chapter 5, proposing **an original equation of Nu-Re invariants**, close to the established values in literature, an equation supported by the results of the analysis of the engine batch [in accordance with Objectives 1.2 and 1.5].

- **The quantification of heat loss through the engine's exterior surfaces, Q_s**, (Chapter 5), a quantity little studied in literature, an important component of the residual term in the energy balance, was experimentally investigated for the case of the AVL 5402 engine. Comsol Multiphysics was used for simulating heat transfer from the exhaust manifold of the D30 engine, thus creating the necessary foundation for carrying out advanced simulations applicable in the optimisation of internal combustion engines [in accordance with Objective 1.5].

- In Chapter 5, the experimentally determined mechanical losses of the investigated engines from the database were compared with prediction formulas from literature, as a function of a series of engine catalogue parameters; **the critical analysis of the mechanical loss predictions against experiments led to the recalibration of four formulas with new coefficients, and a prediction algorithm was also developed.** This approach was necessary for evaluating the exergy term corresponding to mechanical losses [in accordance with Objective 1.5].

- **A contribution to the study of combustion perfection** (Chapter 5), assessed based on the energy remaining in the combustion products (CO, HC, Diesel particulates), was **the updating of the definition formula by separating diesel particulates into two fractions, one carbonaceous and the other containing heavy hydrocarbons** [in accordance with Objective 1.5]. As a result of the difference in heating values of the two fractions, differences appear compared to the case where the difference in composition is not considered. In addition, it was possible to assess, by using the same test cycle according to ECE Regulation 49, how combustion perfection increased, from 0,982 to 0,996, through the decrease of the three pollutants, over a period of two decades in which effective methods for reducing pollutant emissions were applied.

- In Chapter 5, **a contribution to the evaluation of fuel exergy is the proposal to consider the higher heating value, Hs, as a very good predictor for liquid petroleum fuels**, being easier to use than the product $A_{cb} \cdot H_i$ which requires exact knowledge of the fuel's chemical composition [in accordance with Objective 1.4].

- Also in Chapter 5, the proposal **to introduce three new exergy terms associated with heat transfer due to heat losses from compression, combustion (which considers the energy efficiency of combustion), and expansion processes** is motivated and supported, as well as **a residual, undetermined term that closes the exergy balance** [in accordance with Objective 1.5].

- The paragraph dedicated to the extended exergetic balance sums up all these contributions, generating **a set of new Sankey diagrams, with five new exergy loss terms, compared to the first series of charts** [in accordance with Objective 2.3].

- Table 6.2 contains **an ideal comparative characterization of the energy recovery factors of the heat sources existing** on the engine, which have the highest values for exhaust gases, then decreasing for lubricants, coolants, boost air and external surfaces of the engine.

- In section 6.2, for the most advantageous source of recovery, the exhaust gases, based on the high experimental data for the AVL 5402 engine, **the energy recovery potential was studied in detail, finding that the maximum values were obtained at the highest temperatures, which are reached at high speeds and high loads. The quantitative expression of this potential in relation to exhaust gas energy (δ) recorded values of 0,4-0,51, and in relation to fuel exergy (ε) of 0,11-0,25** [according to Objective 2.4].

- For five distinct engine operating cycles, (section 6.5), **the ranking by recovery potential indicates that highway operation is the most advantageous; compared to this, the operating regime on grade roads - mountain roads, has a recovery potential of about three times lower, and when operating in the urban cycle the potential is about six times lower**. These data are particularly valuable for developing strategies for applying energy recovery means.

- The ideal control of exergy recovery should focus on optimising the exergy balance terms with the largest weight, i.e., on the loss caused by combustion irreversibility - π_{irar} and on the loss with the exergy of the heat rejected by the exhaust gases to the environment - π_{QeT} [in accordance with Objective 2.4].

The publication of the main results of the doctoral thesis in specialized journals and the volumes of international conferences with a committee of reviewers can be considered as an important contribution that enriches the technical literature in this field of research.

Regarding **future directions for continuing research**, the principles applied in the exergy balance can be extrapolated to other models and system configurations, beyond the compression ignition engine. The paper [40] focuses on the identification and quantification of irreversibilities, which offers immense potential for application to various other engine types.

The most natural extension of the numerical model is for the case **of spark-combustion engines**, where the application of the exergy model is already presented in section 2.2; there are differences in distinct thermodynamic processes, combustion characteristics, and operating conditions that influence the magnitude of the irreversibilities. The differences in the exergy balance between the spark ignition engine and the compression ignition engine consist in the type of thermodynamic processes that occur during operation, where combustion in SI engines is characterised by higher average temperatures, and combustion irreversibilities are lower compared to CI engines.

Exergy loss from exhaust gases is however lower in CI engines, with a lower exhaust gas temperature as well, also specifying a higher efficiency in the case of the compression ignition engine [41]. Besides these differences, CI engines also differentiate themselves by a higher fuel energy per unit volume than their counterpart, resulting in a better conversion of the fuel's chemical exergy into mechanical work. CI engines are also functionally and constructively advantaged by the higher compression ratio and higher pressures developed, allowing operation closer to the fuel's energy potential.

From the point of view of the numerical model, modifications appear in the engine cycle (ρ =1), in the mass of the thermal agent introduced into the cycle (m_{ag}), as well as in the different values of some input-specific quantities, such as compression ratio, excess air ratio, or fuel exergy.

Furthermore, exergy analysis represents a valuable method in selecting and integrating **alternative fuels** for internal combustion engines, as it identifies in detail the manner and location where exergy is destroyed through irreversibilities due to fuel combustion and heat transfer within the engine, while also quantifying the exergy available in the exhaust gases. Fuel characteristics can directly affect irreversibilities during thermodynamic processes. By precisely quantifying chemical exergy and its destruction, exergy analysis presents a method for improving engine efficiency and optimising fuel utilisation for both conventional and alternative fuels. In the case of the compression ignition engine, the combustion of methane or methanol, which is characterised by an increase in the amount of available oxygen, will lead to lower combustion irreversibility values due to reduced entropy upon mixing the combustion products. This reduction in combustion irreversibilities will lead to an increase in efficiency compared to the case of conventional diesel fuel [190].

The spark ignition engine shows increased efficiency when using ethanol or oxygen-enriched mixture, resulting in reduced combustion irreversibilities compared to the case of pure gasoline [191, 192]. Fuels such as ethanol, compressed natural gas, and oxygen or hydrogen enriched mixtures lead to an increase in useful mechanical work, unlike butanol or adding water to the intake path up to 50% of the mixture, in which case the increase in combustion irreversibilities is significant, resulting in low efficiency [193, 194].

Renewable fuels are of great interest because they reduce CO_2 emissions by reducing the carbon footprint throughout their life cycle and by reducing the combustion of fossil fuels which, through their combustion, supplement the amount of CO_2 in the atmosphere. Paper [195] presents an experimental study carried out on a compression ignition engine powered by biodiesel at 50% and 100%.

The results show that combustion irreversibilities are lower with increasing biodiesel quantity, mainly due to the relatively high oxygen content, about 10-12% (m/m) of this fuel, which helps homogenise the mixture; in contrast, the exhaust gas temperature decreases slightly.

Adding a fraction of up to 15% (m/m) of ethanol in a 50% biodiesel blend leads to increased exergetic efficiency and reduced combustion irreversibilities [196].

Two trends are emerging that would reduce combustion irreversibility, namely the use of lighter hydrocarbons (methane, ethane) than gasoline and diesel fuel, as well as the use of oxygenated compounds (methanol, ethanol).

From the point of view of the numerical model applied to engines with alternative fuels, modifications appear in the formula for calculating fuel exergy, in the compositional components (c, h, o, s), and in the resulting lower heating value.

The exergy model can also be applied to **LHR (Low Heat Rejection)** engines, which are continuations of the concept of an engine, improperly called **adiabatic**, i.e., without heat losses, in which case the cooling system would be eliminated as useless; this technology aims to minimise heat transfer through the engine walls by using insulating materials for the combustion chamber, thus increasing the average temperature inside the cylinder and implicitly the efficiency. By applying the second law of thermodynamics, a reduction in irreversibilities due to fuel combustion and higher exhaust gas temperatures are observed, corresponding to an increased availability of energy for the turbine or other energy recovery systems. A comparison of the behaviour of a thermally insulated diesel engine, compared to the conventional case, shows a slight increase in indicated mechanical work of approximately 3,7%, as well as an increase in exhaust gas exergy of up to 49%, a fact which gives the thermal insulation solution for the cylinder wall a positive evaluation from the point of view of the second principle of thermodynamics [197]; the "flip side of the coin" is that the reduction in heat transfer from the cylinder does not translate notably into an increase in indicated efficiency, but rather into an increase in exhaust gas exergy.

The method for identifying subsystem irreversibilities can even be extended to **cogenerating systems** driven by thermal engines. Cogenerating systems often operate under variable loads and conditions, especially in applications such as urban heating or various industrial processes, and exergy analysis could be applied at the design stage to achieve high efficiency under dynamic conditions. The balance of chemical and thermal exergy is particularly relevant for cogenerating systems, where both electrical and thermal energy must be optimised.

Exergy analysis can be used for integrating waste heat recovery systems, such as thermoelectric generators (TEG) or systems using the Organic Rankine Cycle to utilise exhaust gas heat for producing mechanical work. Furthermore, by extending the analysis to engine auxiliaries, exergy analysis can improve technical solutions for developing and designing turbocharging and intake air intercooling systems by reducing irreversibilities due to compression, heat exchange, and fluid throttling.

By using the presented exergy model, input data can be obtained for the characteristic software programs of energy recovery systems. The experimentally validated model using data from the INAR engine database, including the AVL 5402 engine, can be used to provide the necessary information for determining required boundary conditions, for instance, in the case of determining temperature and pressure data needed for an energy recovery device using the Rankine cycle or data about the hot source of the thermoelectric generator (TEG).

An alternative engine configuration is modern hybrid systems, where internal combustion engines operate in synergy with an electric motor. Exergy analysis can evaluate energy storage losses by estimating losses due to heat transfer and can contribute to optimising the interaction between the thermal energy of the internal combustion engine and the electrical energy from the battery. Hybrid systems are often designed to recover energy from the thermal engine's exhaust gases or from braking. Applying the second principle of thermodynamics can be beneficial in better understanding how energy circulates between the components of the hybrid system and can help in the design stage of energy recovery systems, such as turbochargers or regenerative braking solutions [198]..

Validation of research results

6 scientific articles published, as follows:

	INDEXING					
	ISI Wos	Scopus	IEEE	Google Scholar	High BDI *	
DIARY						
						First author
PROCEEDINGS						
						Corresponding author
						First author

***** *ResearchGate, Academia.edu, EBSCO, CNCSIS, etc*

3 articles indexed in ISI (International Scientific Index) –
Clarivate WoS (Web of Science) Core Collection

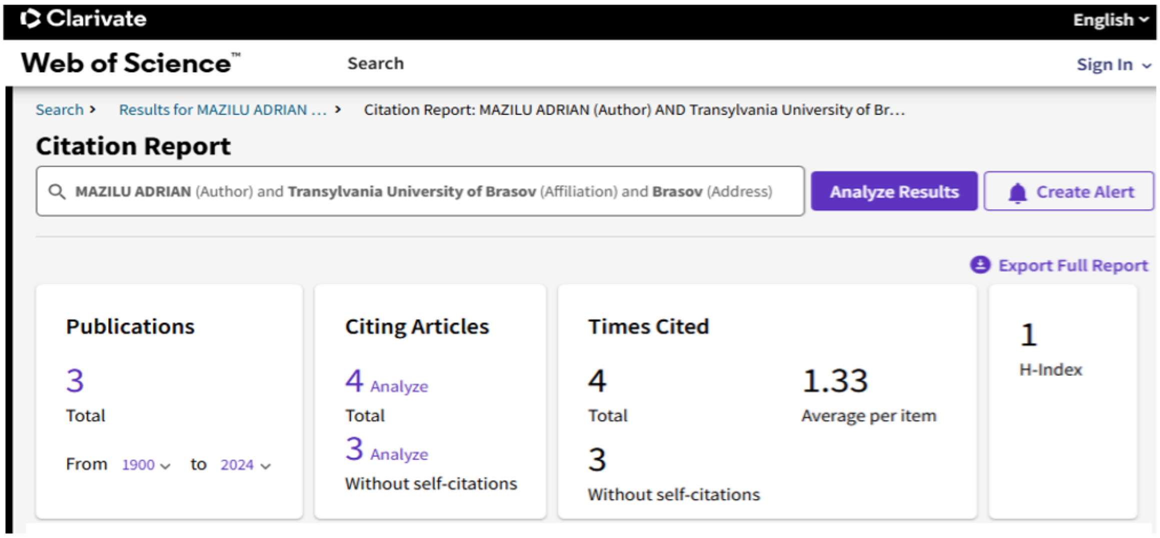

- Sandu V., **Mazilu A.** – "Assessment of Internal Combustion Engine Exergy Based on Theoretical Cycles and Experimental Data" - TEM JOURNAL-TECHNOLOGY EDUCATION MANAGEMENT INFORMATICS, Volume: 8 Issue: 4, Nov. 2019, Pages: 1277-1287, ISSN: 2217-8309, DOI: 10.18421/TEM84-25, Accession Number: WOS:000500710200025, *Indexat și SCOPUS ; Indexat și Google Scholar* ; 1 citare în WoS

- Sandu V., **Mazilu A.** – "Diesel Engine Waste Heat Recovery Potential versus Driving Cycles" – Proceedings of the 8TH International Conference on Renewable Energy Research and Applications (ICRERA 2019), Pages: 331-336, ISSN: 2377-6897, ISBN: 978-1-7281-3587-8, DOI: 10.1109/icrera47325.2019.8996563, Accession Number: WOS:000761668400048 *; Indexat și SCOPUS ; Indexat și IEEE ; Indexat și Google Scholar* ; 3 citări în WoS

- **Mazilu A.**, Sandu V. – „Factors Affecting Exergy Terms in Naturally Aspirated Diesel Engines" – Journal ACTA TECHNICA NAPOCENSIS SERIES-APPLIED MATHEMATICS MECHANICS AND ENGINEERING, Volume: 66, Issue: 1, 2023, Pages: 123-132, ISSN: 1221-5872, Accession Number: WOS:000995805400014, **Autor corespondent Mazilu A** ; *Indexat și Google Scholar*

1 article indexed only SCOPUS

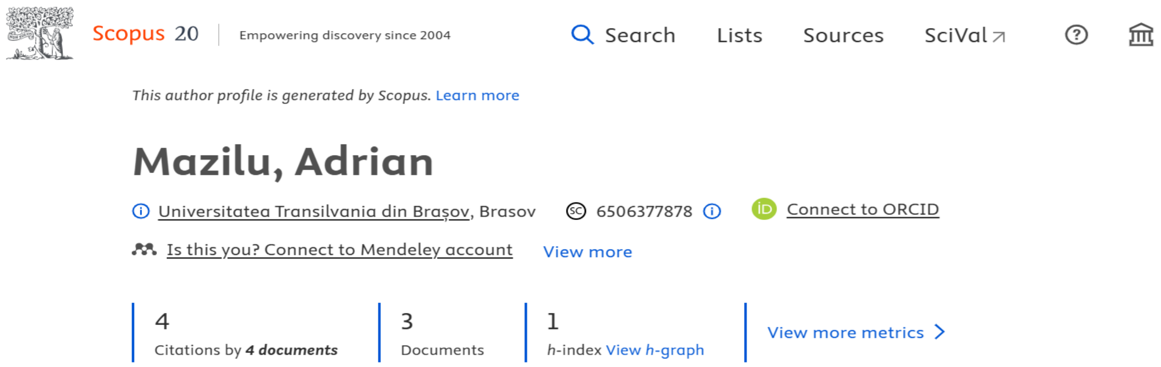

- Sandu V., Ungureanu V.B., Leahu C., **Mazilu A.** – "Predicting vehicle waste heat recovery potential in road gradient driving cycle - A case study" – Proceedings of the International Conference on Advanced Concepts in Mechanical Engineering, ACME 2020, Iasi, June 2020 – ISSN: 1757-8981, Publisher IOP (Institute of Physics – UK / Ireland), DOI: 10.1088/1757-899X/997/1/012155, **Autor corespondent Mazilu A.**

1 article in a journal indexed only in other BDI

- **Mazilu A.**, Costiuc L. – "NUMERICAL MODELLING OF HEAT TRANSFER IN ENGINE EXHAUST MANIFOLDS" - Bulletin of the Transilvania University of Braşov, Vol.15(64), No.2, 2022, DOI:10.31926/but.ens.2022.15.64.2.3, 1 citare în *Google Scholar*.

  https://webbut.unitbv.ro/index.php/Series_I/article/view/5020

1 article indexed only Google Scholar

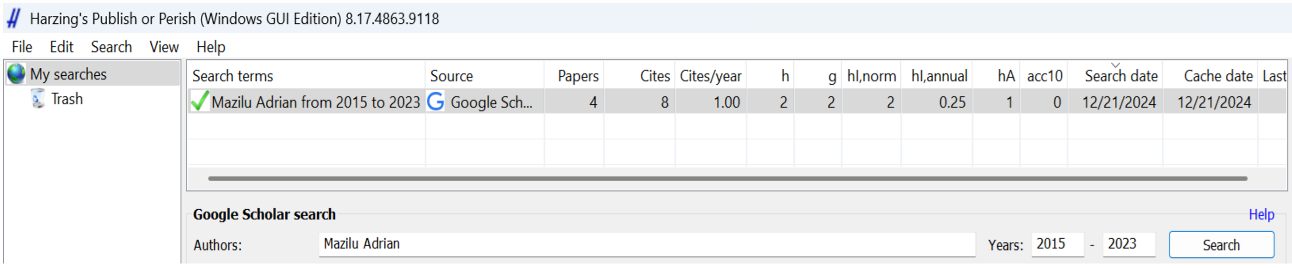

- **Mazilu A.**, Preda I. – " Kinematic Optimization of the Rack and Pinion Steering-System of an Automobile: An Example" – Proceedings of CONAT 2016 - International Automotive Congress, Transilvania University Press ; *4 citări în Google Scholar*

  http://193.254.231.99:8080/jspui/bitstream/123456789/2056/1/11.pdf

REFERENCES

[1] **** Nomenclatorul domeniilor şi al specializărilor / programelor de studii universitare*. Available: https://www.edu.ro/sites/default/files/ANEXA_1_NOMENCLATOR_2020_2021_0.pdf

[2] **** Directiva 2012/27/UE a Parlamentului European și a Consiliului din 25 octombrie 2012 privind eficiența energetică*. Available: https://eur-lex.europa.eu/legal-content/RO/ALL/?uri=celex:32012L0027

[3] *** Raportul special nr. 06/2020 „Mobilitatea urbană durabilă în UE".

[4] **** Planul operational de dezvoltare institutionala a Universitatii Transilvania din Brasov*. Available: https://www.unitbv.ro/documente/despre-unitbv/info-interes-public/transparenta-insitutionala/planuri/plan-operational/Planul_operational_2024.pdf

[5] **** Directiva (UE) 2023/1791 a Parlamentului European și a Consiliului din 13 Septembrie 2023 privind Eficiența Energetică*, 2023.

[6] E. E. Agency, Transport and environment report 2021. Decarbonising road transport—the role of vehicles, fuels and transport demand, ed. European Environment Agency Copenhagen, Denmark, 2022.

[7] J. DeCarolis, A. LaRose, Annual Energy Outlook 2023, *US Energy Information Administration,* 2023.

[8] R. Y. Dahham, H. Wei, J. Pan, Improving thermal efficiency of internal combustion engines: recent progress and remaining challenges, *Energies,* vol. 15, p. 6222, 2022.

[9] J. A. Caton, A review of investigations using the second law of thermodynamics to study internal-combustion engines, *SAE transactions,* pp. 1252-1266, 2000.

[10] S. Jaichandar, P. Tamilporai, Low heat rejection engines–an overview, 2003.

[11] Y. Li, M. Jia, S. L. Kokjohn, Y. Chang, R. D. Reitz, Comprehensive analysis of exergy destruction sources in different engine combustion regimes, *Energy,* vol. 149, pp. 697-708, 2018.

[12] W. Guan, V. B. Pedrozo, H. Zhao, Z. Ban, T. Lin, Variable valve actuation–based combustion control strategies for efficiency improvement and emissions control in a heavy-duty diesel engine, *International Journal of Engine Research,* vol. 21, pp. 578-591, 2020.

[13] Z. Lou, G. Zhu, Review of advancement in variable valve actuation of internal combustion engines, *Applied Sciences,* vol. 10, p. 1216, 2020.

[14] M. Izadi Najafabadi, N. Abdul Aziz, Homogeneous charge compression ignition combustion: challenges and proposed solutions, *Journal of combustion,* vol. 2013, p. 783789, 2013.

[15] J. A. Caton, The thermodynamic characteristics of high efficiency, internal-combustion engines, *Energy Conversion and Management,* vol. 58, pp. 84-93, 2012.

[16] R. K. Maurya, A. K. Agarwal, Experimental study of combustion and emission characteristics of ethanol fuelled port injected homogeneous charge compression ignition (HCCI) combustion engine, *Applied Energy,* vol. 88, pp. 1169-1180, 2011.

[17] S. L. Kokjohn, R. M. Hanson, D. Splitter, R. Reitz, Fuel reactivity controlled compression ignition (RCCI): a pathway to controlled high-efficiency clean combustion, *International Journal of Engine Research,* vol. 12, pp. 209-226, 2011.

[18] J. Zareei, M. Haseeb, K. Ghadamkheir, S. Farkhondeh, A. Yazdani, K. Ershov, The effect of hydrogen addition to compressed natural gas on performance and emissions of a DI diesel engine by a numerical study, *International journal of hydrogen energy,* vol. 45, pp. 34241-34253, 2020.
[19] S. Bari, M. M. Esmaeil, Effect of H2/O2 addition in increasing the thermal efficiency of a diesel engine, *Fuel,* vol. 89, pp. 378-383, 2010.
[20] D. Dogariu, Optimizarea proceselor de formare a amestecurilor și de ardere din motoarele cu ardere internă, Doctoral Thesis, Universitatea Transilvania Brașov, 2020.
[21] Y. Aoyagi, T. Yamaguchi, H. Osada, K. Shimada, Y. Goto, H. Suzuki, Improvement of thermal efficiency of a high-boosted diesel engine with focus on peak cylinder pressure, *International Journal of Engine Research,* vol. 12, pp. 227-237, 2011.
[22] V. Hariram, R. V. Shangar, Influence of compression ratio on combustion and performance characteristics of direct injection compression ignition engine, *Alexandria Engineering Journal,* vol. 54, pp. 807-814, 2015.
[23] M. Meijer, Development and Demonstration of Advanced Engine and Vehicle Technologies For Class 8 Heavy Duty Vehicle (Supertruck II), PACCAR Inc., Bellevue, WA (United States); National Energy Technology 2024.
[24] F. Zhou, S. N. Joshi, R. Rhote-Vaney, E. M. Dede, A review and future application of Rankine Cycle to passenger vehicles for waste heat recovery, *Renewable and Sustainable Energy Reviews,* vol. 75, pp. 1008-1021, 2017.
[25] R. Freymann, J. Ringler, M. Seifert, T. Horst, The second generation turbosteamer, *MTZ worldwide,* vol. 73, pp. 18-23, 2012.
[26] J. Panting, K. Pullen, R. Martinez-Botas, Turbocharger motor-generator for improvement of transient performance in an internal combustion engine, *Proceedings of the Institution of Mechanical Engineers, Part D: Journal of Automobile Engineering,* vol. 215, pp. 369-383, 2001.
[27] A. Boretti, F1 style MGU-H applied to the turbocharger of a gasoline hybrid electric passenger car, *Nonlinear Engineering,* vol. 6, pp. 293-300, 2017.
[28] H. Jääskeläinen, W. A. Majewski, Waste heat recovery for heavy-duty diesel engines: A review of mechanical turbocompounding, in *Internal Combustion Engine Division Fall Technical Conference*, 2017, p. V001T01A012.
[29] S. Park, J. Yoo, S. Kim, A thermoelectric generation waste heat recovery system using engine coolant for light-duty ICE vehicles, in *2010 International Conference on Electrical Machines and Systems*, 2010, pp. 2012-2015.
[30] Volkswagen Shows Thermoelectric Generator for Waste Heat Recovery, in *Green Car Congress*, Berlin, 2008. Available: https://www.greencarcongress.com/2009/02/volkswagen-show.html
[31] J. B. Heywood, Internal Combustion Engine Fundamentals. McGraw-Hill, 1988.
[32] B. Grunwald, Teoria, calculul şi construcția motoarelor pentru autovehicule rutiere. Bucureşti. Editura didacticã şi pedagogicã, 1980.
[33] A. J. Martyr, M. A. Plint, Engine testing: theory and practice. Elsevier, 2011.
[34] F. Payri, P. Olmeda, J. Martín, R. Carreño, Experimental analysis of the global energy balance in a DI diesel engine, *Applied Thermal Engineering,* vol. 89, pp. 545-557, 2015.
[35] W. W. Pulkrabek, Engineering fundamentals of the internal combustion engine, ed, 2004.
[36] V. Radcenco, Criterii de optimizare a proceselor termice. București. Editura Tehnică, 1977.

[37] E. Sciubba, G. Wall, A brief commented history of exergy from the beginnings to 2004, *International Journal of Thermodynamics,* vol. 10, pp. 1-26, 2007.
[38] A. Alkidas, The application of availability and energy balances to a diesel engine, 1988.
[39] P. Flynn, K. Hoag, M. Kamel, R. Primus, A new perspective on diesel engine evaluation based on second law analysis, *SAE transactions,* pp. 198-211, 1984.
[40] C. D. Rakopoulos, E. G. Giakoumis, Second-law analyses applied to internal combustion engines operation, *Progress in Energy and Combustion Science,* vol. 32, pp. 2-47, 2006/01/01/ 2006.
[41] V. Radcenco, Termodinamică tehnică și mașini termice. Procese ireversibile. București. Editura Didactică și Pedagogică, 1976.
[42] V. Sandu, A. Mazilu, Assessment of Internal Combustion Engine Exergy Based on Theoretical Cycles and Experimental Data, *TEM Journal,* vol. 8, p. 1277, 2019.
[43] B. C. Popa, I. Gh. , Manualul inginerului termotehnician. București. Editura Tehnică, 1986.
[44] A. Chiru, S. Țârulescu, Testarea şi omologarea motoarelor cu ardere internă. Matrix Rom, 2018.
[45] *** STAS 6635-87. Motoare cu ardere internă pentru autovehicule și tractoare agricole. Reguli și metode de încercare pe stand., București 1987.
[46] N. Apostolescu, D. Taraza, Bazele cercetării experimentale a maşinilor termice. Editura Didactică şi Pedagogică, 1979.
[47] D. Abăităncei, Motoare pentru automobile şi tractoare, *Editura Tehnică, Bucureşti,* 1980.
[48] R. Atkins, An introduction to engine testing and development. SAE International, 2009.
[49] A. Hijawi, Cam-less Engine Management Unit, 2018.
[50] *** AVL Product Description (2014). Single Cylinder Research Engines, 2014.
[51] A. Sarangi, Diesel low temperature combustion: an experimental study, Loughborough University Loughborough, 2012.
[52] J. Mattson, N. V. Burnete, C. Depcik, D. Moldovanu, N. Burnete, Second law analysis of waste cooking oil biodiesel versus ULSD during operation of a CI engine, *Fuel,* vol. 255, p. 115753, 2019.
[53] *** AVL FLOWSONIX AIR, 2014.
[54] K. Kudlaty, K. Kock, H. Krenn, A novel ultrasonic intake air flow meter for test bed applications, SAE Technical Paper 0148-7191, 2013.
[55] Internal Combustion Engines and Powertrain Systems for Future Transport, in *The International Conference on Internal Combustion Engines and Powertrain Systems for Future Transport*, Birmingham, UK, 2019.
[56] *** Industrial platinum resistance thermometers and platinum temperature sensors EN60751, IEC 2022.
[57] *** Tolerance classes for thermocouples according to the IEC 60 584-2, 1995.
[58] *** Thermocouples - EMF specifications and tolerances IEC 60584-1, 2013.
[59] *** Pressure sensors for combustion analysis. Product catalog, ed. AVL, 2013.
[60] *** Lambda sensor LSU 4.9 Data Sheet, ed. Bosch, 2024.
[61] W. Dongliang, H. Kaisheng, L. Wei, L. Zhihua, W. Yinhui, OBD system oxygen sensor degradation monitoring and mechanism analysis, in *2011 third international conference on measuring technology and mechatronics automation*, 2011, pp. 740-744.
[62] *** AVL Blow-By Meter 442S - 300, ed. AVL, 2009.
[63] S. Hannes, Examination of the Automated Test System for AVL IndiCom, Master Thesis, Graz University of Technology, Graz, 2015.

[64] D. Abăităncei, Motoare pentru automobile şi tractoare fabricate în România. Alma, 2011.
[65] G. Bobescu, T. Nagy, A. Chiru, C. Cofaru, Ridicarea diagramelor indicate și analiza experimentală a proceselor termogazodinamice la motoarele din fabricația Întreprinderii de Autocamioane Brașov, Universitatea Transilvania din Brașov, Brașov 1981.
[66] *** Cercetare preliminară a modelului funcțional D-127T, INAR, Brașov 1997.
[67] *** Dezvoltarea motoarelor din gama de putere 70-100 CP prin turbosupraalimentare în vederea încadrării în normele Euro II, INAR, Brașov 1998.
[68] *** Punerea la punct a motorului D127 ce echipează utilitarele ROCAR, INAR, Brașov 1993.
[69] *** Elaborarea standardelor de ramură (STR) pentru motoarele 392-L4D, DT, DTI cu patru cilindrii în linie, INAR, Brașov 1991.
[70] *** Încercări preliminare motor 392-L4-DT pentru definirea performanțelor, INAR, Brașov 1995.
[71] *** Elaborarea procedurii pentru încercarea și atestarea turbosuflantelor, INAR, Brașov 1996.
[72] *** Încercarea motorului 392-L4-DTI în vederea omologării interne, INAR, Brașov 2000.
[73] *** Elaborarea standardului tehnic de ramură pentru motoarele 550-L6 cu injecție directă în camera de ardere de tip omega, INAR, Brașov 1991.
[74] *** Cercetarea și optimizarea motorului 550-L6-D, INAR, Brașov 1989.
[75] *** Cercetări privind toxicitatea gazelor arse, randamentului volumetric și a vibrațiilor torsionale ale arborelui cotit al motorului 797-05, INAR, Brașov 1985.
[76] *** Determinarea siguranței în funcționare cu motorul 550-L6-DT, INAR, Brașov 1994.
[77] *** Motor 550-L6-DTI cu încadrarea în norma Euro. Cercetări și încercări de scurtă durată în vederea omologării., INAR, Brașov 1994.
[78] *** Încercări pentru determinarea siguranței în funcționare cu motorul orizontal 1035-L6-DTO, INAR, Brașov 1997.
[79] *** Cercetări pentru definitivarea soluțiilor constructive și determinarea performanțelor motorului orizontal 1035-L6-DTO cu puterea de 240 CP la 2100 rpm, INAR, Brașov 1996.
[80] *** Încercări pentru determinarea siguranței în funcționare a motorului 1070-L6-DTI și elaborarea documentelor de omologare, INAR, Brașov 1994.
[81] *** Motor 1230-L6-DTI pentru autovehicule de transport rutier cu putere de 380 CP la 1900 rpm - Cercetare model funcțional, INAR, Brașov 1998.
[82] *** Studiu INAR - Proiectarea modelului funcțional al motorului 1230-L6-DTI, INAR, Brașov 1990.
[83] *** Cercetarea echipamentului de injecție și a grupului de supraalimentare pentru motorul 1230-L6-DTI, INAR, Brașov 1997.
[84] *** Cercetări pentru determinarea performanțelor și reglajelor motorului 1240-V8-DTI, INAR, Brașov 1987.
[85] *** Cercetări pentru determinarea performanțelor motorului 1240-V8-DT/DTI, INAR, Brașov 1985.
[86] *** Motor 1380-V8 DT fiabilizat și cu încadrarea în normele Euro, INAR, Brașov 1995.
[87] *** Proiectarea prototipului motorului 1380-V8-DT și 1380-V8-DTI cu alezaj de 130mm, INAR, Brașov 1986.
[88] *** Încercări în vederea omologării de prototip a motorului 1380- V8- DTI fiabilizat și cu încadrarea în normele Euro, INAR, Brașov 1995.

[89] H. R. Sankey, The Thermal Efficiency of Steam-Engines, *Minutes of the Proceedings of the Institution of Civil Engineers,* vol. 125, pp. 182-212, 1896.
[90] D. C. Kyritsis, C. D. Rakopoulos, Parametric study of the availability balance in an internal combustion engine cylinder, SAE Technical Paper 0148-7191, 2001.
[91] C. Rakopoulos, E. Giakoumis, Speed and load effects on the availability balances and irreversibilities production in a multi-cylinder turbocharged diesel engine, *Applied Thermal Engineering,* vol. 17, pp. 299-313, 1997.
[92] R. J. Primus, P. F. Flynn, The assessment of losses in diesel engines using second law analysis, *Computer-Aided Engineering and Energy Systems,* vol. 3, pp. 61-68, 1986.
[93] C. Rakopoulos, E. Giakoumis, Development of cumulative and availability rate balances in a multi-cylinder turbocharged indirect injection diesel engine, *Energy Conversion and Management,* vol. 38, pp. 347-369, 1997.
[94] B. Challen, R. Baranescu, Diesel engine reference book, 1999.
[95] V. Sandu, Improving diesel engine performance by air-to-air intercooling, *Bulletin of the Transilvania University of Brasov. Series I-Engineering Sciences,* pp. 19-24, 2014.
[96] M. J. da Silva, A. de Oliveira, J. R. Sodré, Analysis of processing methods for combustion pressure measurement in a diesel engine, *Journal of the Brazilian Society of Mechanical Sciences and Engineering,* vol. 41, pp. 1-9, 2019.
[97] Y. A. Cengel, M. A. Boles, Thermodynamics: an engineering approach, *Sea,* vol. 1000, pp. 287-93, 2002.
[98] C. F. Taylor, Internal Combustion Engine in Theory and Practice, revised, Volume 1: Thermodynamics, Fluid Flow, Performance vol. 1. Mit Press, 1985.
[99] K. I. Hamada, M. Rahman, A. R. A. Aziz, Time-averaged heat transfer correlation for direct injection hydrogen fueled engine, *International journal of hydrogen energy,* vol. 37, pp. 19146-19157, 2012.
[100] C. Finol, K. Robinson, Thermal modelling of modern engines: a review of empirical correlations to estimate the in-cylinder heat transfer coefficient, *Proceedings of the institution of mechanical engineers, part D: journal of automobile engineering,* vol. 220, pp. 1765-1781, 2006.
[101] G. Borman, K. Nishiwaki, Internal-combustion engine heat transfer, *Progress in energy and combustion science,* vol. 13, pp. 1-46, 1987.
[102] C. F. Taylor, T.-Y. Toong, Heat transfer in internal-combustion engines, 1957.
[103] G. Blair, Design and simulation of four-stroke engines. SAE International, 1999.
[104] W. Annand, Heat transfer in the cylinder and porting. The thermodynamics and gas dynamics of internal combustion engines, vol II, ed. Oxford University Press, London, 1986.
[105] S. Edition, Ashrae handbook, *Stephen Comstock: Atlanta, GA, USA,* 1993.
[106] T. L. Bergman, Fundamentals of heat and mass transfer. John Wiley & Sons, 2011.
[107] V. Sandu, V.-B. Ungureanu, M. Ivănoiu, L. Costiuc, Experimental Analysis on External Surface Convective-Radiative Heat Transfer in Stationary Diesel Engines, *surfaces,* vol. 1, p. 3, 2014.
[108] A. Mazilu, L. Costiuc, Numerical Modelling of Heat Transfer in Engine Exhaust Manifolds, *Bulletin of the Transilvania University of Brasov. Series I-Engineering Sciences,* pp. 23-30, 2022.
[109] V. Sandu, A.-C. Stanca, A. Pasaroiu, D. Dobre, Experimental investigation of thermoelectric heat recovery from a diesel engine, in *2012 International Conference on Applied and Theoretical Electricity (ICATE)*, 2012, pp. 1-8.

[110] M. Tabatabaian, COMSOL5 for Engineers. Mercury learning and information, 2015.
[111] *** Comsol Multiphysics 5.6. Software documentation., ed. COMSOL AB, 1998-2020.
[112] **** Fluke Ti20 User Manual*. Available: https://www.manualslib.com/manual/52657/Fluke-Ti20.html
[113] E. Giulli, A review of internal combustion engine losses, *Proc. Inst. Mech. Engrs,* vol. 207, pp. 229-240, 1993.
[114] K. McAulay, T. Wu, S. K. Chen, G. L. Borman, P. S. Myers, O. A. Uyehara, Development and evaluation of the simulation of the compression-ignition engine, *SAE Transactions,* pp. 560-593, 1966.
[115] S. Chen, P. FLYNN, International Harvester-LABECO high bmep single cylinder research engine, in *SAE TRANSACTIONS*, 1966, pp. 150-&.
[116] D. Winterbone, D. Tennant, The variation of friction and combustion rates during diesel engine transients, SAE Technical Paper 0148-7191, 1981.
[117] B. W. Millington, E. Hartles, Frictional losses in diesel engines, *SAE Transactions,* pp. 2390-2410, 1968.
[118] *** Motoare cu ardere internă pentru autovehicule și tractoare agricole. Reguli și metode de încercare pe banc., STAS 6635-1987, 1987.
[119] A. J. Martyr, M. A. Plint, Engine testing: the design, building, modification and use of powertrain test facilities. Elsevier, 2012.
[120] D. Taraza, N. A. Henein, W. Bryzik, Experimental determination of the instantaneous frictional torque in multicylinder engines, *SAE transactions,* pp. 2140-2150, 1996.
[121] M. M. Maricq, Chemical characterization of particulate emissions from diesel engines: A review, *Journal of Aerosol Science,* vol. 38, pp. 1079-1118, 2007.
[122] *** Cercetări pe motor pentru determinarea bilanțului energetic general al motorului 1240-V8-DT, INAR, Brașov.
[123] *** Determinarea concentrațiilor compușilor poluanți din gazele de evacuare ale motorului 1240-V8-DT conform Regulamentului nr. 49 al ECE-ONU, INAR, Brașov 1996.
[124] I. Bortel, J. Vavra, M. Takats, Emissions and performance of a passenger car size diesel engine fuelled with hvo diesel fuel mixtures, *fuel,* vol. 7, p. 9, 2017.
[125] *** Regulation No. 49 of the Economic Commission for Europe of the United Nations, in *Uniform Provisions Concerning the Measures to be Taken against the Emission of Gaseous and Particulate Pollutants from Compression-Ignition Engines and Positive Ignition Engines for Use in Vehicles And The Emission Of Gaseous Pollutants From Positive-Ignition Engines Fuelled With Natural Gas Or Liquefied Petroleum Gas For Use In Vehicles* vol. 49, ed. UN/ECE, p. 2013.
[126] V. D. Negrea, V. Sandu, Combaterea poluării mediului în transporturile rutiere, *Ed. Tehnică, Bucureşti,* 2000.
[127] M. J. Moran, Availability analysis: a guide to efficient energy use, 1989.
[128] Z. Rant, Towards the estimation of specific exergy of fuels, *Allg. Wärmetech,* vol. 10, pp. 172-176, 1961.
[129] V. Stepanov, Chemical energies and exergies of fuels, *Energy,* vol. 20, pp. 235-242, 1995.
[130] J. Szargut, T. Styrylska, Approximate evaluation of the exergy of fuels, *Brennst. Wärme Kraft,* vol. 16, pp. 589-596, 1964.
[131] *** Carburanți pentru automobile. Motorină. Cerințe şi metode de încercare, SR EN 590:2022, 2022.

[132] *** The Greenhouse Gases, Regulated Emissions, and Energy Use In Transportation Model, ed. Argonne, Illinois, USA. GREET, Argonne National Laboratory, 2010.
[133] G. Abbaszadehmosayebi, L. Ganippa, Determination of specific heat ratio and error analysis for engine heat release calculations, *Applied Energy,* vol. 122, pp. 143-150, 2014.
[134] R. Saidur, M. Rezaei, W. K. Muzammil, M. Hassan, S. Paria, M. Hasanuzzaman, Technologies to recover exhaust heat from internal combustion engines, *Renewable and sustainable energy reviews,* vol. 16, pp. 5649-5659, 2012.
[135] O. Douadi, R. Ravi, M. Faqir, E. Essadiqi, A conceptual framework for waste heat recovery from compression ignition engines: Technologies, working fluids & heat exchangers, *Energy Conversion and Management: X,* vol. 16, p. 100309, 2022.
[136] S. Brückner, S. Liu, L. Miró, M. Radspieler, L. F. Cabeza, E. Lävemann, Industrial waste heat recovery technologies: An economic analysis of heat transformation technologies, *Applied Energy,* vol. 151, pp. 157-167, 2015.
[137] D. Crane, G. Jackson, D. Holloway, Towards optimization of automotive waste heat recovery using thermoelectrics, SAE Technical Paper 0148-7191, 2001.
[138] X. Zheng, C. Liu, Y. Yan, Q. Wang, A review of thermoelectrics research–Recent developments and potentials for sustainable and renewable energy applications, *Renewable and Sustainable Energy Reviews,* vol. 32, pp. 486-503, 2014.
[139] *Scientific Guide to Understanding Thermoelectric Generators*. Available: https://www.tegmart.com/info/guide-to-understanding-and-using-teg-power-and-products
[140] F. T. Tănăsescu, D. Moraru, C. I. Popescu, Conversia energiei: tehnici neconvenționale. Editura Tehnică, 1986.
[141] N. V. Burnete, F. Mariasiu, C. Depcik, I. Barabas, D. Moldovanu, Review of thermoelectric generation for internal combustion engine waste heat recovery, *Progress in Energy and Combustion Science,* vol. 91, p. 101009, 2022.
[142] A. Schönecker, P.-Y. Pichon, J. König, M. Jägle, M. den Heijer, B. Kraaijveld, Novel Process for Metal Silicide Nanostructures Regarding Cheap and Large-Scale Material Synthesis, in *Proceedings of the 11th European Conference on Thermoelectrics: ECT 2013*, 2014, pp. 43-51.
[143] A. T. Tomescu, I. B. L.; Tomescu, F. M. G.;, Conversiunea directă a energiei. Editura Matrixrom, 2008.
[144] L. Yang, Z. G. Chen, M. S. Dargusch, J. Zou, High performance thermoelectric materials: progress and their applications, *Advanced Energy Materials,* vol. 8, p. 1701797, 2018.
[145] C. Hadjistassou, E. Kyriakides, J. Georgiou, Designing high efficiency segmented thermoelectric generators, *Energy conversion and management,* vol. 66, pp. 165-172, 2013.
[146] X. Liu, Y. Deng, S. Chen, W. Wang, Y. Xu, C. Su, A case study on compatibility of automotive exhaust thermoelectric generation system, catalytic converter and muffler, *Case Studies in Thermal Engineering,* vol. 2, pp. 62-66, 2014.
[147] L. Heber, J. Schwab, Modelling of a thermoelectric generator for heavy-duty natural gas vehicles: Techno-economic approach and experimental investigation, *Applied Thermal Engineering,* vol. 174, p. 115156, 2020.
[148] S. Lan, Z. Yang, R. Chen, R. Stobart, A dynamic model for thermoelectric generator applied to vehicle waste heat recovery, *Applied energy,* vol. 210, pp. 327-338, 2018.

[149] P. Fernández-Yáñez, A. Gómez, R. García-Contreras, O. Armas, Evaluating thermoelectric modules in diesel exhaust systems: potential under urban and extra-urban driving conditions, *Journal of Cleaner Production,* vol. 182, pp. 1070-1079, 2018.
[150] D. T. Crane, G. S. Jackson, Optimization of cross flow heat exchangers for thermoelectric waste heat recovery, *Energy conversion and management,* vol. 45, pp. 1565-1582, 2004.
[151] P. Varshil, D. Deshmukh, A comprehensive review of waste heat recovery from a diesel engine using organic rankine cycle, *Energy Reports,* vol. 7, pp. 3951-3970, 2021.
[152] M. Ghilvacs, Diesel engine exhaust heat recovery using Organic Rankine Cycle, Universitatea Politehnica din Bucuresti, 2018.
[153] C. Sprouse III, C. Depcik, Review of organic Rankine cycles for internal combustion engine exhaust waste heat recovery, *Applied thermal engineering,* vol. 51, pp. 711-722, 2013.
[154] A. Javanshir, N. Sarunac, Z. Razzaghpanah, Thermodynamic analysis of ORC and its application for waste heat recovery, *Sustainability,* vol. 9, p. 1974, 2017.
[155] A. Ganjehkaviri, M. N. M. Jaafar, Energy analysis and multi-objective optimization of an internal combustion engine-based CHP system for heat recovery, *Entropy,* vol. 16, pp. 5633-5653, 2014.
[156] G. Latz, Waste heat recovery from combustion engines based on the Rankine cycle. Chalmers Tekniska Hogskola (Sweden), 2016.
[157] H. Wang, R. Peterson, K. Harada, E. Miller, R. Ingram-Goble, L. Fisher*, et al.*, Performance of a combined organic Rankine cycle and vapor compression cycle for heat activated cooling, *Energy,* vol. 36, pp. 447-458, 2011.
[158] H. Teng, G. Regner, Improving fuel economy for HD diesel engines with WHR Rankine cycle driven by EGR cooler heat rejection, SAE Technical Paper 0148-7191, 2009.
[159] *Directiva 1999/96/CE a Parlamentului European și a Consiliului din 13 decembrie 1999 privind aproximarea legislațiilor statelor membre referitoare la măsurile ce trebuie luate împotriva emisiilor de poluanți gazoși și particule provenite de la motoare cu aprindere prin compresie destinate vehiculelor, precum și a emisiilor de poluanți gazoși provenite de la motoare cu aprindere prin scânteie alimentate cu gaz natural sau gaz petrolier lichefiat destinate vehiculelor și aducerea modificării Directivei 88/77/CEE a Consiliului.* , 2000.
[160] G. Shu, G. Yu, H. Tian, H. Wei, X. Liang, Z. Huang, Multi-approach evaluations of a cascade-Organic Rankine Cycle (C-ORC) system driven by diesel engine waste heat: Part A–Thermodynamic evaluations, *Energy conversion and management,* vol. 108, pp. 579-595, 2016.
[161] A. Mahmoudzadeh Andwari, A. Pesiridis, V. Esfahanian, A. Salavati-Zadeh, A. Karvountzis-Kontakiotis, V. Muralidharan, A comparative study of the effect of turbocompounding and ORC waste heat recovery systems on the performance of a turbocharged heavy-duty diesel engine, *Energies,* vol. 10, p. 1087, 2017.
[162] H. Aghaali, H.-E. Ångström, A review of turbocompounding as a waste heat recovery system for internal combustion engines, *Renewable and sustainable energy reviews,* vol. 49, pp. 813-824, 2015.
[163] C. Ononogbo, E. Nwosu, N. Nwakuba, G. Nwaji, O. Nwufo, O. Chukwuezie*, et al.*, Opportunities of waste heat recovery from various sources: Review of technologies and implementation, *Heliyon,* vol. 9, 2023.
[164] Y. Ismail, D. Durrieu, P. Menegazzi, P. Chesse, D. Chalet, Potential of exhaust heat recovery by turbocompounding, SAE Technical Paper 0148-7191, 2012.

[165] G. He, H. Xie, Fuel saving potential of different turbo-compounding systems under steady and driving cycles. SAE Tech Papers. 2015, ed.

[166] M. A. Abdelkareem, H. M. Maghrabie, E. T. Sayed, E.-C. A. Kais, A. G. Abo-Khalil, M. Al Radi*, et al.*, Heat pipe-based waste heat recovery systems: Background and applications, *Thermal Science and Engineering Progress,* vol. 29, p. 101221, 2022.

[167] I. Dincer, C. Zamfirescu, Advanced power generation systems. Academic Press, 2014.

[168] C. Ladekar, S. Choudhary, S. Khadare, A critical review-optimization of heat pipe, *International J. of Engineering Research & Technology,* pp. 274-280, 2016.

[169] J. Bull, J. M. Buick, J. Radulovic, Heat exchanger sizing for organic rankine cycle, *Energies,* vol. 13, p. 3615, 2020.

[170] C.-T. Hsu, G.-Y. Huang, H.-S. Chu, B. Yu, D.-J. Yao, Experiments and simulations on low-temperature waste heat harvesting system by thermoelectric power generators, *Applied Energy,* vol. 88, pp. 1291-1297, 2011.

[171] H. Lu, T. Wu, S. Bai, K. Xu, Y. Huang, W. Gao*, et al.*, Experiment on thermal uniformity and pressure drop of exhaust heat exchanger for automotive thermoelectric generator, *Energy,* vol. 54, pp. 372-377, 2013.

[172] T. Wang, W. Luan, W. Wang, S.-T. Tu, Waste heat recovery through plate heat exchanger based thermoelectric generator system, *Applied Energy,* vol. 136, pp. 860-865, 2014.

[173] V. Pandiyarajan, M. Chinnappandian, V. Raghavan, R. Velraj, Second law analysis of a diesel engine waste heat recovery with a combined sensible and latent heat storage system, *Energy policy,* vol. 39, pp. 6011-6020, 2011.

[174] Y. Kuze, H. Kobayashi, H. Ichinose, T. Otsuka, Development of new generation hybrid system (THS II)-development of Toyota coolant heat storage system, SAE Technical Paper 0148-7191, 2004.

[175] H. Aghaali, H.-E. Angstrom, Demonstration of air-fuel ratio role in one-stage turbocompound diesel engines, SAE Technical Paper 0148-7191, 2013.

[176] *** Cercetarea efectelor de reducere a particulelor emise de motorul 392-L4-DTI prin utilizarea filtrului de particule 3M, INAR, Brașov 1999.

[177] M. J. Moran, Engineering Thermodynamics/Mechanical Engineering Handbook, ed. Boca Raton: CRC Press LLC, 1999.

[178] T. Wang, Y. Zhang, Z. Peng, G. Shu, A review of researches on thermal exhaust heat recovery with Rankine cycle, *Renewable and sustainable energy reviews,* vol. 15, pp. 2862-2871, 2011.

[179] A. L. GmbH. *** AVL LIST, „Single Cylinder Research Engine 5402 – Users Guide" [Online].

[180] H. Teng, G. Regner, C. Cowland, Waste heat recovery of heavy-duty diesel engines by organic Rankine cycle part I: hybrid energy system of diesel and Rankine engines, SAE Technical Paper 0148-7191, 2007.

[181] V. Sandu, A. Mazilu, Diesel engine waste heat recovery potential versus driving cycles, in *2019 8th International Conference on Renewable Energy Research and Applications (ICRERA)*, 2019, pp. 331-336.

[182] C. Bejan, Studiul critic al ciclurilor în domeniul testelor de anduranță prin raportare la regimurile reale de funcționare şi cerințele testelor de fiabilitate, 1996.

[183] I. S. Rău, Veneția, Discrepancies of international regulations of diesel engine emissions, in *International Symposium on Environmental Protection ECO '96*, București, 1996, pp. pg. 86-93.

[184] **** Directiva 1999/96/EC a Parlamentului European și a Consiliului privitoare la măsurile care trebuie luate împotriva emisiilor de gaze și particule e ale motoarelor cu aprindere prin compresie și ale motoarelor cu aprindere prin scânteie alimentate cu gaz natural sau gaz petrolier lichefiat utilizate pe autovehicule*, 2000.

[185] E. G. Giakoumis, Driving and engine cycles vol. 1. Springer, 2017.

[186] Google. (2019). **** Date obținute de pe traseul Izvoarele-Cheia-Pasul Bratocea, România, folosind Google Earth [Software]*. Available: http://earth.google.com

[187] V. Sandu, V. Ungureanu, C. Leahu, A. Mazilu, Predicting vehicle waste heat recovery potential in road gradient driving cycle-A case study, in *IOP Conference Series: Materials Science and Engineering*, 2020, p. 012155.

[188] F. F. Rovai, C. Mady, Exergetic analysis of an internal combustion engine running on E22 and E100, *Revista de Engenharia Térmica,* vol. 21, pp. 43-50, 2022.

[189] N. Norouzi, A. G. Ebadi, A. Bozorgian, S. J. Hoseyni, E. Vessally, Energy and exergy analysis of internal combustion engine performance of spark ignition for gasoline, methane, and hydrogen fuels, *Iranian Journal of Chemistry and Chemical Engineering,* vol. 40, pp. 1909-1930, 2021.

[190] C. D. Rakopoulos, D. C. Kyritsis, Comparative second-law analysis of internal combustion engine operation for methane, methanol, and dodecane fuels, *Energy,* vol. 26, pp. 705-722, 2001.

[191] W. L. R. Gallo, L. F. Milanez, Exergetic analysis of ethanol and gasoline fueled engines, SAE Technical Paper 0148-7191, 1992.

[192] J. A. Caton, Use of a cycle simulation incorporating the second law of thermodynamics: results for spark-ignition engines using oxygen enriched combustion air, SAE Technical Paper 0148-7191, 2005.

[193] H. Ozcan, M. Sait Soylemez, Effect of water addition on the exergy balances of an LPG fuelled spark ignition engine, *International Journal of Exergy,* vol. 2, pp. 194-206, 2005.

[194] F. Alasfour, Butanol—a single-cylinder engine study: availability analysis, *Applied Thermal Engineering,* vol. 17, pp. 537-549, 1997.

[195] A. Magno, E. Mancaruso, B. M. Vaglieco, Effects of both blended and pure biodiesel on waste heat recovery potentiality and exhaust emissions of a small CI (compression ignition) engine, *Energy,* vol. 86, pp. 661-671, 2015.

[196] A. Paul, R. Panua, D. Debroy, An experimental study of combustion, performance, exergy and emission characteristics of a CI engine fueled by Diesel-ethanol-biodiesel blends, *Energy,* vol. 141, pp. 839-852, 2017.

[197] C. Rakopoulos, E. Andritsakis, D. Kyritsis, Availability accumulation and destruction in a DI diesel engine with special reference to the limited cooled case, *Heat Recovery Systems and CHP,* vol. 13, pp. 261-276, 1993.

[198] Y. D. Lee, K. Y. Ahn, T. Morosuk, G. Tsatsaronis, Exergetic and exergoeconomic evaluation of an SOFC-Engine hybrid power generation system, *Energy,* vol. 145, pp. 810-822, 2018.